UNIVERSITÉ DU QUÉBEC À MONTRÉAL

UNIVERSITÉ PARIS-SUD

THÈSE

présentée à l'Université du Québec à Chicoutimi comme exigence partielle du
DOCTORAT EN RESSOURCES MINÉRALES

offert à
L'UNIVERSITÉ DU QUÉBEC À MONTRÉAL

en vertu d'un protocole d'entente avec l'Université du Québec à Chicoutimi

présentée pour obtenir le grade de
DOCTEUR EN SCIENCES

de
L'UNIVERSITÉ DE PARIS XI

spécialité
SCIENCES DE LA TERRE

par

Pierre DESCHAMPS

TRAÇAGE DE LA MOBILITÉ DES RADIONUCLÉIDES NATURELS EN MILIEU SÉDIMENTAIRE PROFOND À L'AIDE DES DÉSÉQUILIBRES RADIOACTIFS ($^{234}U/^{238}U$): APPLICATION AUX FORMATIONS MÉSOZOÏQUES DE L'EST DU BASSIN DE PARIS

JANVIER 2004

Bibliothèque
Paul-Émile-Boulet

UQAC
Université du Québec
à Chicoutimi

Mise en garde/Advice

Afin de rendre accessible au plus grand nombre le résultat des travaux de recherche menés par ses étudiants gradués et dans l'esprit des règles qui régissent le dépôt et la diffusion des mémoires et thèses produits dans cette Institution, **l'Université du Québec à Chicoutimi (UQAC)** est fière de rendre accessible une version complète et gratuite de cette œuvre.

Motivated by a desire to make the results of its graduate students' research accessible to all, and in accordance with the rules governing the acceptation and diffusion of dissertations and theses in this Institution, the **Université du Québec à Chicoutimi (UQAC)** is proud to make a complete version of this work available at no cost to the reader.

L'auteur conserve néanmoins la propriété du droit d'auteur qui protège ce mémoire ou cette thèse. Ni le mémoire ou la thèse ni des extraits substantiels de ceux-ci ne peuvent être imprimés ou autrement reproduits sans son autorisation.

The author retains ownership of the copyright of this dissertation or thesis. Neither the dissertation or thesis, nor substantial extracts from it, may be printed or otherwise reproduced without the author's permission.

UNIVERSITÉ DU QUÉBEC À MONTRÉAL

UNIVERSITÉ PARIS-SUD

THESIS

presented at Université du Québec à Chicoutimi as a partial requirement of
MINERAL RESSOURCES DOCTORATE

Offered to
UNIVERSITÉ DU QUÉBEC À MONTRÉAL

in accordance to an agreement protocol with Université du Québec à Chicoutimi

presented for the grade of
DOCTEUR EN SCIENCES

of
UNIVERSITÉ DE PARIS XI

spéciality
SCIENCES DE LA TERRE

by

Pierre DESCHAMPS

MOBILITY OF NATURAL RADIONUCLIDES IN DEEP SEDIMENTARY FORMATION AS INFERRED BY ($^{234}U/^{238}U$) RADIOACTIVE DISEQUILIBRIA: APPLICATION TO THE MESOZOIC FORMATIONS OF THE EASTERN PART OF THE PARIS BASIN

JANVIER 2004

UNIVERSITÉ DU QUÉBEC À MONTRÉAL
UNIVERSITÉ PARIS-SUD

THÈSE

présentée à l'Université du Québec à Chicoutimi comme exigence partielle du
DOCTORAT EN RESSOURCES MINÉRALES
offert à
L'UNIVERSITÉ DU QUÉBEC À MONTRÉAL
en vertu d'un protocole d'entente avec l'Université du Québec à Chicoutimi

présentée pour obtenir le grade de
DOCTEUR EN SCIENCES
de
L'UNIVERSITÉ DE PARIS XI
spécialité
SCIENCES DE LA TERRE

par
Pierre DESCHAMPS

TRAÇAGE DE LA MOBILITÉ DES RADIONUCLÉIDES NATURELS EN MILIEU SÉDIMENTAIRE PROFOND À L'AIDE DES DÉSÉQUILIBRES RADIOACTIFS ($^{234}U/^{238}U$): APPLICATION AUX FORMATIONS MÉSOZOÏQUES DE L'EST DU BASSIN DE PARIS

Soutenue le 28 Novembre 2003, devant le jury composé de:

Mr. S. BUSCAHAERT	Examinateur
Mr. L. DEVER	Examinateur
Mr. C. GARIÉPY	Rapporteur
Mr. B. HAMELIN	Rapporteur
Mr. C. HILLAIRE-MARCEL	Co-Directeur de Thèse
Mr. J-L. MICHELOT	Co-Directeur de Thèse

Avant-propos

Nous y voilà. C'est fini et tout commence finalement. Une belle tranche de vie amorcée par hasard sur un terrain de rugby et qui s'achève quelques années plus tard à Montréal. Huit années riches en rencontres et expériences où l'on se construit un pays. "L'âge d'homme" en quelque sorte.

Ce pays n'est peut-être qu'un "vœu de l'esprit", mais il me faut ici remercier les femmes et les hommes qui en font partie.

Merci tout d'abord aux personnes qui ont fait que ce travail existe. Tout d'abord, mes "mentors", Claude, Bassam et Jean-Luc. "On n'emprunte que ce qui peut se rendre augmenté", dit Char. J'espère avoir été à la hauteur de ce qu'ils ont su m'apporter.

Reconnaissance aussi à toutes ces personnes, étudiants, techniciens ou chercheurs, qui m'ont aidé, soutenu et qui ont accepté de partager leur temps et savoir. Reconnaissance aussi à toutes ces personnes, instituteurs et professeurs, qui m'ont donné le goût d'apprendre et plus encore de comprendre.

Merci, enfin, à mes proches, à mes amis, d'ici et d'ailleurs, aux "alliés substantiels" d'exister et d'être là.

Table des matières

Liste des Figures

Partie A: Aspects Analytiques

Chapitre I

Chapitre II

Partie B: Caractérisation de la migration des radionucléides au sein des formations sédimentaires du site ANDRA de l'Est

Chapitre III

Chapitre IV

Liste des Tableaux

Partie A: Aspects Analytiques

Chapitre I

Chapitre II

Partie B: Caractérisation de la migration des radionucléides au sein des formations sédimentaires du site ANDRA de l'Est

Chapitre III

Chapitre IV

Résumé

Cette thèse s'inscrit dans le cadre des études de "faisabilité" du stockage des déchets nucléaires en formations géologiques profondes. Elle s'intègre au programme de recherche conduit par l'agence française pour la gestion des déchets nucléaires (ANDRA) sur le site expérimental Meuse/Haute-Marne de type "argile", situé dans les formations sédimentaires Mésozoïques faiblement perméables de l'Est du bassin parisien. L'étude a pour objet la caractérisation de la migration des radionucléides naturels au sein de la formation argileuse Callovo-Oxfordienne cible et de ses encaissants carbonatés Oxfordien et Bathonien, afin d'estimer les propriétés de confinement à long terme de cette série sédimentaire. Elle repose sur l'analyse de haute précision des déséquilibres radioactifs au sein des familles naturelles de l'uranium et du thorium.

L'intérêt de faire appel aux déséquilibres U-Th réside dans le fait qu'ils sont susceptibles, d'une part, de mettre en évidence et de caractériser les processus contrôlant la mise en solution et la migration *in situ* des radionucléides et, d'autre part, de fournir des indications temporelles sur les processus et perturbations physico-géochimiques auxquelles la formation géologique a été soumise sur des échelles de temps variables, selon les isotopes utilisés, mais pouvant atteindre jusqu'à deux millions d'années environ, via le déséquilibre $^{234}U/^{238}U$.

Les objectifs initiaux de l'étude étaient: i) de déterminer en particulier l'état d'équilibre -ou de déséquilibre- radioactif entre l'uranium-238 et son descendant l'uranium-234 ($T_{1/2}$ (^{234}U) = 245250 a) dans les formations profondes au sein desquelles le laboratoire expérimental de l'ANDRA est en cours d'implantation; ii) de caractériser, le cas échéant, les processus responsables des déséquilibres radioactifs observés; et iii) d'en préciser les implications chronologiques en ce qui a trait à la stabilité chimique de ces formations géologiques.

Compte tenu de ces objectifs, la précision et la justesse analytique des mesures des déséquilibres radioactifs ($^{234}U/^{238}U$) sont apparues comme la clé de la réussite d'une telle entreprise. Une grande partie des travaux a donc été consacrée à la mise au point de l'analyse des déséquilibres radioactifs à l'aide d'un spectromètre de masse à multi-collection et source plasma (MC-ICP-MS). *In fine*, une reproductibilité analytique de l'ordre de 1‰ (2 σ) pour la détermination du rapport $^{234}U/^{238}U$ sur échantillons géologiques a été obtenue.

Haute précision et justesse analytique nous ont ainsi permis de démontrer un état d'équilibre radioactif $^{234}U/^{238}U$ dans les argilites Callovo-Oxfordiennes. Ce résultat indique l'immobilité de l'uranium dans la formation cible et, par suite, atteste

d'un milieu chimiquement inactif et clos, du moins au cours de la période actuelle, pour ce qui concerne l'uranium et, par extension, les actinides naturels. Ce résultat est fondamental au regard de la problématique d'enfouissement des déchets radioactifs car il procure une confirmation *in situ* des capacités de confinement de la couche argileuse cible, dans les conditions physico-chimiques actuelles.

A contrario, des déséquilibres ($^{234}U/^{238}U$) ont été systématiquement observés au niveau de zones soumises à des processus de pression-dissolution (stylolites) dans les formations carbonatées encaissantes de l'Oxfordien et du Bathonien. Ces déséquilibres témoignent d'une remobilisation discrète de l'uranium au cours des derniers deux millions d'années et donc de processus actifs de transport de matière au sein de ces formations. La répartition isotopique de l'uranium telle qu'elle a été révélée, par un sous-échantillonnage systématique au niveau des surfaces de pression-dissolution et par la réalisation d'analyses sériées perpendiculairement à un joint stylolitique, a permis de mettre en évidence une relocalisation de l'uranium depuis la surface stylolitique vers la matrice carbonatée de part et d'autre du stylolite. Bien que soumise à des transferts de matière, une zone stylolitisée fonctionnerait en toute vraisemblance en système fermé vis-à-vis de l'uranium. Ce résultat est surprenant tant ces formations profondes, fortement compactées et peu perméables, ne semblaient pas pouvoir être sujettes à des transferts de matière significatifs à l'échelle de temps des déséquilibres U-Th. Bien qu'il soit pour l'instant difficile de conclure de façon univoque à ce sujet, il est probable que ce phénomène traduit une stylolitisation encore active, ou tout du moins, une réactivation du phénomène au cours des deux derniers millions d'années.

Abstract

This thesis forms part of the geological investigations undertaken by the French agency for nuclear waste management, ANDRA, around the Meuse/Haute-Marne Underground Research Laboratory (URL) located in the Eastern part of the Paris Basin in order to evaluate the feasibility of high-level radioactive waste repository in deep argilite formations. The aim of the study is to examine the radionuclide migration in the deep Callovo-Oxfordian target argilite layer and its surrounding low-permeability Bathonian and Oxfordian limestone formations in order to assess the long term confining capacities of the sedimentary series. This study is based on measurement of radioactive disequilibria within U-series by Multiple-Collector Inductively Coupled Plasma Mass Spectrometry (MC-ICP-MS).

The high precision and accuracy achieved allowed to demonstrate the $^{234}U/^{238}U$ radioactive equilibrium in the Callovo-Oxfordian argilites. This result shows the uranium immobility in the target formation and provides a strong evidence for the current chemical stability and closure of the system for uranium and most probably for the other actinides. This is a fundamental result with respect to the problematic of disposal of high level radioactive waste in deep geological formation since it provides a in situ indication of the confining capacities of the clayey target formation in the current settings.

Conversely, ($^{234}U/^{238}U$) disequilibria are systematically observed within zones, located in the surrounding carbonate formations, that are characterized by pressure dissolution structures (stylolites or dissolution seams). These zones display the systematic features: i) the material within the seams shows a deficit of ^{234}U over ^{238}U (($^{234}U/^{238}U$) down to 0.80) while ii) the surrounding carbonate matrix is characterized by an activity ratio greater than unity (up to 1.05). This distribution of the uranium isotopes throughout the stylolitized zones suggests a relocalization of uranium from the U-rich material within the seams into the surrounding U-low carbonate matrix. These disequilibria provide evidence for a discrete uranium relocation during the last two million years in the vicinity of stylolitic structures. This is a surprising result since it is generally supposed that these deep, low permeability, compact formations behave as closed system at the time scale of the U-series. The nature and the modalities of the driving processes responsible for these disequilibria are not clear, but, it might be possible that these disequilibria highlight an active stylolitization in the limestone formations.

Introduction

Cadre général

Cette thèse s'inscrit dans le cadre général de la caractérisation du transport en solution de matière dans la partie supérieure de la croûte continentale à l'aide des déséquilibres radioactifs au sein des familles naturelles de l'uranium et du thorium. La compréhension de la dynamique et de la modalité de ces transferts est un défi majeur posé à l'hydrogéochimie moderne. L'enjeu est de taille, deux problématiques environnementales, aujourd'hui cruciales, étant directement concernées: (i) l'évaluation, l'évolution, et la gestion, tant quantitative que qualitative, des ressources aquifères et (ii) la sûreté des stockages des déchets nucléaires en formation géologique profonde.

Dans le premier cas, l'enjeu est de développer des outils géochimiques à même de proposer des reconstitutions paléohydrologiques et/ou de préciser le temps de séjour des fluides dans un système aquifère.

Dans le second cas, il s'agit de faire la démonstration des capacités de confinement à long terme d'un site d'enfouissement de déchets radioactifs. Dans de nombreux pays, dont le Canada et la France, le stockage en formation géologique profonde des déchets de moyenne à haute radioactivité et à vie longue (déchets dits des catégories B et C) est une des voies proposées comme solution à la gestion à long terme des déchets nucléaires. Les études de "faisabilité" sont en cours et reposent sur le concept de "multi-barrières", chaque barrière (le colis, la barrière ouvragée, puis la formation géologique) ayant pour objet d'empêcher, ou tout du moins de limiter, la migration des substances toxiques vers la biosphère (Chapman et McKinley, 1987; Alexandre, 1997).

Les capacités de confinement d'un site, une fois les substances toxiques relâchées par les colis et la barrière ouvragée dans l'environnement immédiat du stockage, "le champ proche", dépendent donc *in fine* de la formation géologique, "le

champ large". La voie la plus probable de retour de la radioactivité dans la biosphère est le transfert en solution via la phase fluide du milieu. L'eau constitue donc le principal "ennemi" d'un stockage souterrain (de Marsily et al., 1977; de Marsily, 1997). Elle est d'abord acteur de la corrosion des conteneurs et de la lixiviation des radioéléments, puis vecteur du transport de ces éléments -par convection ou par diffusion moléculaire- vers la biosphère. La sûreté à long terme d'un site de stockage repose donc sur la connaissance des caractéristiques hydrogéologiques du système géologique et sur notre capacité à prédire le comportement des radionucléides, une fois ceux-ci libérés par le stockage.

Dans cette double optique -ressources aquifères et stockages géologiques- et bien que les deux types de milieux concernés soient par nature bien différents (aquifères *vs* aquicludes), l'étude des déséquilibres radioactifs au sein des familles de l'uranium et du thorium présente un intérêt tout particulier. Ces familles sont en effet un des rares outils géochimiques susceptibles de fournir des indications chronologiques sur les transferts, les éventuelles circulations fluides, actuelles ou passées, et les perturbations géochimiques engendrées par ces transferts, auxquels une formation géologique a été soumise. Cette propriété repose sur la diversité des périodes de décroissance radioactive propres aux descendants de l'uranium et du thorium qui donne ainsi accès à un large éventail d'horloges isotopiques pouvant courir jusqu'au million d'années ($T_{1/2}$ (^{234}U) = 245 250 a):

$$^{238}U \xrightarrow[4{,}469.10^{9}\,a]{\alpha} {}^{234}Th \xrightarrow[24{,}1j]{\beta} {}^{234}U \xrightarrow[2{,}445.10^{5}\,a]{\alpha} {}^{230}Th \xrightarrow[75200a]{\alpha} {}^{226}Ra \xrightarrow[1602a]{\alpha} {}^{222}Rn \ldots {}^{206}Pb$$

$$^{235}U \xrightarrow[7.13.10^{8}\,a]{\alpha} {}^{231}Th \xrightarrow[25.6h]{\beta} {}^{231}Pa \xrightarrow[32500a]{\alpha} {}^{227}Ac \ldots {}^{207}Pb$$

Nombre de ces chronomètres (on retiendra ici ^{234}U, ^{230}Th, ^{231}Pa, ^{226}Ra) sont en adéquation avec l'échelle de temps sur laquelle il est nécessaire (i) de considérer le fonctionnement dynamique d'un système aquifère à grande échelle (de l'Holocène au Pléistocène) et (ii) d'envisager la sûreté d'un site d'enfouissement de déchets

radioactifs (jusqu'au million d'années). Ces traceurs sont donc pertinents et susceptibles de compléter avantageusement la panoplie des traceurs radiochronologiques fréquemment employés en hydrogéologie (^{3}H, ^{14}C , ^{36}Cl, ^{81}Kr, voir Figure A.1.).

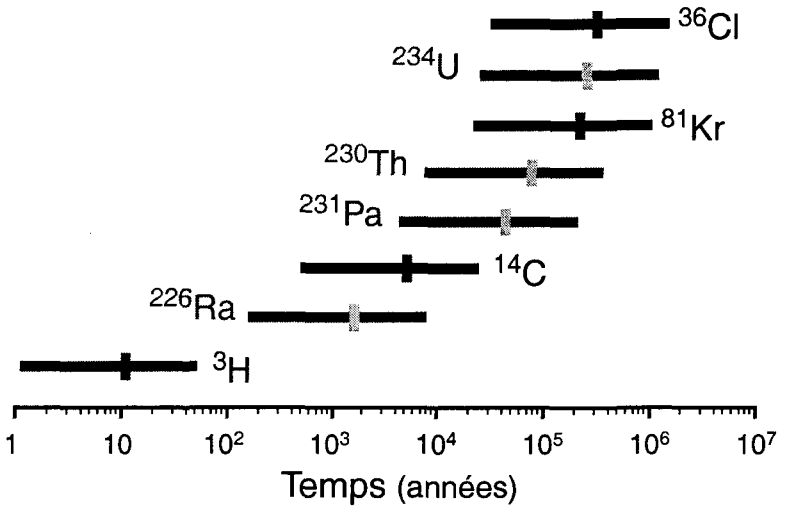

Figure A.1.: Comparaison des échelles de temps caractéristiques des différents traceurs radiochronologiques utilisés en hydrogéologie et paléohydrologie.

Applications des déséquilibres radioactifs au sein des familles U-Th à la problématique du stockage souterrain des déchets nucléaires

Dans le cadre spécifique de la problématique des déchets radioactifs et de leur enfouissement en formation géologique profonde, l'utilité de la systématique U-Th ne se limite pas à ses "propriétés chronologiques". Un intérêt, évident, de ce système géochimique réside dans la nature même des éléments chimiques constitutifs des séries U-Th. Les comportements physico-chimiques d'éléments tels que U, Th, Pa ou Ra sont en effet à rapprocher de ceux des actinides majeurs (Pu et évidemment U) et mineurs (Np, Am, Cm) présents dans les déchets ultimes (déchets de catégorie B et

C) susceptibles d'être stockés en formations géologiques profondes (voir Chapman et Smellie, 1986). L'étude *in situ* de ces éléments présents naturellement dans le système permet de mettre en évidence les processus contrôlant leur remobilisation et leur migration et, par suite, d'anticiper le comportement futur des radionucléides artificiels une fois que ceux-ci auront été libérés des colis et auront atteint le champ large. A ce titre, des gisements uranifères et/ou thoranifères, et les enveloppes d'altérations associées, constituent des analogues naturels de l'évolution à long terme d'un site de stockage et ont été étudiés afin d'illustrer la migration de ces radionucléides naturels à l'échelle géologique (Airey, 1986; Airey et Ivanovich, 1986; Chapman et Smellie, 1986; Chapman et McKinley, 1987; Chapman et al., 1992). L'existence même de ces gisements prouve que la Terre, "l'usine chimique", est non seulement capable de concentrer ces éléments (les actinides) dans un espace géologique limité, mais qu'elle a aussi la faculté de les conserver au cours des temps géologiques.

Ainsi, l'étude des déséquilibres radioactifs au sein des familles de l'uranium et du thorium permet:

- d'une part, de mettre en évidence et de caractériser les processus contrôlant la mise en solution et la migration in situ des radionucléides, et ainsi de mieux comprendre leurs comportements dans le système, en particulier à l'interface phase interstitielle/matrice;
- d'autre part, de fournir des indications tant dynamiques que chronologiques sur les processus et perturbations physico-géochimiques auxquelles la formation géologique est ou a été soumise, et qui sont à l'origine des déséquilibres radioactifs observés au sein des différentes phases constitutives de celle-ci.

C'est sur ces bases que de nombreux travaux s'appuyant sur la systématique U-Th ont été menés dans le cadre des études de faisabilité du stockage souterrain des

déchets radioactifs (voir synthèse par Ivanovich, 1991; Ivanovich et al., 1992). Ces études ont abordé spécifiquement:

- la caractérisation de la phase interstitielle, afin de préciser la mobilité des radionucléides en solution et le temps de transfert des fluides dans le système (e.g. Andrews et al., 1982; Krishnaswami et al., 1982; Andrews et al., 1989; Ivanovich et al., 1991; Krishnamoorthy et al., 1992; Luo et al., 2000; Paces et al., 2002);
- le transport des radionucléides via la phase colloïdale (e.g. Buddemeier et Hunt, 1988; Ivanovich, 1991; Vilks et al., 1991; Vilks et al., 1993; Vilks et al., 1998; voir aussi Kersting et al., 1999);
- la caractérisation et la datation de minéraux secondaires, en particulier des remplissages de fractures, afin d'apporter des éléments quant à la chronologie des circulations de fluides dans le système (e.g. Milton, 1987; Milton et Brown, 1987b; Milton et Brown, 1987a; Griffault et Shewchuk, 1994; Ivanovich et al., 1994; Pomiès, 1999; Neymark et al., 2000; Neymark et Paces, 2000; Neymark et al., 2002);
- l'état d'équilibre radioactif de la matrice hôte afin de déterminer la stabilité chimique du système ou, le cas échéant, la dynamique de la migration des radionucléides naturels au sein de celle-ci (e.g. Schwarcz et al., 1982; Smellie et Stuckless, 1985; Gascoyne et Schwarcz, 1986; Smellie et al., 1986; Gascoyne et Cramer, 1987; Griffault et al., 1993; Pomiès, 1999; Gascoyne et al., 2002).

Objectifs de la thèse

La thèse défendue ici s'inscrit dans la continuité des dernières études citées ci-dessus. L'étude des phénomènes affectant ou ayant affecté un système géologique a donc été envisagée ici sous l'angle des différentes traces -les déséquilibres radioactifs

résiduels- que ces phénomènes ont pu laisser au sein des phases solides du système (matrice et minéraux secondaires). Un des avantages de la systématique U-Th est de permettre l'étude de la dynamique d'un système non pas seulement à partir de la phase mobile, c'est à dire la phase fluide interstitielle, à laquelle les autres radiotraceurs déjà cités (^{36}Cl, ^{14}C, ^{3}H...) sont pour l'essentiel limités, mais aussi à partir des phases solides et des déséquilibres radioactifs dont elles ont hérités à la suite des transferts de matières dans le système. Cette spécificité, qui tient à l'ubiquité des radionucléides dans le système, est particulièrement intéressante dans le cadre de l'étude des milieux faiblement poreux et profonds, et donc au regard de la problématique d'enfouissement des déchets radioactifs, puisque les fluides y sont peu abondants, ou tout du moins difficilement échantillonnables dans des conditions satisfaisantes. Les déséquilibres radioactifs observés sur les phases solides résultent de processus d'interaction eau-roche capables de fractionner et de redistribuer les radionucléides entre les différentes phases du système. Ils tracent donc les processus dynamiques d'échange entre les différentes phases du milieu, faisant suite aux perturbations physico-chimiques subies par le système.

Les processus d'altération chimique accompagnant les circulations de fluides dans le système sont généralement invoqués pour expliquer la remobilisation chimique des radioéléments considérés comme les plus mobiles (e.g. U et Ra) au sein de la matrice, ou du moins au voisinage des axes d'écoulement (voir par exemple Schwarcz et al., 1982; Smellie et al., 1986; Latham et Schwarcz, 1987b; Latham et Schwarcz, 1987a; Schwarcz, 1987; Scott et al., 1992). Bien que cette relation directe entre déséquilibres radioactifs et circulations fluides mérite d'être rediscutée, l'existence de déséquilibres, si elle ne saurait être considérée comme une condition nécessaire de l'existence de transfert au sein du système, témoigne toutefois de son ouverture récente.

Cette étude s'inscrit donc dans le cadre des études de "faisabilité" du stockage des déchets radioactifs en formations argileuses menées par l'agence française pour la gestion des déchets radioactifs (ANDRA) qui en a assumé le financement et l'accès aux échantillons. Elle s'intègre aux différentes investigations entreprises sur le site expérimental Meuse/Haute-Marne de l'ANDRA, situé à Bure au sein des formations sédimentaires Mésozoïques de l'Est du bassin parisien.

Les objectifs fixés étaient:

- de déterminer l'état d'équilibre -ou de déséquilibre- radioactif vis-à-vis des radionucléides à longue période radioactive de la famille de l'uranium-238 (^{230}Th-^{234}U-^{238}U) des formations argileuses et carbonatées profondes à faible perméabilité au sein desquelles le laboratoire expérimental de l'ANDRA est en cours d'implantation;
- de caractériser, le cas échéant, les processus responsables des déséquilibres radioactifs observés et donc de la remobilisation des radionucléides dans le système;
- de préciser les implications chronologiques induites par ces résultats en ce qui a trait à la stabilité chimique des formations géologiques du système.

Organisation du mémoire de thèse

Ce mémoire s'organise en deux parties distinctes abordant dans un premier temps les aspects analytiques puis, dans un second temps, plus spécifiquement la migration des radionucléides au sein des formations sédimentaires du site ANDRA de l'Est. Il est présenté sous forme de quatre publications ou projets de publication, écrits en anglais, formant les quatre chapitres de ce mémoire. Dans la mesure où ces manuscrits sont co-signés par différents collaborateurs, il me semble important de préciser la contribution que j'ai apportée à chacun d'entre eux.

Dans la première partie, certains aspects analytiques développés au cours de ce doctorat sont abordés sous la forme de deux articles. Compte tenu des objectifs fixés dans ce doctorat, la précision et la justesse analytique des mesures des déséquilibres radioactifs est apparue comme la clé de la réussite d'une telle entreprise. Jusque là, les études ayant pour objet la caractérisation, au sein de la matrice, de la migration des radionucléides naturels s'appuyaient sur des techniques de comptage, ne garantissant ainsi qu'une faible précision analytique. Une grande partie de ce doctorat a été consacrée à la mise au point des analyses des déséquilibres radioactifs à l'aide d'une nouvelle génération de spectromètre de masse (spectromètre de masse, multi-collection, à source plasma, MC-ICP-MS). Ce développement analytique m'a permis d'obtenir une précision analytique sur le rapport $^{234}U/^{238}U$ à même de répondre aux objectifs fixés. On pourra toutefois s'étonner de ne trouver dans ce manuscrit aucune analyse isotopique du thorium (^{232}Th-^{230}Th) par MC-ICP-MS. Des difficultés d'ordre technique (non linéarité du compteur d'ion de type Daly, difficulté de calibration du gain Daly/Faraday) en sont la cause et expliquent le choix de réaliser les analyses isotopiques de l'uranium en n'utilisant que les cages de Faraday.

Le premier article, publié dans la revue *Chemical Geology* (2003, Vol. 201 (1-2), pp 141-160) sous le titre "*Further investigations on optimized tail correction and high-precision measurement of uranium isotopic ratios using multi-collector ICP-MS*", présente donc le protocole analytique que j'ai mis au point afin d'obtenir des analyses précises et justes du rapport $^{234}U/^{238}U$ par MC-ICP-MS. Ce développement analytique a été essentiel puisque c'est en s'appuyant sur ce protocole que l'ensemble des données présentées dans la Partie B ont pu être obtenues. Ce travail a été mené à bien, grâce en particulier à une collaboration étroite avec le Dr. Régis Doucelance pour ce qui concerne l'élaboration d'un modèle commun de correction de "l'effet de *tailing*", Régis travaillant plus spécifiquement sur la mise au point des analyses isotopiques du plomb. Les analyses et tests effectués, ainsi que l'écriture de l'article, sont de mon fait.

Le second manuscrit, sur lequel je figure en troisième et dernier auteur, propose une procédure de séparation et purification du radium en vue de mesures précises de cet élément par spectrométrie de masse à ionisation thermique. Cet article a été soumis à *Chemical Geology* sous le titre "*Improved method for radium extraction from environmental samples and its analysis by Thermal Ionisation Mass Spectrometry*". L'originalité de la procédure chimique revient au Dr. Bassam Ghaleb. Ma contribution à cet article concerne essentiellement l'intercalibration entre les différents traceurs utilisés (2 traceurs ^{228}Ra enrichis + 2 traceurs ^{236}U-^{233}U), ainsi que les mesures précises effectuées sur un squelette de corail (un standard interne du GEOTOP) qui ont permis de valider la justesse des mesures de ^{226}Ra. J'ai également collaboré activement à la rédaction de l'article.

Dans la seconde partie, les résultats obtenus sur les échantillons des formations sédimentaires Mésozoïques au droit du site de Bure sont présentés. Le troisième article a été soumis à la revue *Hydrology and Earth System Sciences*; il présente une partie des résultats (^{234}U/^{238}U) obtenus lors de la première partie de la thèse sur les échantillons provenant des formations carbonatées. Cette soumission a été faite sur la demande de cette revue dans le cadre d'un prix (*Young Scientist Outstanding Poster Paper award*) décerné par l'*American Geophysical Union* et l'*European Geophysical Society* pour la présentation d'un poster (Deschamps et al., 2003) lors de la réunion annuelle de ces deux associations à Nice, France, en Mai 2003.

Le quatrième et dernier article présente l'ensemble des résultats obtenus sur les échantillons du site de l'Est (formations argileuses cibles et formations carbonatées aux épontes). Il devrait faire l'objet d'une soumission à la revue *Earth and Planetary Science Letters* sous une forme réduite, la taille actuelle de l'article dépassant les critères définis par cette revue.

Pour ces deux articles, l'ensemble des analyses relèvent de ma seule responsabilité, exception faite de quatre analyses "TIMS" présentées dans le chapitre IV qui ont été réalisées en collaboration avec le Dr. B. Ghaleb. La rédaction des articles a été effectuée sous la supervision de mes deux co-directeurs de thèse, le Pr. C. Hillaire-Marcel et le Dr. J.L. Michelot, et a bénéficié de discussions avec les autres co-auteurs, le Dr. R. Doucelance, le Dr. B. Ghaleb et le Dr. S. Buschaert.

Enfin, on trouvera en annexe, enregistré sur un cédérom, un rapport bibliographique (Annexe A) qui synthétise les connaissances sur le comportement des isotopes de l'uranium dans les eaux souterraines. Ce rapport (D RP 0 UNQ 99-001) a été réalisé en 1998-1999 sous la supervision du Pr. C. Hillaire-Marcel dans le cadre d'un contrat avec l'ANDRA (Deschamps et Hillaire-Marcel, 1999). Cette étude visait à préciser l'utilité des déséquilibres radioactifs entre l'uranium-234 et son ascendant, l'uranium-238, en tant que traceur géochimique et chronomètre dans les eaux souterraines. Ce rapport dépasse la problématique spécifique du stockage des déchets nucléaires en formations géologiques et s'inscrit donc dans le cadre plus général que nous avons présenté au début de cette introduction. Un résumé détaillé, reprenant les principales conclusions du rapport, est présenté au début de cette annexe.

Deux autres annexes de taille plus réduite accompagnent ce rapport bibliographique et développent plus spécifiquement la géochimie de l'uranium en solution (Annexe B) et l'abondance de cet élément dans l'environnement (Annexe C).

Par souci de commodité, ces annexes, représentant un volume conséquent (plus de 200 pages), ont été regroupées sur un cédérom sous la forme de fichiers au format PDF. Le présent mémoire y est aussi inclu sous la forme de deux fichiers PDF, un au format *US letter*, l'autre au format A4.

Références

Alexandre, D., 1997. Conditionnement des déchéts nucléaires. In: R. Turlay (Editor), Les déchets nucléaires; un dossier scientifique. Les éditions de Physique, pp. 181-202.

Andrews, J.N., Ford, D.J., Hussain, N., Trivedi, D. et Youngman, M.J., 1989. Natural radioelement solution by circulating groundwaters in the Stripa Granite. Geochimica et Cosmochimica Acta, 53: 1791-1802.

Andrews, J.N., Giles, I.S., Kay, R.L.F., Lee, D.J., Osmond, J.K., Cowart, J.B., Fritz, P., Barker, J.F. et Gale, J., 1982. Radioelements, radiogenic helium and age relationships for groundwaters from the granites at Stripa, Sweden. Geochimica et Cosmochimica Acta, 46(9): 1533-1543.

Buddemeier, R.W. et Hunt, J.R., 1988. Transport of colloidal contaminants in groundwater; radionuclide migration at the Nevada Test Site. Applied Geochemistry, 3(5): 535-548.

Chapman, N.A. et McKinley, I.G., 1987. The geological disposal of nuclear waste. John Wiley & Sons, Chichester, United Kingdom, 280 pp.

Chapman, N.A. et Smellie, J.A.T., 1986. Natural analogues to the conditions around a final repository for high-level radioactive waste. Chemical Geology, 55(4): 167-173.

de Marsily, G., 1997. Enfouissement des déchets nucléaires en formation géologique. In: R. Turlay (Editor), Les déchets nucléaires; un dossier scientifique. Les éditions de Physique, pp. 203-246.

de Marsily, G., Barbreau, A., Ledoux, E. et Margat, J., 1977. Nuclear waste disposal; can the geologist guarantee isolation? Science, 197(4303): 519-527.

Deschamps, P. et Hillaire-Marcel, C., 1999. Bilan des connaissances sur le comportement des isotopes de l'uranium dissous en milieu réduit - Applications chronologiques. D RP 0 UNQ 99-001, ANDRA.

Deschamps, P., Hillaire-Marcel, C., Michelot, J.L., Doucelance, R. et Ghaleb, B., 2003. $^{234}U/^{238}U$ Disequilibria along sedimentary discontinuities in a deep formation: late diagenetic U-relocation processes vs. large scale fluid circulation evidence?, EGU-AGU Joint Assembly. Geophysical Research Abstract, Nice, France.

Gascoyne, M. et Cramer, J.J., 1987. History of actinide and minor element mobility in an Archean granitic batholith in Manitoba, Canada. Applied Geochemistry, 2(1): 37-53.

Gascoyne, M., Miller, N.H. et Neymark, L.A., 2002. Uranium-series disequilibrium in tuffs from Yucca Mountain, Nevada, as evidence of pore-fluid flow over the last million years. Applied Geochemistry, 17(6): 781-792.

Gascoyne, M. et Schwarcz, H.P., 1986. Radionuclide migration over recent geologic time in a granitic pluton. Chemical Geology; Isotope Geoscience Section, 59(1): 75-85.

Griffault, L.Y., Gascoyne, M., Kamineni, C., Kerrich, R. et Vandergraaf, T.T., 1993. Actinide and Rare Earth Element characteristics of deep fracture zones in the Lac du Bonnet granitic batholith, Manitoba, Canada. Geochimica et Cosmochimica Acta, 57(6): 1181-1202.

Griffault, L.Y. et Shewchuk, T.A., 1994. Permeability effects on radionuclide migration in a highly fractured zone in the Lac du Bonnet batholith, Canada. Radiochimica Acta, 66/67: 495-503.

Ivanovich, M., 1991. Aspects of uranium/thorium series disequilibrium applications to radionuclide migration studies. Radiochimica Acta, 52/53: 257-268.

Ivanovich, M., Froehlich, K. et Hendry, M.J., 1991. Dating very old groundwater, Milk River Aquifer, Alberta, Canada. Applied Geochemistry, 6; 4: 112.

Ivanovich, M., Hernandez Benitez, A., Chambers, A.V. et Hasler, S.E., 1994. Uranium series isotopic study of fracture infill materials from el Berrocal Site, Spain. Radiochimica Acta, 66/67: 485-494.

Kersting, A.B., Efurd, D.W., Finnegan, D.L., Rokop, D.J., Smith, D.K. et Thompson, J.L., 1999. Migration of plutonium in ground water at the Nevada Test Site. Nature, 397: 56-59.

Krishnamoorthy, T.M., Nair, R.N. et Sarma, T.P., 1992. Migration of radionuclides from a granite repository. Water Resources Research, 28(7): 1927-1934.

Krishnaswami, S., Graustein, W.C., Turekian, K.K. et Dowd, J.F., 1982. Radium, thorium and radioactive lead isotopes in groundwaters; application to the in situ determination of adsorption-desorption rate constants and retardation factors. Water Resources Research, 18(6): 1663-1675.

Latham, A.G. et Schwarcz, H.P., 1987a. On the possibility of determining rates of removal of uranium from crystalline igneous rocks using U-series disequilibria; 1: a U-leach model, and its applicability to whole-rock data. Applied Geochemistry, 2(1): 67-71.

Latham, A.G. et Schwarcz, H.P., 1987b. On the possibility of determining rates of removal of uranium from crystalline igneous rocks using U-series disequilibria; 2: Applicability of a U-leach model to mineral separates. Applied Geochemistry, 2(1): 67-71.

Luo, S., Ku, T.L., Roback, R., Murrell, M. et McLing, T.L., 2000. In-situ radionuclide transport and preferential groundwater flows at INEEL (Idaho); decay-series disequilibrium studies. Geochimica et Cosmochimica Acta, 64(5): 867-881.

Milton, G.M., 1987. Paleohydrological inferences from fracture calcite analyses; an example from the Stripa Project, Sweden. IApplied Geochemistry, 2; 1: 33-36.

Milton, G.M. et Brown, R.M., 1987a. Adsorption of uranium from groundwater by common fracture secondary minerals. Canadian Journal of Earth Sciences, 24(7): 1321-1328.

Milton, G.M. et Brown, R.M., 1987b. Uranium series dating of calcite coatings in groundwater flow systems of the Canadian Shield. Chemical Geology; Isotope Geoscience Section, 65(1): 57-65.

Neymark, L.A., Amelin, Y., Paces, J.B. et Peterman, Z.E., 2002. U-Pb ages of secondary silica at Yucca Mountain, Nevada: implications for the paleohydrology of the unsaturated zone. Applied Geochemistry, 17(6): 709-734.

Neymark, L.A., Amelin, Y.V. et Paces, J.B., 2000. ^{206}Pb-^{230}Th-^{234}U-^{238}U and ^{207}Pb-^{235}U geochronology of Quaternary opal, Yucca Mountain, Nevada. Geochimica et Cosmochimica Acta, 64(17): 2913-2928.

Neymark, L.A. et Paces, J.B., 2000. Consequences of slow growth for ^{230}Th/ U dating of Quaternary opals, Yucca Mountain, NV, USA. Chemical Geology, 164(1-2): 143-160.

Paces, J.B., Ludwig, K.R., Peterman, Z.E. et Neymark, L.A., 2002. 234U/238U evidence for local recharge and patterns of ground-water flow in the vicinity of Yucca Mountain, Nevada, USA. Applied Geochemistry, 17(6): 751-779.

Pomiès, C., 1999. Traçage isotopique des migrations d'uranium dans l'environnement granitique de la minéralisation uranifère de Palmottu (Sud-Ouest Finlande). Ph. D. Thesis, Université Montpellier 2.

Schwarcz, H.P., 1987. Uranium-series disequilibrium as a criterion for stability of radwaste sites. Isotope geochemistry of groundwater and fracture material in plutonic rock., 2(1): 136.

Schwarcz, H.P., Gascoyne, M. et Ford, D.C., 1982. Uranium-series disequilibrium studies of granitic rocks. Chemical geology, 36(1-2): 87-102.

Scott, R.D., MacKenzie, A.B. et Alexander, W.R., 1992. The interpretation of ^{238}U-^{234}U- ^{230}Th- ^{226}Ra disequilibria produced by rock-water interactions. Journal of Geochemical Exploration, 45(1-3): 345-363.

Smellie, J.A.T., Mackenzie, A.B. et Scott, R.D., 1986. An analogue validation study of natural radionuclide migration in crystalline rocks using uranium-series disequilibrium studies. Chemical Geology, 55(4): 233-254.

Smellie, J.A.T. et Stuckless, J.S., 1985. Element mobility studies of two drill-cores from the Goetemar Granite (Kraakemaala test site), Southeast Sweden. Chemical Geology, 51(1-2): 55-78.

Vilks, P., Caron, F. et Haas, M.K., 1998. Potential for the formation and migration of colloidal material from a near-surface waste disposal site. Applied Geochemistry, 13; 1: 31-42.

Vilks, P., Cramer, J.J., Bachinski, D.B., Doern, D.C. et Miller, H.G., 1993. Studies of colloids and suspended particles in the groundwaters of the Cigar Lake uranium deposit in Saskatchewan. In: J.F. McCarthy et F.J. Wobber (Editors),

Manipulation of groundwater colloids for environmental restoration. Lewis Publishers, Boca Raton, FL, United States, pp. 331-334.

Vilks, P., Miller, H.G. et Doern, D.C., 1991. Natural colloids and suspended particles in the Whiteshell Research Area, Manitoba, Canada, and their potential effect on radiocolloid formation. Applied Geochemistry, 6(5): 565-574.

PARTIE A:

ASPECTS ANALYTIQUES

PARTIE A: ASPECTS ANALYTIQUES

Présentation

C'est sans nul doute à la fin des années 80 que la systématique U-Th a pris un nouvel essor. Jusque là, les analyses des radionucléides à longue période de décroissance radioactive issus des séries uranium et thorium (^{238}U, ^{234}U, ^{230}Th et dans une moindre mesure ^{231}Pa, via ^{227}Ac) étaient réalisées par comptage α (Barnes et al., 1956; Rosholt et al., 1963; Condomines et Allègre, 1980; Lalou et Brichet, 1980; Allègre et Condomines, 1982; Rosholt, 1983; Condomines et al., 1988). Bien que, théoriquement, la précision accessible par les méthodes de comptage dépende du temps de comptage, les erreurs rapportées dans la littérature sur les rapports d'activité ne dépassent pas, à de rares exceptions près, 5% (2σ). Le développement des analyses isotopiques de l'uranium et du thorium à l'aide de la spectrométrie de masse à ionisation thermique (TIMS), dans les années 80, et le gain en termes de précision (0,5-1%), de temps requis pour l'analyse et de sensibilité que cette technique a permis, a largement élargi les possibilités et les champs d'application des déséquilibres radioactifs. Historiquement, l'utilisation de la thermo-ionisation pour l'analyse des séries U-Th découle des développements analytiques menés par Chen et Wasserburg (1981a; 1981b) dans le but de déterminer la composition isotopique de l'uranium ($^{238}U/^{235}U$) d'échantillons météoritiques de taille réduite (inclusions réfractaires d'Allende, minéraux phosphatés) pour lesquels les quantités d'uranium sont inférieures au picogramme. L'enjeu était alors de confirmer ou non l'existence d'anomalies isotopiques en rapport avec les radioactivités éteintes ^{244}Pu et ^{247}Cm au sein de la nébuleuse protosolaire.

La technique mise au point par l'équipe du California Institute of Technology (Caltech) permettant une efficacité d'ionisation de l'uranium de l'ordre du 1% (dépôt

sur filament simple de rhénium, utilisation de graphite comme activateur) autorisait ainsi l'analyse des déséquilibres radioactifs à l'aide de la spectrométrie de masse à ionisation thermique. Dans un premier temps, Chen et al. (1986) déterminent précisément la composition isotopique de l'uranium de l'eau de mer. Puis, L. Edwards (1988) démontre la faisabilité des analyses isotopiques de haute précision du thorium (^{230}Th-^{232}Th) par TIMS et, par suite, de celles de la chaîne ^{238}U-^{234}U-^{230}Th . Comparativement à la spectrométrie α, la technique de l'équipe du Caltech améliore la précision analytique d'un facteur 10 et diminue dans les mêmes proportions les quantités d'échantillons nécessaires (Chen et al., 1992).

C'est donc à partir de ce développement analytique majeur que la systématique U-Th va connaître une nouvelle impulsion aboutissant en très peu de temps à des avancées déterminantes tant dans le domaine de la paléoclimatologie que dans celui des processus magmatiques (voir par exemple Goldstein et al., 1989; Goldstein et al., 1991; Chabaux et Allègre, 1994). En particulier, la datation U-Th maintenant extrêmement précise des coraux a permis i) de déterminer les variations du niveau marin et ainsi de rediscuter, en relation avec la théorie de Milankovitch, les variations climatiques de la Terre au cours du Quaternaire (Edwards et al., 1987a; Edwards et al., 1987b; Bard et al., 1990a), ou bien ii) de mettre en évidence, puis de déterminer les variations du taux de production du ^{14}C dans l'atmosphère (Bard et al., 1990b). Depuis ces premiers travaux, de nombreuses autres contributions significatives s'appuyant sur la spectrométrie de masse à ionisation thermique ont vu le jour. A titre d'exemple, on citera: la datation précise du stade isotopique 5e (e.g. Stein et al., 1991; Hillaire-Marcel et al., 1996) ou la reconstitution de paléoclimats continentaux grâce à la datation de dépôts endokarstiques (e.g. Ludwig et al., 1992; Winograd et al., 1992).

L'amélioration constante des spectromètres de masse à ionisation thermique, ainsi que l'avènement, depuis la fin des années 90, d'une nouvelle génération de spectromètre de masse à source plasma (MC-ICP-MS), font qu'aujourd'hui la reproductibilité analytique obtenue, par certains laboratoires, sur les rapports $^{230}Th/^{234}U$ et $^{234}U/^{238}U$ est respectivement de l'ordre de 2 ‰ et 1‰, aussi bien par TIMS (e.g. Cheng et al., 2000; Delanghe et al., 2002) que par MC-ICP-MS (e.g. Luo et al., 1997; Stirling et al., 2001; Henderson, 2002; Pietruszka et al., 2002; Robinson et al., 2002; Shen et al., 2002). L'obtention de telles précisions et reproductibilités analytiques a souvent été le fruit de long travaux de mise au point, tant de la part des manufacturiers que des utilisateurs, travaux ayant fait par la suite l'objet de nombreuses publications.

C'est dans ce cadre qu'il faut replacer l'article qui constitue le premier chapitre de cette thèse. Cet article, publié dans la revue *Chemical Geology* (2003, Vol. 201(1-2), pp 141-160) sous le titre "*Further investigations on optimized tail correction and high-precision measurement of uranium isotopic ratios using multi-collector ICP-MS*", développe le protocole analytique mis au point afin de réaliser des analyses hautement précises et justes du rapport $^{234}U/^{238}U$ sur un spectromètre de masse, multi-collection, à source plasma, de type Isoprobe™. Le choix initial, qui avait été fait au GEOTOP de réaliser les analyses isotopiques de l'uranium sur cages de Faraday, a conduit au développement d'un modèle de correction de "l'effet de *tailing*" dû à la faible sensibilité en abondance de cet instrument (de l'ordre de 25 ppm). Le protocole mis au point a permis d'obtenir une reproductibilité de l'ordre du 1‰, tant sur standard (NBS 960) que sur échantillons géologiques, la justesse des mesures étant validée par l'excellent accord entre la valeur proposée pour le standard NBS 960 et celles publiées récemment dans la littérature (voir Figure I.5). Cette partie de la thèse revêt un aspect essentiel puisqu'elle est la base sur laquelle s'appuient l'ensemble des résultats présentés dans la partie 2.

Le second chapitre présente une contribution soumise à la revue *Chemical Geology* sous le titre "*Improved method for radium extraction from environmental samples and its analysis by Thermal Ionisation Mass Spectrometry*". Ce manuscrit décrit une procédure originale de séparation et de purification du radium d'échantillons géologiques, développé au GEOTOP et à laquelle j'ai contribuée. Contrairement à l'uranium et au thorium, la préparation chimique, en particulier à partir de matrices carbonatées, est encore problématique et constitue un facteur limitant en ce qui a trait à de la précision analytique obtenue par spectrométrie de masse à ionisation thermique. Le protocole analytique proposé ici permet d'améliorer significativement l'efficacité totale d'ionisation du radium et donc, *in fine*, la précision analytique.

Références

Allègre, C.J. et Condomines, M., 1982. Basalt genesis and mantle structure studied through Th-isotopic geochemistry. Nature (London), 299(5878): 21-24.

Bard, E., Hamelin, B. et Fairbanks, R.G., 1990a. U-Th ages obtained by mass spectrometry in corals from Barbados; sea level during the past 130,000 years. Nature (London), 346(6283): 456-458.

Bard, E., Hamelin, B., Fairbanks, R.G. et Zindler, A., 1990b. Calibration of the ^{14}C timescale over the past 30,000 years using mass spectrometric U-Th ages from Barbados corals. Nature (London), 345(6274): 405-410.

Barnes, J.W., Lang, E.J. et Potratz, H.A., 1956. Ratio of ionium to uranium in coral limestone. Science, 124(3213): 175-176.

Chabaux, F. et Allègre, C.J., 1994. ^{238}U-^{230}Th-^{226}Ra disequilibria in volcanics; a new insight into melting conditions. Earth and Planetary Science Letters, 126(1-3): 61-74.

Chen, J.H., Edwards, R.L. et Wasserburg, G.J., 1986. ^{238}U, ^{234}U and ^{232}Th in seawater. Earth and Planetary Science Letters, 80(3-4): 241-251.

Chen, J.H., Edwards, R.L. et Wasserburg, G.J., 1992. Mass spectrometry and applications to uranium-series disequilibrium. In: M. Ivanovich et R.S. Harmon (Editors), Uranium-series disequilibrium; applications to earth, marine, and environmental sciences. Clarendon Press, Oxford, United Kingdom, pp. 174-206.

Chen, J.H. et Wasserburg, G.J., 1981a. The isotopic composition of uranium and lead in Allende inclusions and meteoritic phosphates. Earth and Planetary Science Letters, 52(1): 1-15.

Chen, J.H. et Wasserburg, G.J., 1981b. Isotopic determination of uranium in picomole and subpicomole quantities. Analytical Chemistry, 53: 2060-2067.

Cheng, H., Edwards, R.L., Hoff, J., Gallup, C.D., Richards, D.A. et Asmerom, Y., 2000. The half-lives of Uranium-234 and Thorium-230. Chemical Geology, 169(1-2): 17-33.

Condomines, M. et Allègre, C.J., 1980. Age and magmatic evolution of Stromboli Volcano from (super 230) Th- (super 238) U disequilibrium data. Nature (London), 288(5789): 354-357.

Condomines, M., Hemond, C. et Allègre, C.J., 1988. U-Th-Ra radioactive disequilibria and magmatic processes. Earth and Planetary Science Letters, 90(3): 243-262.

Delanghe, D., Bard, E. et Hamelin, B., 2002. New TIMS constraints on the uranium-238 and uranium-234 in seawaters from the main ocean basins and the Mediterranean Sea. Marine Chemistry, 80(1): 79-93.

Edwards, R.L., 1988. High precision thorium-230 ages of corals and the timing of sea level fluctuations in the late Quaternary. Ph.D. Thesis, California Institute of Technology, Pasadena, United States.

Edwards, R.L., Chen, J.H., Ku, T.L. et Wasserburg, G.J., 1987a. Precise timing of the last interglacial period from mass spectrometric determination of thorium-230 in corals. Science, 236(4808): 1547-1553.

Edwards, R.L., Chen, J.H. et Wasserburg, G.J., 1987b. ^{238}U-^{234}U-^{230}Th-^{232}Th systematics and the precise measurement of time over the past 500,000 years. Earth and Planetary Science Letters, 81(2-3): 175-192.

Goldstein, S.J., Murrell, M.T. et Janecky, D.R., 1989. Th and U isotopic systematics of basalts from the Juan de Fuca and Gorda ridges by mass spectrometry. Earth and Planetary Science Letters, 96(1-2): 134-146.

Goldstein, S.J., Murrell, M.T., Janecky, D.R., Delaney, J.R. et Clague, D.A., 1991. Geochronology and petrogenesis of MORB from the Juan de Fuca and Gorda ridges by ^{238}U-^{230}Th disequilibrium. Earth and Planetary Science Letters, 107(1): 25-41.

Henderson, G.M., 2002. Seawater ($^{234}U/^{238}U$) during the last 800 thousand years. Earth and Planetary Science Letters, 199(1-2): 97-110.

Hillaire-Marcel, C., Gariepy, C., Ghaleb, B., Goy, J.L., Zazo, C. et Barcelos, J.C., 1996. U-series measurements in Tyrrhenian deposits from Mallorca; further evidence for two last-interglacial high sea levels in the Balearic Islands. Quaternary Science Reviews, 15(1): 53-62.

Lalou, C. et Brichet, E., 1980. Anomalously high uranium contents in the sediment under Galapagos hydrothermal mounds. Nature (London), 284(5753): 251-253.

Ludwig, K.R., Simmons, K.R., Szabo, B.J., Winograd, I.J., Landwehr, J.M., Riggs, A.C. et Hoffman, R.J., 1992. Mass-spectrometric ^{230}Th-^{234}U-^{238}U dating of the Devils Hole calcite vein. Science, 258(5080): 284-287.

Luo, X., Rehkämper, M., Lee, D.C. et Halliday, A.N., 1997. High precision $^{230}Th/^{232}Th$ and $^{234}U/^{238}U$ measurements using energy-filtered ICP Magnetic Sector Multi-Collector mass spectrometry. International Journal of Mass Spectrometry and Ion Processes, 171: 105-117.

Pietruszka, A.J., Carlson, R.W. et Hauri, E.H., 2002. Precise and accurate measurement of ^{226}Ra-^{230}Th-^{234}U disequilibria in volcanic rocks using plasma ionization multicollector mass spectrometry. Chemical Geology, 188(3-4): 171-191.

Robinson, L.F., Henderson, G.M. et Slowey, N.C., 2002. U-Th dating of marine isotope stage 7 in Bahamas slope sediments. Earth and Planetary Science Letters, 196(3-4): 175-187.

Rosholt, J.N., 1983. Isotopic composition of uranium and thorium in crystalline rocks. Journal of Geophysical Research. B, 88(9): 7315-7330.

Rosholt, J.N., Shields, W.R. et Garner, E.L., 1963. Isotopic fractionation of uranium in sandstone. Science, 139(3551): 224-226.

Shen, C.-C., Edwards, L.R., Cheng, H., Dorale, J.A., Thomas, R.B., Bradley, M., S., Weinstein, S.E. et Edmonds, H.N., 2002. Uranium and thorium isotopic and concentration measurements by magnetic sector inductively coupled plasma mass spectrometry. Chemical Geology, 185(3-4): 165-178.

Stein, M., Wasserburg, G.J., Lajoie, K.R. et Chen, J.H., 1991. U-series ages of solitary corals from the California coast by mass spectrometry. Geochimica et Cosmochimica Acta, 55: 3709-3722.

Stirling, C.H., Esat, T.M., Lambeck, K., McCulloch, M.T., Blake, S.G., Lee, D.C. et Halliday, A.N., 2001. Orbital forcing of the marine isotope stage 9 interglacial. Science, 291: 290-293.

Winograd, I.J., Coplen, T.B., Landwehr, J.M., Riggs, A.C., Ludwig, K.R., Szabo, B.J., Kolesar, P.T. et Revesz, K.M., 1992. Continuous 500,000-year climate record from vein calcite in Devils Hole, Nevada. Science, 258(5080): 255-260.

Chapitre I

Further investigations on optimized tail correction and high-precision measurement of Uranium isotopic ratios using Multi-Collector ICP-MS

Pierre Deschamps, Régis Doucelance, Bassam Ghaleb and Jean-Luc Michelot

Chemical Geology, 2003, 201 (1-2), page 141-160

Abstract

In the present paper, we further examine the optimum conditions for rapid, precise and accurate determination of $^{234}U/^{238}U$ ratios in geological materials by multiple-collector (magnetic-sector) inductively coupled plasma mass spectrometry (MC-ICP-MS). In our experiments, isotopic measurements were performed on a Micromass IsoProbe™ instrument, using Faraday collectors in static mode only. Unlike the ion counting system coupled with an energy filter, this technique eliminates the difficulty of proper calibration of the Daly/Faraday gain ratio. On the other hand, since our Micromass instrument has a poor abundance sensitivity (the proportion of the ^{238}U ion beam measured at mass 237 is ~25 ppm), the major issue to be addressed is the tail correction. For this purpose, we have developed a tail correction method slightly modified from Thirlwall (2001). This method is based on correction of the actual tail contribution under each peak, as assessed by the tail shape measurements on mono-isotopic ion beams, instead of the usual half-mass zeroes baseline estimation. Our approach enabled us to correct for the large offset that can be observed on isotopic data when tail correction is done by means of linear interpolation between half-mass zeroes, and showed that this latter tail correction method results in nearly 3%

underestimation of $^{234}U/^{238}U$ ratios on the GEOTOP IsoProbe™ for material at secular equilibrium.

A ^{236}U-^{233}U double spike was employed to correct for mass discrimination bias. Using an Aridus™ micro-concentric, desolvating nebulizer sample introducing system, a minimum of 200 ng of sample-U was consumed to carry out a precise $^{234}U/^{238}U$ analysis, thereby allowing a ^{234}U signal of ~4-5 mV to be monitored for 50 measurement cycles of 5 seconds each. This time-consuming, 10-minute procedure allowed us to obtain an external reproducibility of 0.8‰ (2σ) for isotopic measurements of the NBL-112a standard solution. Replicate measurements of this reference material yielded a mean $\delta^{234}U$ value of -36.42±0.80‰ (2σ, n = 19), which is highly consistent with values reported by other laboratories. The total reproducibility, including both chemical separation and spectrometric measurement, was assessed using geological samples (a coral and a carbonate rock); the long-term reproducibility obtained was about 1.3‰ (2σ).

Keywords: Uranium Isotopes; Multiple-Collector ICP-MS; Tail correction; Standard; Accuracy; Precision

I.1. Introduction

Multiple collector inductively coupled plasma mass spectrometry (MC-ICP-MS) has proved to be a powerful tool for high-precision measurement of isotopic compositions, leading to a wide array of new applications in Earth and planetary sciences and cosmochemistry (Halliday et al., 1998).

This technique has been successfully used for precise measurements of U and Th isotopic compositions (Luo et al., 1997; Stirling et al., 2000; Stirling et al., 2001; Henderson, 2002; Robinson et al., 2002; Shen et al., 2002). MC-ICP-MS, and more generally, ICP sources, have several advantages over conventional thermal ionization mass spectrometry (TIMS), which many other studies have already reported (e.g. Halliday et al., 1998; Stirling et al., 2000):

- The plasma source yields a very high ionization efficiency (>90%) of nearly all elements having a low first ionization potential (Jarvis et al., 1992; Taylor, 2001);
- Ionization efficiency is not a function of load size;
- To a first approximation, the mass discrimination is time-independent during data acquisition, since fresh aerosol sample is continuously introduced into the ICP;
- Fewer chemical steps are needed during sample preparation.

Nevertheless, MC-ICP-MS has two major drawbacks not encountered in TIMS with respect to U(-Th) isotopic analysis: i) high plasma-generated ion source instability (Shen et al., 2002); and ii) poor abundance sensitivity of some instruments (Thirlwall, 2001). The abundance sensitivity is a parameter that allows the estimation of the magnitude of the tail contribution, and is usually defined as the proportion of ^{238}U ion beam measured at mass 237 (Chen et al., 1992; Thirlwall, 2001). Because of the large atom ratios encountered in the U(-Th) systematics (for example, the

$^{238}U/^{234}U$ atom ratio is close to 18,200 for a sample in secular equilibrium), the tail effect may limit the analytical accuracy (see discussion in Chen et al., 1992). With TIMS analyses, this problem is generally circumvented by using a Daly detector coupled with an energy filter: electrostatic (ESA), Retarding Potential Quadripole (RPQ) or Wide Aperture Retarding Potential (WARP) filter (Edwards, 1988; Chen et al., 1992; Cheng et al., 2000; Rubin, 2001). With such a system, abundance sensitivity is greatly improved to <<1ppm, and the remaining tail contribution is corrected by using a linear interpolation between half-mass zeroes. The stable thermal-generated ion source allows an analysis in magnet-controlled peak jumping mode on a single detector placed behind the energy filter.

In MC-ICP-MS, the high instability of the ion beam produced by the plasma source makes this approach impractical. Depending on the instrument, different protocols were adopted to overcome this problem.

In this paper, we outline and discuss the advantages and limitations of the technique we developed for precise measurement of uranium concentration and isotopic composition using a Micromass IsoProbe™ MC-ICP-MS instrument. In contrast to what other MC-ICP-MS users have done (Luo et al., 1997; Robinson et al., 2002; Shen et al., 2002), we used Faraday detectors in static mode only. This strategy obviates many of the problems related to gain calibration of the Daly-Faraday detectors. However, since we did not use a Daly detector and the energy filter normally coupled with it, the tail contribution induced by the high abundance sensitivity of the instrument (~25 ppm) proved to be a critical bias. We addressed this issue following an approach slightly modified from Thirlwall (2001).

In the forthcoming sections, we outline the general protocol used to optimize correction for significant tailing effects. We also describe the entire mass spectrometric procedure that can be used with an IsoProbe™ MC-ICP-MS instrument for precise measurement of $^{234}U/^{238}U$ ratios. Finally, based on measurements of

standard reference materials and geological samples (corals and limestones), we address the issue of the overall analytical precision and accuracy that can be achieved using this technique.

I.2. Overview of current procedures for U isotopic analysis by ICP-MS

Using a VG Elemental Plasma 54™ MC-ICP-MS instrument, Luo et al. (1997) proposed to perform U(-Th) analyses by combining Faraday cups and a Daly detector coupled with an energy filter, either in static or in multi-static mode. Since Faraday and Daly detectors are used simultaneously, their relative gain must be carefully determined in order to achieve maximum precision and accuracy. Two data acquisition protocols were developed. They differ in the way variations in the relative Faraday/Daly gain are monitored. With the static procedure, it is determined externally by a standard bracketing method. With the multi-static procedure, the relative Faraday/Daly gain is monitored and calibrated during the sample analysis by comparing the results of two sequential $^{235}U/^{238}U$ measurements with two different collector configurations (Daly/Faraday and Faraday/Faraday). Luo et al. (1997) and Stirling et al. (2000) argued that the latter approach is superior even though it requires slightly larger sample sizes and is more time-consuming. Because a Daly detector coupled with an energy filter is used to measure the minor mass (^{234}U), the contribution of the tail effect underneath this peak may be considered negligible or, at least, well corrected for by the linear interpolation between half-mass zeroes.

Using a Nu™ MC-ICP-MS, Robinson et al. (2002) proposed to perform measurements in static mode on Faraday collectors for major peaks and on an ion counting channel for the minor peak (^{234}U). In contrast to observations made on the Daly detector of the Plasma 54™ instrument (Luo et al., 1997) and our IsoProbe™ instrument, the relative gain between the ion counting channel and the Faraday cups

remains constant throughout an analysis with the Nu™ collector system, so that no internal drift correction is required. However, because the ion counting channel is not coupled with an energy filter, abundance sensitivity is in the order of 5 ppm at 1 amu. With this instrument, this causes an offset of <0.5‰ to the measured $^{235}U/^{234}U$ ratio (Robinson et al., 2002). Robinson et al. (2002) argued that the standard bracketing measurement procedure they followed corrects not only for the relative gain between Faraday cups and the ion counting channel, but for this tail offset as well. This means that all sample measurements are taken with reference to a given standard, in this case, CRM-145, and that one makes the assumption that the system behaves linearly. They assessed the validity of their approach by comparing analyses of the CRM-145 standard (also called NBL-112a, NIST-4321, and formerly U-960 or NBS SRM-960) with analyses of the Harwell uraninite (HU-1), which Cheng et al. (2000) have shown to be in secular equilibrium for the ^{238}U-^{234}U sequence.

Using a sector-field ICP-MS equipped with a single electron multiplier, Shen et al. (2002) also performed a precise, accurate U-Th isotopic analysis. Their approach obviates many of the problems associated with the intercalibration of ion-counting and Faraday detectors, but requires (i) that the error introduced by source instabilities be minimized; and (ii) more particularly, that the tail correction problem be addressed. The first problem is overcome by installing a guard electrode (GE) sheath around the torch and by employing a rapid peak switching method. The second problem requires precise determination of the tail shape between each mass. Furthermore, the intensity bias inherent in the electron multiplier (see also Cheng et al., 2000) must be corrected for. The correction value is determined once a day by comparing the CRM-145 measured $\delta^{234}U$ with its accepted value. In much the same way as the experiments conducted by Robinson et al. (2002), this protocol requires that all sample analyses be done with reference to a standard sample.

I.3. Experimental procedure used for U-isotope measurements

I.3.1. Instrumentation and data acquisition

All the results presented here were obtained using a Micromass IsoProbe™ MC-ICP-MS at the GEOTOP-UQAM-McGILL Research Center from July 2001 to May 2002. The instrument is similar to that used by Thirlwall (2001; 2002). It is equipped with an array of nine Faraday cups with 10^{11} Ω positive feedback resistors, two ion counting detectors (Channeltron) and a Daly ion counting system inserted immediately behind a retarding filter (WARP).

Table 1 : Collector configuration for U isotopic analysis on the GEOTOP IsoProbe™ MC-ICP-MS

Collector	Axial	High 1	High 2	High 3	High 4	High 5	High 6
Uranium	-	^{233}U	^{234}U	^{235}U	^{236}U	(237)	^{238}U

The U isotopic data are acquired in static multicollection mode by means of Faraday collectors with cup efficiencies set at unity. The Faraday amplifier gain is calibrated daily before the analytical session. Ignition of the plasma and application of the accelerating high voltage is followed by a warm-up period of about 90 min. Collectors are aligned H1: mass 233 to H6: mass 238, using the configuration shown in Table 1. For uranium isotopic determinations, since the ^{234}U ion beam has to be measured on a Faraday cup with a minimum intensity of ~4-5 mV, the ^{238}U beam would exceed 80 V for a sample assumed to be in secular equilibrium for the ^{238}U-^{234}U sequence. This greatly exceeds the capacity of Faraday cups equipped with a 10^{11} Ω resistor. In such cases, the H6 detector is moved away from the ^{238}U beam in order to avoid any beam collection. However, this collector is occasionally used to determine U concentration in low U-content samples as well as to conduct specific tests (for instance, spike calibration). Abundance sensitivity, usually defined as the proportion of the ^{238}U ion beam tail measured at mass 237, is monitored online during each analysis from H5 output, with H5 set for mass 237. The ^{238}U intensity is

calculated from the ^{235}U ion beam (H3) using the natural $^{238}U/^{235}U$ ratio of 137.88 (see section 4.2). A double spike (^{236}U-^{233}U) with a ratio of ≈ 0.7 is used to correct for mass discrimination. The measured isotope ratios are then normalized using a linear law (see section 5.2.). In general, samples are spiked so that the resulting $^{235}U/^{233}U$ and $^{233}U/^{234}U$ ratios are close to 11, thereby optimizing dynamic range and precision.

All measurements are performed using a high-efficiency desolvating microconcentric nebulizer system, the ARIDUS MCN 6000™. The sweep gas (Ar and N_2) settings are optimized to maximize the sensitivity and minimize oxide levels. The uptake rate of the nebulizer is kept constant at ~50 µl/min. Under such conditions, a 6-7 ppb ^{238}U solution generates a signal over 1 V. The total sensitivity, combining ionization with MS transmission efficiencies, is about 5%. Argon flows are set at ~15.0 l/min for the cool gas, at ~1.03 l/min for the intermediate gas and at ~0.90-0.99 l/min for the nebulizer gas.

The sample is introduced into the mass spectrometer in a 2% HNO_3 solution. The inlet system is cleaned with 4% HNO_3 followed by 2% HNO_3 between sample runs until a negligible U background is achieved (see section 3.2.). Depending on the cleanliness of the nebulizer, the washout procedure requires from 10 to 20 min. The first step of the data acquisition procedure consists of a 1-min measurement of the electronic backgrounds of each Faraday cup, subsequently defined as the Mass Spectrometer Background (MSB), with no ion beam (valve off) in the analyzer, in order to determine the amplifier drifts. After the valve (LOS) is opened, the "on-peak zero" baseline (OPZ) is measured for 1 min with the same 2% HNO_3 batch solution that was used to dilute samples. Finally, samples are analyzed for one block of 50 scan cycles with a 5 s integration time per cycle. A routine analytical procedure time is around 10 min. With this protocol, the amount of U consumed per analysis is at least 200 ng. This produces a signal of ~1 V for ^{235}U and >0.005 V for ^{234}U (for samples close to ^{238}U-^{234}U secular equilibrium).

Raw signal intensities are corrected for resistor gains only. They are then transferred to an Excel spreadsheet for further offline cycle-by-cycle manipulations (correction for OPZs, tailing and mass discrimination).

I.3.2. Accuracy and background

In the Excel spreadsheet, the on-peak zeroes (OPZs), determined before sample acquisition, are subtracted from sample peak intensities to correct for: i) amplifier drifts; ii) U in the blank solution; iii) U memory effect in the inlet system; and iv) potential isobaric interferences that may be associated with the 2% HNO_3 solution. The OPZ correction significantly controls the precise determination of the small ^{234}U signal and thus the accuracy of U isotopic measurements. The effect of MS backgrounds and absolute on-peak zero (OPZ_{abs}) intensities (estimated by subtracting the MSB from OPZ) on accuracy and precision are discussed separately in the next sections.

I.3.2.1. MS Background

Daily variations in the electronic background (MSB) were monitored during 64 seconds on each Faraday cup throughout the first step of the sample analytical procedure. These were around 20-30 μV (2σ; $n\approx20$ analysis per day) depending on the day of analysis. However, a general drift was observed on all the Faraday cup baselines in the course of a day, demonstrating that, to a first approximation, the electronic backgrounds monitored on each cup co-varied with time. This phenomenon might be associated with temperature fluctuations of the system (MC-ICP-MS, room temperature).

We define dark noise here as the fluctuation around this first-order drift. This noise is below 10 μV (2σ) for the MSB measurements of each Faraday cup, based on a 64-second integration time. Included in this value is the intrinsic error associated

with the amplifier noise (see discussion in Ludwig, 1997), and also the error related to the drift in the amplifier background, during the integration. This value represents the actual irreproducibility associated with the background correction. It also provides an estimate of the limits, in terms of precision and accuracy, that can be achieved on the GEOTOP IsoProbe™. Thus, in order to obtain an external reproducibility and an internal precision of 1 to 2‰ on each measured ratio, the signal/dark noise ratio must be equal to or greater than 500 for each ion beam. For the minor isotope (^{234}U), this requires monitoring a signal intensity of at least 5 mV. Under such conditions, baseline variations occurring during data collection will not affect signals measured within the desired level of precision. However, large fluctuations we observed within a day made it necessary to monitor the MS background during each analysis.

I.3.2.2. Absolute OPZ values

The OPZ_{abs} values give direct indications about the U content in the blank solution, U-memory effects in the inlet system and potential isobaric contributions. The 2% HNO_3 blank solution is prepared with ultra-pure reagents and is identical to the blank solution used to dilute samples and standards. Theoretically, this should make it possible to thoroughly correct for any U contamination present and to avoid any change in the acid molarity that could remove additional U from the inlet system (Thirlwall, 2002). During our U isotopic measurements, constant contamination associated with the 2% HNO_3 remained undetectable on ^{235}U and thus, *a fortiori*, on ^{234}U.

Concerning sample cross-contamination, a longer washout time (up to 20 min) is sometimes required between two successive analyses in order to make OPZ_{abs} values negligible in comparison with signal intensities (i.e., signal/OPZ_{abs} >> 500). Memory effects do not appear to be directly related to the most recent sample intensity. In practice, for uranium isotopic determinations, data acquisition is initiated when measured OPZs do not differ from MS background values for masses 233, 234

and 236 within the range of dark noise irreproducibility (i.e., -20 μV < OPZ_{abs} < 20 μV , where OPZ_{abs} = OPZ - MBS). With respect to ^{235}U measurement, the analysis criterion is that the OPZ_{abs} value on H3 remains < 50 μV. However, while memory effects are well constrained using the suggested cleaning procedure for routine $^{234}U/^{238}U$ isotopic measurements, they remain a serious problem for standards such as U-500 or NBL-117, as well as for tests and spike analyses that require monitoring ^{238}U ion beams. In fact, such standard or spike solutions have $^{238}U/^{235}U$ ratios (e.g., $^{238}U/^{235}U \approx 1$, for NBL-117 and U-500) that are very different from natural uranium ($^{238}U/^{235}U$ = 137.88). During such analyses, any variations in the uranium baseline from the OPZ measurement will cause significant inaccuracies in the final results.

No isobaric interferences were observed on the monitored masses of uranium. If there were any, they remained within the dark noise range. However, we identified a substantial constant interference on mass 237, with an OPZ_{abs} significantly higher than the MS background (OPZ_{abs}(mass 237) ≈ 60 to 100 μV). This suggests a mono-isobaric interference, which might be associated with the presence of Au (gold coating of the hexapole ion guide, cf. Rehkämper and Mezger, 2000) and Ar in the inlet system.

I.4. The tailing contribution

I.4.1. The half-mass zero estimation of the baseline

Correction for tail from adjacent peaks onto a given mass is commonly done by subtracting values interpolated from signals measured at half-mass positions (±0.5 amu) from the peak to be corrected (Chen et al., 1986; Edwards et al., 1987). This approach has the advantage of an online correction of the tailing contribution, but also has two major drawbacks. First, each peak is corrected for its own tailing. Second, because the tail profile has a negative curvature, linear interpolation between half-mass backgrounds overestimates the actual tail contribution under the peak. This

problem was first reported by Chen et al. (1986) and Bard et al. (1990) for U/Th analyses. Bard and co-workers (1990) have shown that the linear tailing correction is no longer appropriate for U-Th TIMS analyses when abundance sensitivity increases due to vacuum deterioration. They proposed a parabolic interpolation to correct for the total tail contribution under the ^{234}U and ^{235}U peaks. Nevertheless, they acknowledged that this parabolic fit was not able to correct properly for tailing biases under the ^{236}U peak. Shen et al. (2002) also used the log-mean of the signals measured at half-masses to subtract tail contribution from ^{233}U, ^{234}U and ^{235}U intensity beams. However, they showed that this calculation was no longer appropriate for mass 236 because of the significant contribution of the ^{235}U peak, superimposed on the major ^{238}U tailing, over the mass interval 235.5 - 236.5. They therefore established an empirical formula, which was a function of the signal measured at mass 236.5, to estimate the total tail contribution at mass 236.

When applied to our IsoProbe™ MC-ICP-MS data, the linear and exponential interpolation result in a systematic offset, which is illustrated by $\delta^{234}U$ values of -26‰ and -15‰, respectively, for the Harwell uraninite standard (see Fig. I.1 and section 6.1 for more details) instead of the expecteed value for secular equilibrium, $\delta^{234}U = 0$‰ (Ludwig et al., 1992; Cheng et al., 2000). This large offset is due to the poor abundance sensitivity (~25 ppm) of the GEOTOP IsoProbe MC-ICP-MS. Below, we will show that with this instrument, even exponential corrections (i.e., the log-mean of the signals measured at half-mass positions) overestimate the real tail contribution.

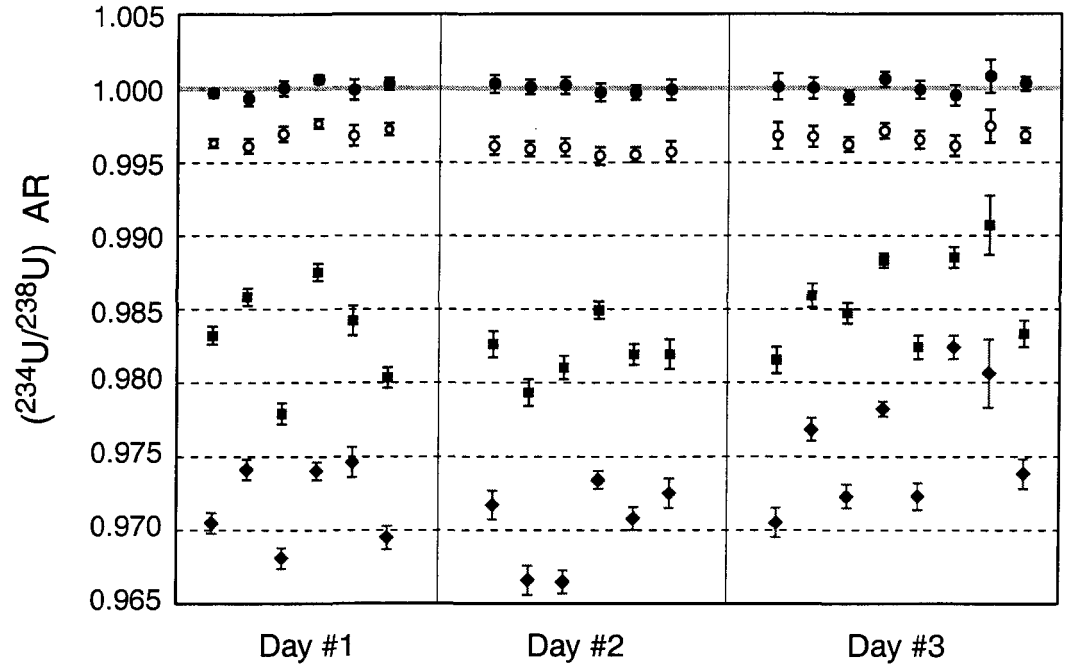

Figure I.1.: Repeated analyses of the ($^{234}U/^{238}U$) activity ratio of the HU-1 uraninite conducted on the Micromass IsoProbe™ MC-ICP-MS instrument over a 3-day analytical run. Results obtained using a tail correction based either on linear (filled diamonds) or exponential (filled squares) interpolation of half-mass zeroes are compared with results obtained using the tail correction method we developed (circles). The latter approach is based on the actual, precise quantification of tail contributions underneath each peak due to adjacent ion beams, as assessed by tail shape measurements on mono-isotopic ion beams. Blank circles refer to the correction which is done when the measured tail shape only is used; filled circles refer to results obtained by this same model using the tail shape corrected according to the θ coefficient (see full explications in the text).

I.4.2. The tail correction method

The method that we finally retained for tail correction is based on the actual, precise quantification of tail contributions underneath each peak due to adjacent ion beams. Thirlwall (2001; 2002) used the same method for optimizing tail corrections on MC-ICP-MS instruments with poor abundance sensitivity, such as the IsoProbe™. He

showed, for example, that for high-precision Pb isotope measurements, his method corrects for discrepancies of up to ~700 ppm relative to the standard half-mass zero correction for the $^{208}Pb/^{206}Pb$ ratio on the NIST SRM-982 reference standard (Thirlwall, 2001).

Our approach requires precise determination of the tail profile on both sides of a mono-isotopic peak in an array of several atomic mass units (amu). This is accomplished by measuring mono-isotopic solutions within the mass range of the element of interest (see section 4.3). The total tail under a given peak then becomes the sum of contributions from all adjacent peaks. This can be mathematically formalized by:

$$I^{m}_{Tailcor} = I^{m}_{Measured} - \sum_{\substack{i=-5 \\ i\neq 0}}^{+3} Z_i \times I^{m-i}_{Tailcor} \qquad (S)$$

where $I^{m}_{Tail\,cor}$ is the tail-corrected beam intensity on mass m, $I^{m}_{Measured}$ is the measured beam intensity, and Z_i is the proportional tail, expressed in ppm, at i amu away from a mono-isotopic peak. This expression is similar to that proposed by Thirlwall (2001), but it dispels one ambiguity. From a theoretical point of view, one must consider the tail-corrected beam intensity in the right part of the expression (S). In the equation proposed by Thirlwall (2001), it is unclear whether the tail-corrected intensities or the measured ones are considered. However, for uranium analysis, the artefact induced by using the measured intensities is small: 0.2‰ for the $^{234}U/^{238}U$ ratio and 0.5‰ for the concentration.

Since we do not monitor the ^{238}U ion beam, its intensity is calculated using ^{235}U intensity, corrected for mass discrimination according to:

$$I^{238}_{Estimate} = 137.88 \times I^{235}_{Tail\,coor} \times (1 + \Delta_m \times \varepsilon)^{-1}$$

where ε is the linear discrimination bias (see section 5) calculated by using the $^{236}U/^{233}U$ double-spike ratio and Δ_m is the mass difference between ^{238}U and ^{235}U.

Thus, for the determination of the $^{234}U/^{238}U$ ratios, this approach leads to a linear system of 4 equations for 4 unknowns ($I^{233}_{Tailcor}$, $I^{234}_{Tailcoo}$, $I^{235}_{Tailcor}$, $I^{236}_{Tailcor}$) which is solved offline by inverting the associated matrix in the Excel spreadsheet. This calculation is done cycle by cycle.

I.4.3. Determination of the tail profile

The tail profile was determined using separate isotope solutions. ^{233}U solutions were used for the range from -5 to -1 amu. Both ^{238}U and ^{232}Th solutions were analyzed for the range from +1 to +3 amu. Before dilution and analysis, the parent solutions of ^{233}U and ^{232}Th were purified by means of anion exchange resin to avoid any presence of uranium in ^{232}Th solutions and of thorium in ^{233}U solutions.

We took great care in precise quantification of the tail profile over the range from -5 to -1 amu because this is the tail contribution of the major ^{238}U ion beam that mainly controls the accuracy of uranium isotopic analysis. Four ^{233}U mono-isotopic solutions were prepared in order to yield ^{233}U ion beam intensity over the range from 25 to 140 V. That way, the experiments were carried out in the same intensity conditions as for uranium analyses. The alignment of the Faraday cups, optimized for uranium isotope analysis (H1: mass 233 to H5: mass 237; see Table 1), was conserved. The ion beams monitored at masses 228 (H1) to 232 (H5) were measured with an intensity of at least 0.05 mV. Since the ^{233}U intensity beam was not monitored for these solutions, the "abundance sensitivity", defined here as Z_{-1}, could not be determined online. However, we were able to determine the (Z_{-1}/Z_{-1}) ratios precisely.

Two dilute solutions of a shelf of thorium and two HU-1 uraninite solutions were prepared to yield ion beam intensities on the main peak (^{238}U or ^{232}Th) over the 4-8.5 V range. The major isotope was monitored on the H2 Faraday cup. This

permitted online calculation of abundance sensitivity Z_{-1}, using the H1/H2 ratio, as well as the other $Z_{\geq+1}$ parameters.

Tests were performed on two days in July and November 2001. In July, three ^{233}U solutions yielding a ^{233}U beam intensity over the 25-100V range and the two ^{232}Th solutions were analyzed. In November, we performed three analyses of a ^{233}U solution with a 140 V signal intensity together with the two ^{238}U solutions. Each analysis consisted of three blocks of 12-scan cycles with a 5 s integration time per cycle. Prior to each block, half-mass zeroes (+0.5 and -0.5 amu) were measured for one minute. Using this protocol, we determined the tail contribution at half-masses (that is to say the $Z_{\pm i.5}$ values) with the same precision as at unit masses.

The results are presented in Tables 2a and 2b and illustrated in Fig. I.2. For the ^{233}U tests, we determined all the results ($Z_{-5.5}$ to $Z_{-0.5}$), fixing the abundance sensitivity (Z_{-1}) arbitrarily at 27 ppm. That way, the GEOTOP tail profile could be directly compared with the one determined by Thirlwall in 2001, who measured a mean abundance sensitivity of 27 ppm on the Royal Holloway IsoProbe™ (Thirlwall, 2001). Since then, following repairs to two major leaks in the analyzer, the abundance sensitivity of the Royal Holloway Isoprobe™ has been improved to 8 ppm (Thirlwall, 2002).

For the ^{238}U and ^{232}Th tests, the data were also normalized to the reference value of 27 ppm. In correcting for tail effect on standard and sample data, we used the average results obtained in July and November, except for Z_{+2} and Z_{+3}, for which the half-mass log-mean estimation appears to be better. In fact, for these two parameters, we observed interferences and/or contamination during measurements at unit mass. For the ^{232}Th tests, this can be easily attributed to the presence of ^{235}U traces on H5. For the ^{238}U tests, however, interferences observed on masses 240 and 241 are not explained.

Table 2a : Tail profile for a mono isotopic uranium peak in the range of -5.5 to -0.5 amu from the central peak, as estimated in this study on the GEOTOP IsoProbe" instrument.

Test / Analysis period	Intensity	Tail contribution (ppm) from central peak										
		$Z_{-5.5}$	Z_{-5}	$Z_{-4.5}$	Z_{-4}	$Z_{-3.5}$	Z_{-3}	$Z_{-2.5}$	Z_{-2}	$Z_{-1.5}$	Z_{-1}	$Z_{-0.5}$
Royal Holloway IsoProbe (Thirlwall, 2001)												
^{238}U Solution	~8 V	-	-	**1.2**	**2.3**	**3.5**	**4.7**	**6.8**	**8.5**	**13.5**	**27**	**370**
~2SE				0.3	0.7	1.0	0.7	0.9	0.6	0.6	1.4	35.8
GEOTOP IsoProbe (this study)												
Test ^{233}U July 2001												
Solution 1	~25 V	*1.70*	*1.77*	*1.65*	*2.41*	*2.36*	*4.07*	*4.65*	*8.41*	*11.20*	*27*	*173*
Solution 2	~85 V	1.27	1.48	1.98	2.52	3.06	4.13	5.84	8.46	13.41	27	226
Solution 3	~100 V	1.27	1.59	1.89	2.41	3.02	4.35	5.67	8.70	13.07	27	211
Mean July		**1.27**	**1.53**	**1.93**	**2.47**	**3.04**	**4.24**	***5.75***	***8.58***	***13.24***	**27**	***218***
Test ^{233}U November 2001												
Solution 4 Run #1	~140 V	1.39	1.69	1.98	2.46	3.01	4.34	5.24	8.51	12.86	27	326
Solution 4 Run #2	~140 V	1.39	1.71	1.95	2.49	3.08	4.14	5.47	8.40	13.18	27	287
Solution 4 Run #3	~140 V	1.48	1.73	2.04	2.57	3.17	4.15	5.54	8.37	13.35	27	271
Mean November		**1.42**	**1.71**	**1.99**	**2.50**	**3.09**	**4.21**	**5.41**	**8.43**	**13.13**	**27**	**295**
Mean Study		**1.36**	**1.64**	**1.97**	**2.49**	**3.07**	**4.22**	**5.55**	**8.49**	**13.17**	**27**	**264**
-2σ		0.09	0.11	0.06	0.06	0.06	0.11	0.22	0.13	0.22		47
			1.66		**2.52**		**4.31**		**9.36**		**139**	
Δ_{mean}			0.02		0.03		0.09		0.88		112	
Half mass zero log-mean			**1.64**		**2.46**		**4.13**		**8.55**		**59**	
$\Delta_{log\text{-}mean}$			0.00		-0.03		-0.09		0.06		32	

The tail profile, as determined by Thirlwall (2001) on the Royal Holloway IsoProbe" for ^{238}U, is also given.

The theoretical tail correction (in ppm) for a mono-isotopic peak (estimated by the linear or the exponential interpolation of half-mass zeroes), and the differences (Δ) between these corrections and the effective tail contribution, are calculated.

Table 2b : Tail profile for a mono isotopic uranium peak in the range of +0.5 to +3.5 amu from the central peak, as estimated in this study on the GEOTOP IsoProbe" instrument.

Test / Analysis period	Intensity	Tail contribution (ppm) from central peak								
		Z_{-1}	$Z_{-0.5}$	$Z_{+0.5}$	Z_{+1}	$Z_{+1.5}$	Z_{+2}	$Z_{+2.5}$	Z_{+3}	$Z_{+3.5}$
Royal Holloway IsoProbe (Thirlwall, 2001)										
^{238}	~8 V	27		30.2	12.6	**6.6**	**3.8**	**2.5**	**1.3**	**0.3**
~2SE		1.4		3.5	0.8	1.0	0.4	0.6	0.5	0.5
GEOTOP IsoProbe (this study)										
Test ^{232}Th July 2001										
Solution 1	~4.1 V	27	261	35.2	16.9	8.0	5.3	3.1	3.2	0.9
Solution 2	~6.7 V	27	248	33.9	15.0	7.8	5.2	2.6	3.7	0.6
Mean July		**27**	**255**	**34.6**	**15.9**	**7.9**	**5.2**	**2.9**	**3.4**	**0.7**
Test ^{238}U November 2001										
Solution 1	~7.4 V	27	260	32.4	14.2	6.0	6.6	2.7	4.5	2.1
Solution 2	~8.4 V	27	294	35.6	16.4	7.6	7.1	3.3	5.3	2.0
Mean November		**27**	**277**	**34.0**	**15.3**	**6.8**	**6.9**	**3.0**	**4.9**	**2.1**
Mean Study		**27**	**266**	**34.3**	**15.6**	**7.3**	**6.0**	**2.9**	**4.2**	**1.4**
-2σ				1.4	1.3	0.9	1.0	0.3	0.9	0.8
Final Values for this study		**27**		**34.3**	**15.6**	**7.3**	***4.6***	**2.9**	***2.0***	**1.4**

The tail profile, as determined by Thirlwall (2001) on the Royal Holloway IsoProbe" for ^{238}U, is also given.

Values in italic correspond to log-mean estimations. The measured Z_i values for these masses are certainly affected by interferences or contamination.

In Tables 2a and 2b, we calculate (1) the theoretical tail correction, expressed in ppm, as generated by linear and exponential interpolations of half-mass zeroes for a mono-isotopic peak, and (2) the differences (Δ) between these corrections and the actual tail contribution. Our results confirm the previous work done by Thirlwall (2001), in that the total contribution for a given peak is significantly lower than the average of half-mass zeroes. However, the tail shape as a whole is not identical to Thirlwall's, especially at -5 and -4 amu. This may be due to the specific methods in which Thirlwall and we determined our profiles.

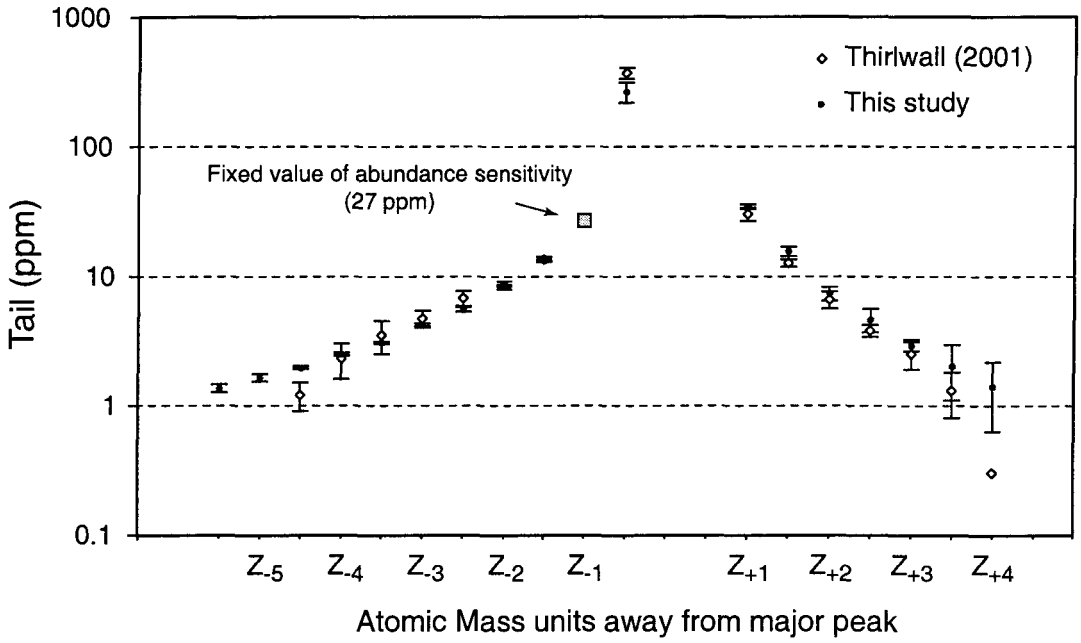

Figure I.2.: Tail shape between –5.5 and +3 amu, as determined for uranium on the GEOTOP IsoProbe™ instrument (filled circles; data from Table 2a and 2b). Also reported are the results obtained by Thirlwall (2001) on the Royal Holloway IsoProbe™ instrument (open diamonds). For comparison purposes, the tail profile observed on the GEOTOP instrument was normalized to the average abundance sensitivity value observed on the Royal Holloway IsoProbe™ (27 ppm).

For exponential tail correction, the difference between the log-mean calculations and the effective contributions is negligible, at -5, -4, -3 and +3 amu. However, this exponential interpolation significantly overestimates the real tail contribution near the peak between -2 to +2 amu (see Tables 2a and 2b). Thus, for uranium isotopic analysis, the exponential estimation cannot optimize the tail correction around the major ^{235}U peak. In this mass range, the juxtaposed ^{235}U and ^{238}U tails do not display an exponential shape. This implies that, for our IsoProbe™ instrument, exponential tail correction onto the ^{236}U beam and onto the ^{234}U beam is inappropriate (see Tables 2a and 2b and Fig. I.2).

I.4.4. Time fluctuation of the abundance sensitivity

During a U isotope analysis, abundance sensitivity can be estimated online by means of intensity monitoring on mass 237 (H5). In fact, considering the dynamic of such an analysis, the tail contribution of the minor peaks integrated onto mass 237 is negligible compared with that of the ^{238}U peak. Since the intensity measured on H5 is essentially associated with the tail contribution of the ^{238}U peak, the proportion of the ^{235}U peak contribution is only of the order of 0.1%, for example (see Table 2b). Therefore, I_{237} provides an online approximation of the abundance sensitivity, via:

$$Z_{-1} = I^{237} / I^{238}_{Estimate}$$

where $I^{238}_{Estimate}$ is determined in the same way as in section 4.2., by means of an average linear discrimination bias, ε.

While estimating abundance sensitivity in this way, we observed variations from 23 to 32 ppm (mean ~25 ppm) in the course of this study. These variations might be due to the irreproducibility of the cup alignment or pressure fluctuation within the analyzer from one day to the next. However, we also observed significant variations in abundance sensitivity in the course of a single day (usually a decrease of

a few ppm). This phenomenon cannot be caused by the irreproducibility of the Faraday cup alignment. Fluctuations in the vacuum within the analyzer in the course of the day could account for it. Nevertheless, we are not able to clearly explain such variations at this time.

These abundance sensitivity variations were taken into account for the tail correction. In each analysis, we used the Z_{-1} value determined online, and the Z_i parameters were normalized to this value (see section 4.3.). This way, the daily reproducibility obtained on the HU-1 standard is significantly improved (see section 6.1.) in comparison with the consideration of a daily mean value for the abundance sensitivity. This demonstrates that (i) the interference measured on mass 237 during the OPZ monitoring is constant at the time scale of an analysis (see section 3.2.) and (ii) that its measurement is sufficiently accurate to properly determine the abundance sensitivity and its fluctuations.

I.4.5. Linearity of the system

An inherent condition for using the tail profile correction method described above is that the system must behave linearly. This means that:

- Tail shape is independent of the peak considered. First, we could consider this assumption to be true at a first order over the mass range of the element analyzed (here, 233 to 238). It must be observed that this is not the case over a broader mass spectrum (see for example, the tail shape difference for ^{238}U and ^{209}Bi, as shown by Thirlwall, 2001).
- The tail shape remains independent of the peak height over the range of beam intensities monitored during analysis: a few mV for ^{234}U to 200 V for ^{238}U. It is clear that for uranium isotopic analysis this assumption has to be essentially verified over the entire range of beam intensities of the two largest peaks (^{238}U

and ^{235}U) monitored during an analysis, since the tail contributions of the minor peaks (^{233}U, ^{234}U and ^{236}U) are negligible.

The ^{233}U tests carried out to determine the tail shape provide the first clue that the second assumption is true, since the results we obtained over a wide range of ^{233}U signals are reproducible (Tables 2a and 2b).

To obtain further confirmation of this assumption, we analyzed, over a one-day period, 7 unspiked HU-1 solutions over a wide range of intensities. By monitoring the total tail contribution at each half-mass and at U-free unit mass, we were able to test the constancy of tail shape over the mass spectrum of uranium over a period of time (one day) at different intensities. The results, which are illustrated in Fig. I.3, are expressed in the form of (I_{233}/I_{237}), $(I_{233.5}/I_{237})$, $(I_{234.5}/I_{237})$, $(I_{235.5}/I_{237})$, (I_{236}/I_{237}) ratios as a function of the I_{238} intensity, as estimated according to I_{235} intensity. These values represent the total tail contribution of ^{238}U, ^{235}U and ^{234}U peaks at mass (237-i), normalized to the tail contribution monitored at mass 237. This normalization makes it possible to take into account variations in abundance sensitivity observed in the course of the day (see above). The (I_{237-i}/I_{237}) ratios remained constant (see Fig. I.3.); the greater irreproducibility is observed in analyses carried out at low ^{238}U intensities and is due to the very low intensities monitored at half-masses and at U-free unit masses for these analyses.

These experiments confirm that the integrated tail contribution of ^{238}U, ^{235}U and ^{234}U peaks onto a given mass is constant over a wide range of intensities in the course of a single day. Therefore, if one assumes that tail shape is independent of the peak considered, these tests demonstrate that tail shape, characterized by the (Z_{-i}/Z_{-1}) ratios, is independent of peak height.

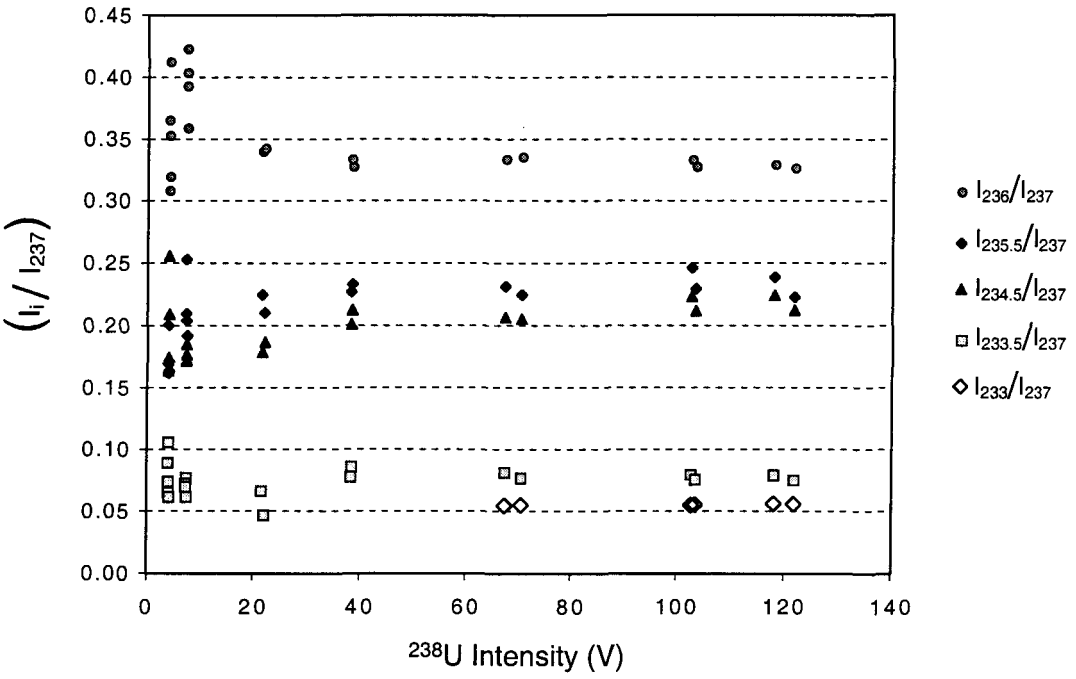

Figure I.3.: Linearity of the tailing effect. Total tail contributions at half-mass and at U-free unit mass were monitored during successive analyses of seven unspiked HU-1 solutions covering a wide range of intensities. Results are expressed in the form of (I_{233}/I_{237}), ($I_{233.5}/I_{237}$), ($I_{234.5}/I_{237}$), ($I_{235.5}/I_{237}$), (I_{236}/I_{237}) ratios as a function of I_{238} intensity. The good reproducibility that can be observed for each ratio demonstrates the constancy of the tail shape, in the course of a day, over 1) the mass spectrum of uranium; and 2) different intensity scales.

I.5. Correction for mass discrimination

I.5.1. Spike calibration

The ^{236}U-^{233}U double spike used to monitor and correct for mass discrimination was prepared from pure ^{236}U and ^{233}U solutions. To calibrate it, we developed a method similar to that proposed for Pb double/triple-spike calibration against the NIST SRM-982 reference standard (Hamelin et al., 1985; Galer, 1999). The spike composition is calibrated in reference to natural uranium with the accepted nominal value of 137.88 for the ^{238}U/^{235}U ratio (see Cowan and Adler, 1976; Cheng et al., 2000). In practice,

we used a solution of the natural uraninite HU-1 in much the same way as NIST SRM-982 is used for Pb double/triple-spike calibration. The true isotopic composition of the spike is determined by considering the mathematical system built by: (i) analysis of the spike alone, and (ii) analysis of a mixed solution of spike and natural uranium (HU-1) (see Hofmann, 1971).

To our knowledge, this approach is new for the U-Th community. In the past, ^{236}U-^{233}U double spikes have been calibrated by using a certified reference material, the CRM U-500 (Chen and Wasserburg, 1981; Chen et al., 1986; Edwards et al., 1987; Cheng et al., 2000). In this case, the isotopic composition of the spike is determined by analyzing a mixed solution of the spike and this standard. This provides the absolute $^{236}U/^{233}U$ ratio of the spike, normalized for mass discrimination to the reference $^{238}U/^{235}U$ value of U-500 (Cheng et al., 2000). The abundance of trace isotopes in the spike (^{234}U, ^{235}U, ^{238}U) is then determined by another analysis (Cheng et al., 2000).

The double-spike calibration method we propose here has certain advantages. First, the precise determination of the $^{236}U/^{233}U$ ratio is done relative to a natural uranium solution (HU-1), which avoids having to take into account the trace impurities contained in standard reference materials such as U-500 (essentially ^{236}U for this standard) and their associated errors. Second, this spike calibration protocol takes into account only the widely accepted and used reference value of natural uranium ($^{238}U/^{235}U$ = 137.88). For instance, for mono spike techniques, correction for mass discrimination is performed by normalizing the measured $^{238}U/^{235}U$ ratio against the nominal value of 137.88 (e.g. Bard et al., 1990; Luo et al., 1997; Delanghe et al., 2002; Robinson et al., 2002). For double-spike techniques, the $^{234}U/^{238}U$ ratio is calculated by dividing the calculated $^{234}U/^{235}U$ ratio by the natural $^{238}U/^{235}U$ value of 137.88 when the ^{238}U is not monitored (e.g. Chen et al., 1986; Ludwig et al., 1992; Cheng et al., 2000; Shen et al., 2002 or this study). Since this is the only reference

value we take into account throughout our protocol (including spike calibration and analysis procedures), we avoid accumulating systematic errors associated with both the $^{238}U/^{235}U$ of the U-500 standard and the nominal value of natural uranium in determining the total error propagation in a $^{234}U/^{238}U$ analysis. Moreover, we can disregard the error associated with the nominal value of natural uranium as is often done, in practice, with $^{234}U/^{238}U$ isotopic analysis on geological samples.

I.5.2. Mass discrimination correction models

Unlike in TIMS, the mass discrimination effect in a plasma source can be considered independent of time during the analysis and is characterized by the preferential transport of heavier isotopes of a given element into the mass analyzer. Various mass fractionation laws, namely linear, power and exponential laws, are commonly used to correct for this mass bias. It should be observed that, for the "exponential" law, different mathematical forms are described in the literature. Taylor et al. (1995) have evaluated these three mass discrimination correction models and have shown that, for their Plasma-54 MC-ICP-MS, the power and exponential functions result in the best correction for uranium analysis.

In our opinion, the linear law corrects with sufficient accuracy at the level of precision we need for our experiments. In fact, in the course of this study, the GEOTOP IsoProbe™ displayed a bias factor of 0.2-0.4% per amu in the mass range of U isotopes. Since this bias is low, unlike the bias observed on the Plasma 54 (~1%) by Taylor et al. (Taylor et al., 1995; see also Luo et al., 1997), the difference between the linear mass bias correction and the power or exponential corrections is negligible in comparison to the total analytical precision. This is illustrated in Fig. I.4, which shows the simulated difference between the exponential and power corrections of the $^{235}U/^{233}U$ ratio relative to the linear correction as a function of the measured reference ratio ($^{236}U/^{233}U$), varying over the mass bias range observed in the course of this

study. This difference does not exceed 33 ppm for the $^{235}U/^{233}U$ ratio (Fig. I.4) and is of the same order for the $^{234}U/^{233}U$ ratio (not shown).

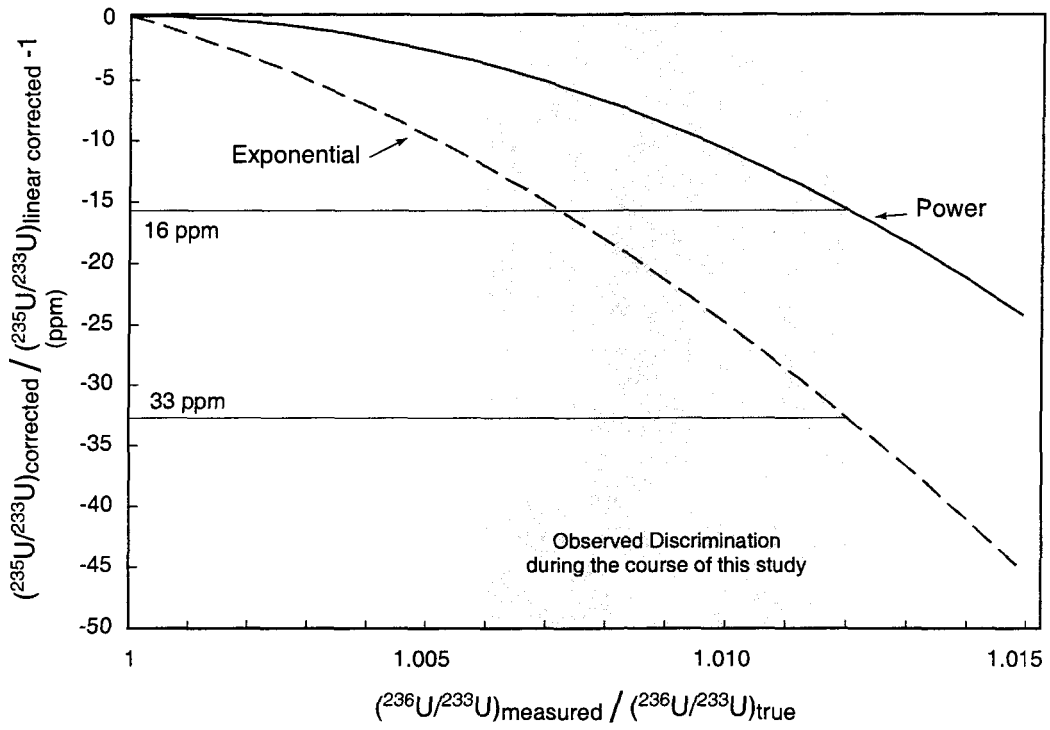

Figure I.4.: Simulation of the difference between the "exponential" or the "power" law mass discrimination corrections and the linear law correction for the $^{235}U/^{233}U$ ratio as a function of the measured spike reference ratio ($^{236}U/^{233}U$). The mass discrimination, expressed by the ratio $(^{236}U/^{233}U)_{measured}/(^{236}U/^{233}U)_{true}$, varied from 1.006 to 1.012 in the course of this study. Within this range of variation, the error induced on corrected $^{235}U/^{233}U$ ratios does not exceed 33 ppm, irrespective of the mass discrimination law used. This error is insignificant relative to the total error of a $^{234}U/^{238}U$ analysis (~1‰).

There are two main advantages in using the linear law. The error-correlation calculations and error propagations in mass discrimination correction are made easier. In the same way, resolution of the double-spike system (Hofmann, 1971; Hamelin et

al., 1985; Galer, 1999), as described above for uranium, becomes simpler with the linear mass discrimination model than with any other one.

I.6. Precision and Accuracy

I.6.1. HU-1 uraninite

The HU-1 uraninite is commonly assumed and used as a secular equilibrium standard (Ludwig et al., 1992). This was recently proved by Cheng et al. (2000) for the ^{238}U-^{234}U series. In fact, these authors have shown that this uraninite solution exhibits a $^{234}U/^{238}U$ atomic ratio that is highly consistent with geological materials that were likely to have behaved as closed systems and to have reached the secular equilibrium state. These results enabled Cheng et al. (2000) to precisely re-determine the half-life of ^{234}U. For the remainder of the text, all the results are presented in the form of activity ratios using the ^{234}U half-life value calculated by these authors ($T_{1/2}$ = 245,250±490 yr). However, the error associated with this value is not propagated.

The HU-1 uraninite was analyzed according to the method described in section 3.1. Figure I.1. compares the results of 20 analyses measured over a 3-day period with the results obtained for the same analysis using linear and exponential tail correction (see section 4.1). Several conclusions can be drawn from this figure.

First, besides having greater analytical precision, our "tail form correction" model dramatically improves external reproducibility over the other two tail correction models (~1%, 2σ). This significant irreproducibility is due to imprecise measurement of the signal monitored at half-masses. In fact, since the half-mass correction of tail represents up to ~4% of the signal measured at mass 234 (for a sample at secular equilibrium), a precise estimate of the baseline is required. This entails a sufficient integration time for these signals. For the analyses presented in

Fig. I.1., the time acquisition of a half-mass signal consists of 12 scan cycles with a 5 s integration time per cycle. This 1-minute integration time is certainly insufficient to measure this signal accurately. Moreover, because the half-mass sequence is monitored before the main analytical sequence, the signal measured at half-mass position is not necessarily representative of the true signal monitored during the main sequence. More particularly, it does not take into account any signal fluctuations that can occur during the analysis. Since the tail correction model we propose obviates the need to measure the half-mass baselines, the external reproducibility obtained by this method is improved to around 0.1% (2σ) for each analysis day (see Fig. I.1.).

Second, although our procedure improves analytical precision significantly, it systematically induces an offset of ~0.3% (see Fig. I.1.). Although the reasons for this gap are not fully understood, this bias might result from the way we determine the tail shape (see section 4.3.). For this determination, we conserved the Faraday cup alignment, even though they were optimized for uranium isotope analysis (H1: mass 233 to H5: mass 237), and assumed that the tail shape produced by a ^{233}U beam (i.e. Z_i parameters) was equivalent to the tail shape produced by the ^{238}U peak. This assumption may not be completely valid, and may result in a distortion in our tail estimates with respect to the actual tail shape of the ^{238}U peak. Since this model leads to a result lower than the expected value, the estimated tail shape and, more specifically, the most sensitive parameter Z_{-4} are overestimated. Moreover, small variations in the daily mean of HU-1 analyses are observed from day to day (from 0.996 to 0.999). We think that this variation is caused by the irreproducibility of the Faraday cup alignment, especially the H5 cup that monitors mass 237.

To deal with these two problems, we applied a correction coefficient, θ, to the Z_{-4} parameter for each day of analysis. This coefficient, calculated from more than ten days of analyses, spread over a 6-month period, varies from 0.91 to 0.98, which

represents a decrease of 2 to 9% below the expected value of Z_{-4}. This pragmatic approach translates the results so that the daily mean of HU-1 analyses is set to 1 (see Fig. I.1.).

In practice, we analyzed at least 6 spiked HU-1 samples per day. This enabled us to determine the θ correction coefficient which was then applied to the other analyses carried out during the day. This implies that, in much the same way as Robinson et al. (2002) and Shen et al. (2002), the analyses are done with reference to the accepted value of a standard material (here HU-1).

I.6.2. NBL-112a Standard

The New Brunswick Laboratory Certified Reference Material 112a (NBL-112a standard, also called CRM-145 —formerly NBS SRM-960) was analyzed to assess the validity of our approach. Corrected $^{234}U/^{238}U$ isotope ratios are listed in Table 3 and shown in Fig. I.5.. Between 200 to 800 ng of uranium were consumed per analysis. Analyses were performed on four different days, with at least one-week intervals between each day of analysis. The results yield a mean $\delta^{234}U$ value of -36.42±0.80‰ (2σ, n = 19). This is consistent with values previously reported by other laboratories and determined on MC-ICP-MS, as well as on TIMS (see compiled values in Table 3). Two major conclusions can be drawn from these results. First, the pragmatic approach that consists in applying a correction coefficient θ (estimated from HU-1 analyses) to the Z_{-4} parameter for each day of analysis, is validated. Second, these results confirm that the HU-1 and the NBL-112a admitted values are consistent within error, and therefore, that the HU-1 uraninite is indeed in secular equilibrium for the ^{238}U-^{234}U series.

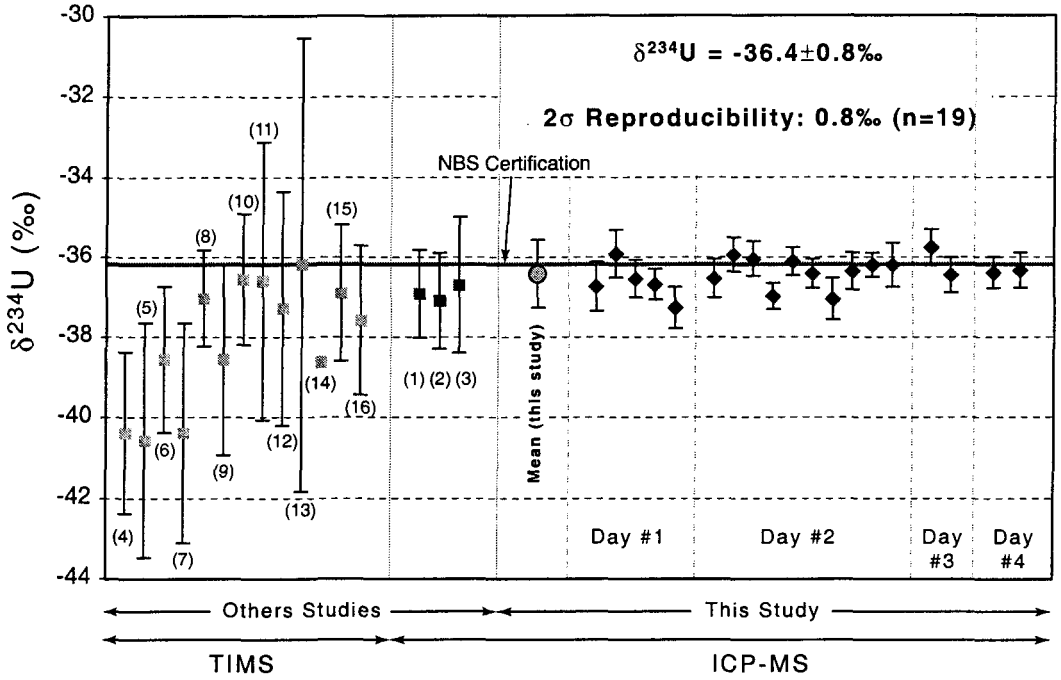

Figure I.5.: Assessment of the $^{234}U/^{238}U$ external reproducibility (expressed as $\delta^{234}U$ values) with the NBL-112a standard solution (formerly NIST NBS-960). For comparison purposes, previously published results (squares) are also reported. Numbers in brackets refer to the reference column in Table 3. All $\delta^{234}U$ values were re-calculated using half-life values from Cheng et al. (2000). Mean $\delta^{234}U$ value (present study): -36.42±0.80‰ (2σ, n=19). All error bars refer to 2σ analytical precision. Within-run 2σ analytical precision typically ranges from 0.3 to 0.6‰.

The use of this second standard allows us to assess our external analytical reproducibility, which was 0.8 ‰ (2σ, n = 19) when measured on 4 different days. This is consistent with the error anticipated according to Faraday cup irreproducibility.

Table 3 : Comparison between $^{234}U/^{238}U$ measurements for the NBL-112a standard (formely NIST NBS-960) on the GEOTOP MicroMass IsoProbe" MC-ICP-MS and TIMS or ICP-MS compiled values given by other laboratories.

Method	Analysis		$^{234}U/^{238}U$ Atomic Ratio	$\delta^{234}U$(‰)*	
MC-ICP-MS					
This Study	Day #1	#1	0.00005287 ± 3	-36.7 ± 0.6	
	Day #1	#2	0.00005291 ± 3	-35.9 ± 0.6	
	Day #1	#3	0.00005288 ± 3	-36.5 ± 0.5	
	Day #1	#4	0.00005287 ± 2	-36.7 ± 0.4	
	Day #1	#5	0.00005284 ± 3	-37.3 ± 0.5	
	Day #2	#6	0.00005288 ± 3	-36.5 ± 0.5	
	Day #2	#7	0.00005291 ± 2	-35.9 ± 0.4	
	Day #2	#8	0.00005291 ± 2	-36.0 ± 0.4	
	Day #2	#9	0.00005286 ± 2	-37.0 ± 0.3	
	Day #2	#10	0.00005290 ± 2	-36.1 ± 0.3	
	Day #2	#11	0.00005289 ± 2	-36.4 ± 0.4	
	Day #2	#12	0.00005285 ± 3	-37.1 ± 0.5	
	Day #2	#13	0.00005289 ± 3	-36.3 ± 0.5	
	Day #2	#14	0.00005290 ± 2	-36.2 ± 0.3	
	Day #2	#15	0.00005290 ± 3	-36.2 ± 0.6	
	Day #3	#16	0.00005292 ± 2	-35.8 ± 0.5	
	Day #3	#17	0.00005289 ± 2	-36.5 ± 0.4	
	Day #4	#18	0.00005289 ± 2	-36.4 ± 0.4	
	Day #4	#19	0.00005289 ± 2	-36.4 ± 0.4	
	Mean (– 2σ, n = 19)		**0.00005289** ± 4	**-36.42** ± 0.80	n=19
	2σ (‰)		**0.8‰**		
Luo et al. (1997)		(1)	0.00005286 ± 6	-36.9 ± 1.1	n=8
Shen et al. (2002)		(2)	0.00005285 ± 7	-37.1 ± 1.2	n=10
Robinson et al. (2002)		(3)	0.00005287 ± 9	-36.7 ± 1.7	n=8
TIMS					
Chen et al. (1986) I		(4)	0.00005267 ± 11	-40.4 ± 2.0	n=6
Chen et al. (1986) II		(5)	0.00005266 ± 16	-40.6 ± 2.9	n=4
Banner et al. (1990)		(6)	0.00005277 ± 10	-38.6 ± 1.8	n=4
Stein et al. (1991)		(7)	0.00005267 ± 15	-40.4 ± 2.7	n=9
Edwards et al. (1993)		(8)	0.00005285 ± 7	-37.0 ± 1.2	n=8
Gari py et al. (1994)		(9)	0.00005277 ± 13	-38.6 ± 2.4	n=12
Stirling et al. (1995)		(10)	0.00005288 ± 9	-36.6 ± 1.6	n=6
Bard et al. (1996)		(11)	0.00005288 ± 19	-36.6 ± 3.5	n=6
Luo et al. (1997)		(12)	0.00005284 ± 16	-37.3 ± 2.9	n=15
Israelon and Wohlfarth (1999)		(13)	0.00005290 ± 31	-36.2 ± 5.6	n=7
McCulloch and Esat (2000)		(14)	0.00005277	-38.6	n=5
Cheng et al. (2000)		(15)	0.00005286 ± 10	-36.9 ± 1.7	n=21
Delanghe et al. (2002)		(16)	0.00005283 ± 10	-37.6 ± 1.9	n=33
NBS *Certification* *(in Delanghe et al., 2002)*			0.00005290 ± 20	-36.2 ± 3.6	

* $\delta^{234}U = [(^{234}U/^{238}U)-1]x1000$, where $(^{234}U/^{238}U)$ is the activity ratio. All the $\delta^{234}U$ values are calculated using the half-life values given by Cheng et al. (2000).

I.6.3. Experiments with natural samples

In order to assess our total long-term reproducibility (chemical and analytical combined) on natural samples, replicated measurements of carbonate samples were performed during the study. Two types of carbonates were analyzed: one coral from the Rendez-Vous Hill, Barbados (5a isotope stage), and a sedimentary carbonate rock core sample taken from a borehole at a depth of 470 m in the Mesozoic sedimentary rocks of the eastern Paris basin. These two kinds of material were chosen because they are representative of two major applications of the U-Th systematics in the Earth sciences, which have a growing need for high precision and accuracy:

- Absolute dating of marine carbonates such as corals, used for paleo-sea level studies (Stirling et al., 2001; Gallup et al., 2002) and paleo-reconstitution of ($^{234}U/^{238}U$) seawater (Henderson, 2002), for instance.
- Studies of radionuclide migration in deep geological formations conducted to assess the safety of radioactive waste disposal in such environments (see, for example Schwarcz et al., 1982; Smellie and Stuckless, 1985; Gascoyne and Schwarcz, 1986; Smellie et al., 1986; Gascoyne and Cramer, 1987; Ivanovich et al., 1992; Griffault et al., 1993).

The second application is primarily concerned with determining whether a geological system is at secular equilibrium or not. Most of the studies in this field were conducted by means of α-counting techniques. The results obtained by this analytical method generally do not have a precision better than 4-5% (2σ), based on counting statistics. Excluding highly altered and/or fractured zones, this is not accurate enough for host-rock studies, in which disequilibria should not be significant. The application of advanced analytical techniques, such as MC-ICP-MS, should open up new perspectives in this field.

I.6.3.1. Rendez-Vous Hill Coral Sample (Barbados)

About one hundred grams of the coral were finely ground to ensure homogeneity of the sample. The coral sub-samples weighed from 100 to 400 mg. After addition of the ^{236}U-^{233}U spike, the sub-samples were dissolved in HNO_3. U and Th were then co-precipitated with Fe carrier. Finally, the samples were processed through anion exchange columns in order to separate and purify the uranium fraction, using a procedure similar to that reported by Edwards et al. (1987).

We prepared eleven samples over three distinct series. The MC-ICP-MS analyses were performed in the course of five days of analysis spread over a five-month period. The results are listed in Table 4 and presented in Figure I.6.. The external reproducibility on this in-house standard is 1.3‰ (2σ, n = 11) and the results are consistent within error with (i) our TIMS measurements and (ii) an external analysis of this sample carried out by Henderson and Robinson (pers. com.) at Oxford University on a NU™ MC-ICP-MS (see Tab. 4 and Fig. I.6.). Moreover, the measurements were taken over a range of ^{234}U intensities from 5 to 22 mV, indicating that the tail contribution can be modelled as a linear system.

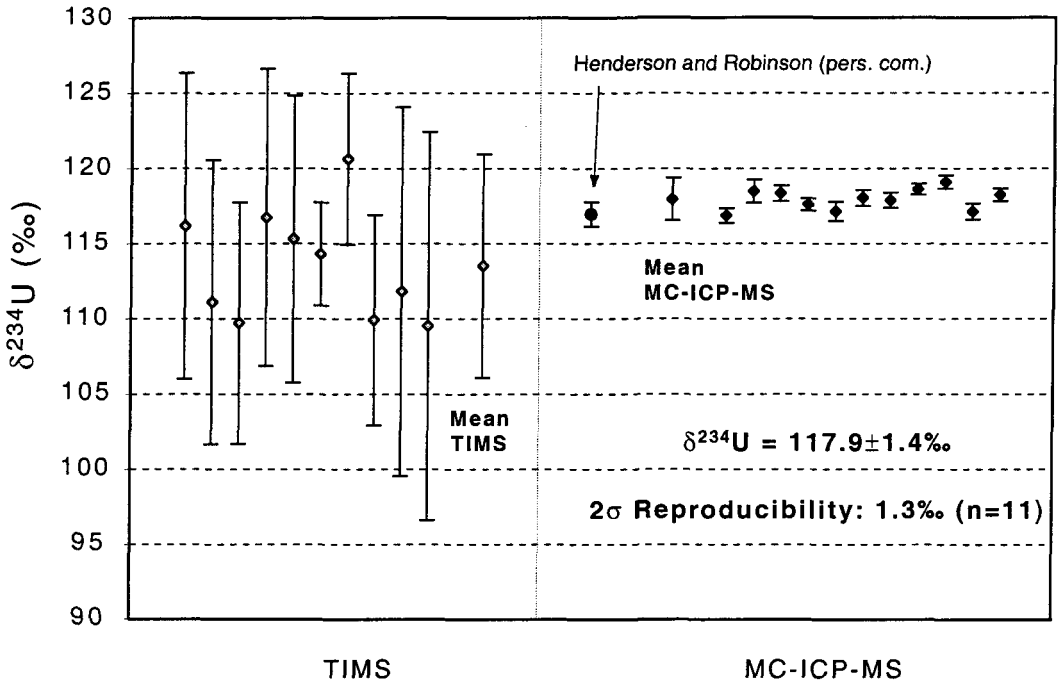

Figure I.6.: External reproducibility of the $^{234}U/^{238}U$ ratio (expressed as $\delta^{234}U$ values) determined by replicate analyses of a coral sample (Barbados). Data are listed in Table 4. MC-ICP-MS results are compared with TIMS measurements also obtained at GEOTOP on a VG Sector™ mass spectrometer equipped with a 10 cm electrostatic analyzer and a pulse-counting Daly detector. Also reported is the analysis performed by Henderson and Robinson (pers. com.) on a Nu™ MC-ICP-MS at Oxford University (filled circle). All $\delta^{234}U$ values are calculated using the half-life values determined by Cheng et al. (2000). Error bars represent 2σ analytical precision. The MC-ICP-MS total external reproducibility is estimated to be ±1.3‰ (2σ, n=11).

I.6.3.2. Carbonate Rock Sample

The sedimentary carbonate sample we used here as another in-house standard is part of a study in relation to investigations conducted by ANDRA (Agence nationale pour la gestion des déchets radioactifs —the French agency for nuclear waste management) into the feasibility of high-level-waste repository in a deep clayey

environment. ANDRA is building a scientific Underground Research Laboratory at a depth of 450 m in a deep Jurassic clay layer of the Paris basin (Callovo-Oxfordian argilites). Borehole core samples from the target formation and its bounding limestone formations were analyzed for their uranium content and isotopic composition in order i) to document the mobility of this element in such deposits, and ii) to constrain the time scale of the geological phenomena responsible for an eventual remobilization.

The sample (HTM 02924 A #1) we chose as an internal standard belongs to a transect performed perpendicular to a major sub-horizontal stylolitic joint located in the Bathonian limestone, near the interface with the Callovo-Oxfordian formation (Deschamps et al., 2002). The chemical procedure developed for these types of carbonates is quite different from the usual chemical procedure, as described above, because of the large amount of clay and organic impurities in the matrix. This chemical protocol will be described more precisely elsewhere.

The sample was finely powdered. Nine sub-samples, weighed from 0.8 to 1.9 g, were then chemically prepared over six distinct series. The MC-ICP-MS analyses were performed in the course of seven days of analysis spread over an eight-month period. The results are listed in Table 4 and illustrated in Figure I.7.. The results of some sub-sample solutions that were analyzed twice on two different days of analysis are also given. These duplicate measurements are consistent, within error, with previous analyses. Considering only the first MC-ICP-MS analysis of each sub-sample, the total reproducibility on this internal standard is about 1.3‰ (2σ, n = 9). This is of the same order as the reproducibility obtained from the coral standard, indicating that the heavy chemical protocol does not induce significant drift in the results.

Table 4 : Replicate $\delta^{234}U$ and [U] measurements of two in-house standards on the GEOTOP VG Sector TIMS and MicroMass IsoProbe" MC-ICP-MS.

Method	Sub-Sample	^{238}U (ppb)	$\delta^{234}U$ (‰)*
Rendez-Vous Hill Coral (Barbados)			
TIMS			
GEOTOP	#1	3163.2 ± 15.3	116.2 ± 10.2
	#2	3130.1 ± 18.6	111.1 ± 9.4
	#3	3152.9 ± 15.6	109.7 ± 8.0
	#4	3146.5 ± 18.2	116.7 ± 9.9
	#5	3179.8 ± 17.3	115.3 ± 9.6
	#6	3184.7 ± 13.0	114.3 ± 3.4
	#7	3181.0 ± 14.0	120.6 ± 5.7
	#8	3204.4 ± 14.7	109.9 ± 7.0
	#9	3210.8 ± 16.4	111.8 ± 12.3
	#10	3208.7 ± 8.4	109.5 ± 12.9
	Mean (– 2σ, n = 10)	**3194.9** ± 29.1	**113.5** ± 7.4
	2σ (%)	**0.91%**	**0.67%**
MC-ICP-MS			
GEOTOP	#1	3209.2 ± 2.9	116.8 ± 0.5
	#2	3205.9 ± 2.4	118.5 ± 0.8
	#3	3204.8 ± 2.4	118.3 ± 0.5
	#4	3207.4 ± 2.4	117.6 ± 0.4
	#5	3201.6 ± 2.4	117.1 ± 0.6
	#6	3211.0 ± 3.3	118.0 ± 0.5
	#7	3200.9 ± 4.6	117.9 ± 0.5
	#8	3203.3 ± 2.4	118.6 ± 0.4
	#9	3220.6 ± 3.1	119.1 ± 0.4
	#10	3216.8 ± 4.9	117.1 ± 0.5
	#11	3202.5 ± 2.4	118.2 ± 0.4
	Mean (– 2σ, n = 11)	**3208.1** ± 12.9	**117.9** ± 1.4
	2σ (%)	**0.40%**	**0.13%**
Oxford University (Henderson and Robinson, pers. com)			116.9 – 0.8
Carbonate Rock Sample (HTM-02924 A #1, ANDRA)			
MC-ICP-MS			
	#1	526.7 ± 0.4	9.6 ± 0.8
	#1 bis#	*527.0 ± 0.4*	*10.6 ± 1.0*
	#2	524.0 ± 0.5	10.3 ± 0.9
	#2 bis	*524.3 ± 0.5*	*11.2 ± 0.7*
	#3	527.9 ± 0.4	9.5 ± 1.0
	#3 bis	*528.2 ± 0.4*	*11.3 ± 0.4*
	#4	526.4 ± 0.4	11.5 ± 1.0
	#5	528.4 ± 0.5	9.8 ± 1.3
	#5 bis	*528.1 ± 0.5*	*11.1 ± 0.8*
	#6	528.4 ± 0.5	11.0 ± 1.1
	#7	528.0 ± 0.5	9.9 ± 1.2
	#7 bis	*527.6 ± 0.5*	*11.1 ± 1.3*
	#8	526.4 ± 0.5	10.6 ± 0.6
	#9	527.7 ± 0.5	10.2 ± 0.7
	Mean (– 2σ, n = 14)	**527.1** ± 2.9	**10.5** ± 1.4
	2σ (%)	**0.54%**	**0.13%**
	Mean (– 2σ, n = 9)	**527.1** ± 2.8	**10.3** ± 1.3
	2σ (%)	**0.54%**	**0.13%**

* $\delta^{234}U = [(^{234}U/^{238}U)-1]\times1000$, *where* $(^{234}U/^{238}U)$ *is the activity ratio. The* $\delta^{234}U$ *values are calculated using the half-life values given by Cheng et al. (2000).*

#: the suffixe "bis" indicates a duplicated measurement of the sample solution.

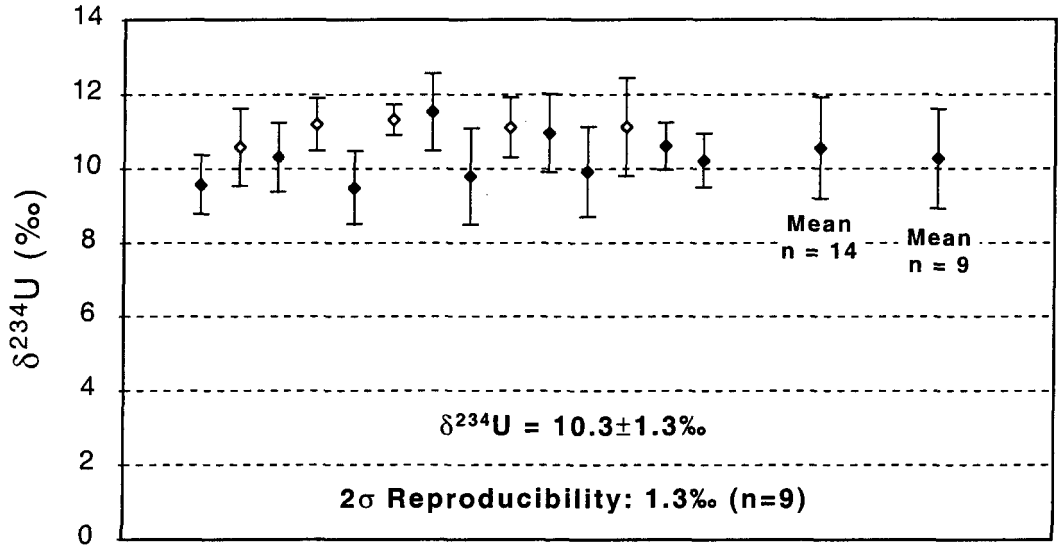

Figure I.7.: $\delta^{234}U$ (‰) replicate analyses of the HTM 02924 A #1 carbonate rock sample using the GEOTOP IsoProbe™ instrument. Data are from Table 4. Filled diamonds: single measurements; open diamonds: duplicate measurement of the previous sub-sample solution. $\delta^{234}U$ values are calculated using the half-life values determined by Cheng et al. (2000). Error bars indicate 2σ analytical precision. The total external reproducibility is estimated to be ±1.3‰ (2σ, n=9).

This sample displays a significant disequilibrium ($\delta^{234}U$ = +10.3±1.3‰), as do all the transect samples (see Deschamps et al., 2002), indicating that U remobilization has occurred in the system within a period of 1Ma. These results highlight the importance of using highly precise and accurate techniques, such as MC-ICP-MS, as opposed to α-counting spectrometry, in studies on natural radionuclide migration over recent geologic time in host-rock formations.

I.7. **Conclusion**

In this paper, we have shown that precise, accurate $^{234}U/^{238}U$ measurements can be achieved using Faraday collectors only. However, the problem caused by the poor

abundance sensitivity of the GEOTOP IsoProbe™ instrumentation needed to be fully addressed. The tail correction method we developed enabled us to correct for the large offset observed in the results obtained with the usual linear or exponential interpolation of baseline measurement monitored at ±0.5 amu of each peak. This model can be of great relevance to the precise, accurate analysis of isotopic ratios with a wide dynamic range, such as those in the U-Th series, on instruments with relatively poor abundance sensitivity.

Our external analytical precision and reproducibility, as determined on replicate analyses of the NBL-112a standard solution, is 0.8‰ at the 95% confidence level. On natural carbonate samples, the external reproducibility (combined chemical separations plus spectrometric measurements) is about 1.3‰. The technique we developed on the GEOTOP IsoProbe™ is therefore a robust tool for U isotopic studies, especially when very high precision data are required and large amounts of uranium (at least 200 ng) are available, such as in radionuclide migration studies on radioactive waste repository safety.

Acknowledgements

The authors thank Pr. C. Hillaire-Marcel, Dr. H. Isnard, A. Poirier and Dr. Dan Sinclair for their constructive help and comments. We are also very grateful to G. Henderson and L. Robinson for agreeing to perform an external analysis of our in-house coral standard on the Oxford University NU™ MC-ICP-MS. Dr. A. Simonetti's assistance with MC-ICP-MS measurement was also appreciated. The paper benefited from careful and helpful reviews from S. Galer and an anonymous reviewer. ANDRA provided drill-core samples and financial support for PD's Ph.D. RD was supported by a Lavoisier post-doctoral fellowship.

References

Banner, J.L., Wasserburg, G.J., Chen, J.H. and Moore, C.H., 1990. ^{234}U-^{238}U-^{230}Th-^{232}Th systematics in saline groundwaters from central Missouri. Earth and Planetary Science Letters, 101(2-4): 296-312.

Bard, E., Hamelin, B., Arnold, M., Montaggioni, L., Cabioch, G., Faure, G. and Rougerie, F., 1996a. Deglacial sea-level record from Tahiti corals and the timing of global meltwater discharge. Nature, 382: 241-244.

Bard, E., Hamelin, B., Arnold, M., Montaggioni, L., Cabioch, G., Faure, G. and Rougerie, F., 1996b. Pleistocene sea levels and tectonic uplift based on dating of corals from Sumba Island, Indonesia. Geophysical Research Letters, 23(12): 1473-1476.

Bard, E., Hamelin, B., Fairbanks, R.G., Zindler, A., Mathieu, G. and Arnold, M., 1990. U/Th and ^{14}C ages of corals from Barbados and their use for calibrating the ^{14}C time scale beyond 9000 years BP. Nuclear Instrument and Methods in Physics Research, B-52: 461-468.

Chen, J.H., Edwards, R.L. and Wasserburg, G.J., 1986. ^{238}U, ^{234}U and ^{232}Th in seawater. Earth and Planetary Science Letters, 80(3-4): 241-251.

Chen, J.H., Edwards, R.L. and Wasserburg, G.J., 1992. Mass spectrometry and applications to uranium-series disequilibrium. In: M. Ivanovich and R.S. Harmon (Editors), Uranium-series disequilibrium; applications to earth, marine, and environmental sciences. Clarendon Press, Oxford, United Kingdom, pp. 174-206.

Chen, J.H. and Wasserburg, G.J., 1981. Isotopic determination of uranium in picomole and subpicomole quantities. Analytical Chemistry, 53: 2060-2067.

Cheng, H., Edwards, R.L., Hoff, J., Gallup, C.D., Richards, D.A. and Asmerom, Y., 2000. The half-lives of Uranium-234 and Thorium-230. Chemical Geology, 169(1-2): 17-33.

Cowan, G.A. and Adler, H.H., 1976. The variability of the natural abundance of ^{235}U. Geochimica et Cosmochimica Acta, 40: 1487-1490.

Delanghe, D., Bard, E. and Hamelin, B., 2002. New TIMS constraints on the uranium-238 and uranium-234 in seawaters from the main ocean basins and the Mediterranean Sea. Marine Chemistry, 80(1): 79-93.

Deschamps, P., Doucelance, R., Ghaleb, B., Hillaire-Marcel, C. and Michelot, J.L., 2002. Evidence for micro-scale U-mobility along sedimentary discontinuities in a deep limestone formation as inferred by $^{234}U/^{238}U$ disequilibria. Abstracts of the 12th Annual V.M. Goldschmidt Conference, Geochimica et Cosmochimica Acta, Special Supplement, 66: 179.

Edwards, R.L., 1988. High precision thorium-230 ages of corals and the timing of sea level fluctuations in the late Quaternary. Ph.D. Thesis, California Institute of Technology, Pasadena, United States.

Edwards, R.L., Beck, J.R., Burr, G.S., Donahue, D.J., Chappell, J.M.A., Bloom, A.L., Druffel, E.R.M. and Taylor, F.W., 1993. A large drop in atmospheric $^{14}C/^{14}C$ and reduced melting in the Younger Dryas, documented with ^{230}Th ages of corals. Science, 260: 962-968.

Edwards, R.L., Chen, J.H. and Wasserburg, G.J., 1987. ^{238}U-^{234}U-^{230}Th-^{232}Th systematics and the precise measurement of time over the past 500,000 years. Earth and Planetary Science Letters, 81(2-3): 175-192.

Galer, S.J.G., 1999. Optimal double and triple spiking for high precision lead isotopic measurement. Chemical Geology, 157: 255-274.

Gallup, C.D., Cheng, H., Taylor, F.W. and Edwards, R.L., 2002. Direct determination of the timing of sea level change during termination II. Science, 295: 310-313.

Gascoyne, M. and Cramer, J.J., 1987. History of actinide and minor element mobility in an Archean granitic batholith in Manitoba, Canada. Applied Geochemistry, 2(1): 37-53.

Gascoyne, M. and Schwarcz, H.P., 1986. Radionuclide migration over recent geologic time in a granitic pluton. Chemical Geology; Isotope Geoscience Section, 59(1): 75-85.

Griffault, L.Y., Gascoyne, M., Kamineni, C., Kerrich, R. and Vandergraaf, T.T., 1993. Actinide and Rare Earth Element characteristics of deep fracture zones in the Lac du Bonnet granitic batholith, Manitoba, Canada. Geochimica et Cosmochimica Acta, 57(6): 1181-1202.

Halliday, A.N., Lee, D.C., Christensen, J.N., Rehkämper, M., Yi, W., Luo, X., Hall, C.M., Ballentine, C.J., Pettke, T. and Stirling, C., 1998. Applications of multiple collector-ICPMS to cosmochemistry, geochemistry and paleoceanography. Geochimica et Cosmochimica Acta, 62(6): 919-940.

Hamelin, B., Manhès, G., Albarède, F. and Allègre, C.J., 1985. Precise lead isotope measurements by the double spike technique: a reconsideration. Geochimica et Cosmochimica Acta, 49: 173-182.

Henderson, G.M., 2002. Seawater ($^{234}U/^{238}U$) during the last 800 thousand years. Earth and Planetary Science Letters, 199(1-2): 97-110.

Hofmann, A.W., 1971. Fractionation corrections for mixed-isotope spikes of Sr, K and Pb. Earth and Planetary Science Letter, 10: 397-402.

Israelson, C. and Wohlfarth, B., 1999. Timing of the last-interglacial high sea level on the Seychelles Islands, Indian Ocean. Quaternary Research, 51: 306-316.

Ivanovich, M., Latham, A.G., Longworth, G. and Gascoyne, M., 1992. Applications to radioactive waste disposal studies. In: M. Ivanovich and R.S. Harmon (Editors), Uranium-series disequilibrium; applications to earth, marine, and environmental sciences. Clarendon Press, Oxford, United Kingdom, pp. 583-630.

Jarvis, K.E., Gray, A.L. and Houk, R.S., 1992. Handbook of Inductively Coupled Plasma Spectrometry. Blackie, Glasgow.

Ludwig, K.R., 1997. Optimization of multicollector isotope-ratio measurement of strontium and neodymium. Chemical Geology, 135(3-4): 325-334.

Ludwig, K.R., Simmons, K.R., Szabo, B.J., Winograd, I.J., Landwehr, J.M., Riggs, A.C. and Hoffman, R.J., 1992. Mass-spectrometric ^{230}Th-^{234}U-^{238}U dating of the Devils Hole calcite vein. Science, 258(5080): 284-287.

Luo, X., Rehkämper, M., Lee, D.C. and Halliday, A.N., 1997. High precision $^{230}Th/^{232}Th$ and $^{234}U/^{238}U$ measurements using energy-filtered ICP Magnetic Sector Multi-Collector mass spectrometry. International Journal of Mass Spectrometry and Ion Processes, 171: 105-117.

McCulloch, M.T. and Esat, T., 2000. The coral record of last interglacial sea levels and sea surface temperatures. Chemical Geology, 169: 107-129.

Rehkämper, M. and Mezger, K., 2000. Investigation of matrix effects for Pb isotope ratio measurements by multiple collector ICP-MS: verification and application of optimized analytical protocols. Journal of Analytical Atomic Spectrometry, 15: 1451-1460.

Robinson, L.F., Henderson, G.M. and Slowey, N.C., 2002. U-Th dating of marine isotope stage 7 in Bahamas slope sediments. Earth and Planetary Science Letters, 196(3-4): 175-187.

Rubin, K.H., 2001. Analysis of $^{232}Th/^{230}Th$ in volcanic rocks: a comparison of thermal ionization mass spectrometry and other methodologies. Chemical Geology, 175(3-4): 723-750.

Schwarcz, H.P., Gascoyne, M. and Ford, D.C., 1982. Uranium-series disequilibrium studies of granitic rocks. Chemical geology, 36(1-2): 87-102.

Shen, C.-C., Edwards, L.R., Cheng, H., Dorale, J.A., Thomas, R.B., Bradley, M., S., Weinstein, S.E. and Edmonds, H.N., 2002. Uranium and thorium isotopic and concentration measurements by magnetic sector inductively coupled plasma mass spectrometry. Chemical Geology, 185(3-4): 165-178.

Smellie, J.A.T., Mackenzie, A.B. and Scott, R.D., 1986. An analogue validation study of natural radionuclide migration in crystalline rocks using uranium-series disequilibrium studies. Chemical Geology, 55(4): 233-254.

Smellie, J.A.T. and Stuckless, J.S., 1985. Element mobility studies of two drill-cores from the Goetemar Granite (Kraakemaala test site), Southeast Sweden. Chemical Geology, 51(1-2): 55-78.

Stein, M., Wasserburg, G.J., Lajoie, K.R. and Chen, J.H., 1991. U-series ages of solitary corals from the California coast by mass spectrometry. Geochimica et Cosmochimica Acta, 55: 3709-3722.

Stirling, C.H., Esat, T.M., Lambeck, K., McCulloch, M.T., Blake, S.G., Lee, D.C. and Halliday, A.N., 2001. Orbital forcing of the marine isotope stage 9 interglacial. Science, 291: 290-293.

Stirling, C.H., Esat, T.M., McCulloch, M.T. and Lambeck, K., 1995. High-precision U-series dating of coral from Wetsern Australia and implication for the timing

and duration of the Last Interglacial. Earth and Planetary Science Letters, 135: 115-130.

Stirling, C.H., Lee, D.C., Christensen, J.N. and Halliday, A.N., 2000. High-precision in situ ^{238}U-^{234}U-^{230}Th isotopic analysis using laser ablation multiple-collector ICP-MS. Geochimica et Cosmochimica Acta, 64(21): 3737-3750.

Taylor, H.E., 2001. Inductively Coupled Plasma Mass Spectrometry. Practice and Techniques. Academic Press, San Diego, California, 294 pp.

Taylor, P., De Bievre, P., Walder, A. and Entwistle, A., 1995. Validation of the analytical linearity and mass discrimination correction model exhibited by a multiple collector inductively coupled plasma mass spectrometer by means of a set of synthetic uranium isotope mixtures. Journal of Analytical Atomic Spectrometry, 10: 395-398.

Thirlwall, 2001. Inapropriate tail corrections can cause large inaccuracy in isotope ratio determination by MC-ICP-MS. Journal of Analytical Atomic Spectrometry, 16: 1121-1125.

Thirlwall, M.F., 2002. Multicollector ICP-MS analysis of Pb isotopes using a ^{207}Pb-^{204}Pb double spike demonstrates up to 400 ppm/amu systematic errors in Tl-normalization. Chemical Geology, 184(3-4): 255-279.

Chapitre II

Improved method for radium extraction from environmental samples for its analysis by Thermal Ionisation Mass Spectrometry

Bassam Ghaleb, Edwige Pons-Branchu and Pierre Deschamps

Submitted to Chemical Geology

Abstract

We have developed an efficient procedure for the chemical separation of ^{226}Ra from environmental samples and its measurement by thermal ionization mass spectrometry. The original step in this procedure consists in a pre-concentration by co-precipitation of radium onto manganese dioxide. This pre-concentration step permits an efficient separation of radium from major elements including, most importantly, calcium. Thus, the present protocol provides a very useful technique for the precise and accurate analysis of radium-226 in carbonate samples. Furthermore, this procedure is also well-suited for seawater sample Ra analysis since it does not require a preliminary evaporation stage, thereby eliminating problems due to the precipitation of large quantities of salts.

Reproducibility and accuracy of ^{226}Ra concentration measurements were estimated by replicate measurements of a homogenized reef coral skeleton and several seawater samples. The external reproducibility obtained on the carbonate sample was ±0.55% at the 95% confidence level (n = 9) using between 300 to 600 fg of ^{226}Ra. The chemical yield averages 80% for carbonate matrix. For seawater

samples, the external reproducibility was 2.3% (2σ, n = 5) using less than 10 fg of ^{226}Ra (i.e. ~200 ml of seawater).

The ability to extract with a high efficiency radium from carbonate and seawater samples allows wider investigations of the use of ^{226}Ra either as a Holocene chronometer for carbonates or as a tracer of oceanic processes.

Keywords: Radium; TIMS; Carbonate matrix; Coral; Seawater; Chemical Separation.

II.1. Introduction

The measurement of ^{226}Ra by Thermal Ionization Mass Spectrometry -TIMS- has several advantages compared with conventional radioactive counting methods: greater precision, smaller sample size and much faster determination (Cohen and O'Nions, 1991; Volpe et al., 1991). This new technique allowed to use ^{226}Ra as a tracer and/or chronometer for: i) recent magmatic processes (Volpe and Goldstein, 1993; Chabaux and Allègre, 1994; Sigmarsson, 1996; Bourdon et al., 1998; Claude-Ivanaj et al., 1998; Sigmarsson et al., 2002), ii) Holocene studies (Pons-Branchu, 2001; Staubwasser et al., submitted), iii) river, groundwater and hydrothermal systems (Rihs et al., 2000; Vigier et al., 2001) and iv) oceanographic studies (Liebetrau et al., 2002). However, the determination of ^{226}Ra by TIMS requires the separation of a very high purity Ra fraction, because the presence of trace of elements such as Ca and Ba tends to inhibit the ionization of radium (Cohen and O'Nions, 1991; Volpe et al., 1991; Chabaux et al., 1994). Usually, Ra extraction and purification have been performed in two distinct steps. Firstly, Ra and Ba are extracted from bulk samples using a cationic exchange resin. Secondly, the Ra-Ba separation is carried out by using either a cationic resin with ammonium EDTA elution (Cohen and O'Nions, 1991; Volpe et al., 1991) or a chromatographic Sr spec™ resin in HNO_3 (Chabaux et al., 1994). This last procedure provides an easier and more efficient Ba-Ra separation technique (Rihs et al., 1997).

However, in samples such as carbonate (speleothems, corals, molluscs...), problems still persist with respect to the separation of Ra from other alkaline-earth elements (Ca, Sr....) on cationic resins. They are due to the high Ca/Ra or Sr/Ra ratios in carbonates compared to silicate materials. For example, a coral sample has a $Ca/^{226}Ra$ atomic ratio of $\sim 2 \times 10^{12}$ assuming a 3 μg/g uranium concentration and a secular radioactive equilibrium state for the ^{226}Ra-U series. For comparison purposes, a Mid-Ocean Ridge Basalt sample would have a ratio of $\sim 1 \times 10^{7}$.

For seawater analysis, the low concentrations of ^{226}Ra (from 0.07 dpm/kg to 0.2 dpm/kg, see Broecker et al., 1976) make necessary the processing of a large volume of water (a few hundred ml to several litres) even using the TIMS technique. Therefore, Ra extraction through a co-precipitation step is more suitable than a direct ion exchange resin procedure, since it allows to eliminate the evaporation step and the subsequent, and difficult, re-dissolution of salts in acidic media. Cohen and O'Nions (1991) proposed a procedure based on the precipitation of $Sr(Ra)SO_4$ and its conversion to an acid-soluble $Sr(Ra)CO_3$ according to the classical Curie-Debierne method (Curie and Debierne, 1910). However, this reaction is relatively complex and time consuming.

Here, we present an improved procedure allowing a highly efficient separation of Ra and Ba from sample matrix based on a pre-concentration step of Ra and Ba by MnO_2 precipitation. This procedure has been applied to natural samples. We report results for an in-house reef coral standard and Labrador seawater samples to illustrate the sensitivity, reproducibility and accuracy of the method.

II.2. Analytical method

II.2.1. Chemical procedure

II.2.1.1. Chemical separation and purification

All acids were purified by sub-boiling distillation in PTFE stills. De-ionized 18 MΩ water and analytical grade $KMnO_4$, $MnCl_2.4H_2O$ and NaOH from Alldrich Ltd. were used.

The following chemical procedure is for the analysis of a carbonate matrix material (the GEOTOP in-house coral standard). The procedure for seawater samples is very similar and will be described below. From 0.4 to 1.8 g of coral powder is weighed into a 250 ml Teflon™ beaker into which an enriched ^{228}Ra spiked was

previously added. The sample is dissolved in nitric acid, evaporated to dryness, and re-dissolved into 1 to 2 ml of 6M HCl, before adding 200 ml of water. At this stage, 100 µl of a 0.5M $KMnO_4$ solution are added, turning the solution to a purple color. This solution is then heated to 80 °C, and the pH adjusted to 8-9 by adding 1M NaOH. In a following stage, 200 µl of a 0.5M $MnCl_2.4H_2O$ solution are added (twice the quantity of $KMnO_4$ previously added). This causes MnO_2 to appear as a dark brown precipitate following the chemical reaction:

$$2MnO_4^- + 3Mn^{2+} + 2H_2O \Rightarrow 5MnO_2 + 4H^+$$

The supernatant contains most of the Ca and part of the Sr, whereas Ba and Ra are co-precipitated with the manganese dioxide.

The solution is stirred and, after at least one hour, the MnO_2 precipitate is recovered by centrifugation. The precipitate is washed with Milli-Q water, centrifuged, dissolved in 5 to 10 ml of 6M HCl and transferred to a 50 ml Teflon™ beaker. The solution is heated at 80°C. The reduction of MnO_2 to Mn^{2+} then occurs as shown by the gradual disappearance of the brownish color. When a slightly brownish coloration remains, a few mg of reducing agents such as ascorbic acid or hydroxylamine can be added. The solution should become instantly colorless. The solution is then evaporated to dryness and re-dissolved into 2 ml of 3M HCl. At this stage, the sample is ready to go through a slightly modified version of the cation exchange purification method (Cohen and O'Nions, 1991). Details of the different steps of the procedure are given in Table 1.

Table 1: Procedure for the separation and purification of Ra from carbonate matrix or seawater after a co-precipitation step of Ra with manganese dioxide

	Column 1	Column 2	Column 3
Resin type	BioRad® AG50W-X8, 200-400 mesh	BioRad® AG50W-X8, 200-400 mesh	Sr Spec®
Column type	BioRad Poly-Prep (10 ml)	8 cm length, 4 mm diameter	8 cm length, 4 mm diameter
Resin Volume	2 ml	1 ml	1 ml
Introducing	2 ml HCl 3N	2 ml HCl 3N	1 ml HNO_3 3N
Washing	8 ml HCl 3N	6 ml HCl 3N	1 ml HNO^3 3N
Elution	8 ml HNO_3 5M	6 ml HCl 6N	2.5 ml HNO^3 3N
Eluted fraction	Ra + Ba	Ra + part of Ba	Ra

A similar procedure was applied to seawater samples. The analysis was carried out on 200 ml of water (~ 10 fg of ^{226}Ra). The co-precipitation was directly performed on this water volume after prior acidification to pH ~1 with HCl. For such seawater sample volumes, the amounts of reagents needed are identical to those used for coral samples. However, for larger seawater samples the amount of reagents will have to be adjusted proportionally.

II.2.1.2. Blank and Recovery

The blank of the total chemical procedure was measured regularly. Spiked blank analyses were indistinguishable from the spike value within the uncertainty. Therefore, the ^{226}Ra blank shall be considered as negligible (< 0.1 fg).

The total recovery of the chemical procedure described above was estimated by three independent analyses of the in-house coral reef standard. Co-precipitation, chromatographic separation and purification steps were carried out on three unspiked coral sub-samples. The spike was added at the end of the chemical preparation, just before TIMS measurement. The difference between the measured ^{226}Ra concentrations and its actual value (see section 3.1.) provides an estimates for the chemical yield of radium. It varied from 73% to 86%.

II.2.2. Spike calibration

The data presented here were obtained using two different ^{228}Ra spikes. These enriched ^{228}Ra tracers were prepared at a two-year interval by milking the radium fraction from a $Th(NO_3)_4$ salt according to the procedure proposed by Volpe et al. (1991). The initial $^{228}Ra/^{226}Ra$ ratios of these spikes were ~7 and ~3.5 respectively. However, because of the short half-life of ^{228}Ra ($T_{1/2}$ = 5.75 y), the isotopic composition of the spike and its ^{228}Ra concentration were measured before each batch of analyses. The spike concentrations were calibrated against the HU-1 uraninite standard solution assuming that this uraninite is at secular equilibrium for the ^{226}Ra-^{238}U series (as has previously assumed for the ^{230}Th-^{234}U-^{238}U series by Ludwig et al., 1992). However, Cheng et al. (2000) showed recently that the GEOTOP HU-1 solution is slightly out of equilibrium for the ^{230}Th-^{238}U series at a 3‰ level. This point will be discussed later.

The minimum amount of ^{228}Ra spike used per analysis was 60 fg. In borderline cases (e.g. seawater), the spike quantity added to a natural sample was set in order to insure that ^{226}Ra from the sample represented at least 35% of the total ^{226}Ra.

II.2.3. Mass spectrometry

The final Ra fraction was loaded with 1 µl of Ta-HF-H_3PO_4 activator (Birck, 1986) on a single, zone-refined Re filament. Prior to data collection, the filament temperature was slowly increased to 1200°C during at least 15 min. The acquisition procedure was started when the interferences (polyatomic isobars) were reduced to background level. Ra isotopes and background were measured using the Daly-ion counter of a VG Sector-54™ mass spectrometer operated in peak jumping mode. The ^{228}Ra signal typically yielded signals greater than 2000 counts per second (cps), thereby allowing a direct focusing on this mass. Peak measurements (^{226}Ra and ^{228}Ra)

were integrated for 4 seconds each. The background was monitored at mass 224.5 for 6 seconds. A minimum of 3 blocks of 15 cycles were collected per analysis which allowed an internal precision better than 0.5% on the measured $^{228}Ra/^{226}Ra$ ratio. The ionization efficiency, as estimated within this short time interval (~40 min), was at least of 1% of the total amount of atoms loaded on the filament. The mass fractionation can be considered as negligible at the level of the external reproducibility achieved and therefore should not affect the results significantly (see Cohen and O'Nions, 1991).

II.3. Application to natural samples : coral and seawater

II.3.1. Coral samples

II.3.1.1. Reproducibility

Nine independent ^{226}Ra analyses of the in-house coral standard were performed over a period of two years using two distinct spikes. The results are reported in Table 2 and shown on Figure II.1.. The mean value was 583.3±3.2 fg/g, or 1.279±0.007 dpm/g (using a ^{226}Ra half-life of 1602 a). This yields an external and long-term reproducibility, including both chemical preparation and spectrometric measurement, of 5.5‰ at the 95% confidence level, using a minimum amount of 250 fg of ^{226}Ra.

II.3.1.2. Accuracy

The accuracy of replicate coral measurements can be assessed by comparing the measured ^{226}Ra with the expected ^{226}Ra activity of this coral assuming a closed system behaviour for U-series.

Table 2: Replicate ^{226}Ra TIMS measurements of the GEOTOP in-house coral standard

Replicate	Spike	(^{226}Ra) (dpm/g)	^{226}Ra (fg/kg)
#1	Spike 2001	1.280 ± 0.005	583.8 ± 2.1
#2	Spike 2001	1.282 ± 0.006	584.8 ± 2.7
#3	Spike 2001	1.284 ± 0.004	585.6 ± 1.8
#4	Spike 2001	1.280 ± 0.004	583.8 ± 1.9
#5	Spike 2003	1.278 ± 0.004	583.1 ± 2.0
#6	Spike 2003	1.280 ± 0.002	584.1 ± 1.1
#7	Spike 2003	1.272 ± 0.005	580.5 ± 2.2
#8	Spike 2003	1.278 ± 0.003	583.1 ± 1.5
#9	Spike 2003	1.274 ± 0.007	581.4 ± 3.3
	Mean (± 2σ)	1.279 ± 0.007	583.3 ± 3.2
	2σ (%)	**0.55%**	

The uranium concentration, $^{234}U/^{238}U$, $^{230}Th/^{234}U$ activity ratios of this in-house coral standard have been determined by TIMS and/or MC-ICP-MS with replicate measurements spanning a period of two years (Deschamps et al., 2003). The up-to-date best estimates of U concentration, $^{234}U/^{238}U$ activity ratio and ^{230}Th age are 3.194±0.023 ppm, 1.1179±0.0014 and 73.0±1.9 ka, respectively. They are determined using the ^{230}Th and ^{234}U half-lives proposed by Cheng et al. (2000). These values are in good agreement with an external analysis of this sample performed by Henderson and Robinson (pers. com.) at Oxford University on a NU™ MC-ICP-MS instrument (3.185±0.003 ppm, 1.1169±0.0008 and 73.4±1.4 ka). The calculated initial $(^{234}U/^{238}U)_0$ of this coral is 1.1450±0.0021, which is consistent within error bars with seawater values determined by Chen et al. (1986) and Henderson et al. (1999) with TIMS instruments and with a value we determined (P.D.) using a MC-ICP-MS instrument ($(^{234}U/^{238}U)_{seawater}$ = 1.1486±0.0017, n=5). The $(^{234}U/^{238}U)_0$ of this coral appears slightly lower than the $(^{234}U/^{238}U)$ values given by Delanghe et al. (2002) for seawater (1.1496±0.0020), although it is in agreement with their determination of $(^{234}U/^{238}U)$ on modern corals (1.1466±0.0028). Nevertheless, the marine $(^{234}U/^{238}U)_0$ signature of our standard coral is a strong indication for a closed system behaviour for its ^{230}Th-^{234}U-^{238}U series (Hamelin et al., 1991).

Using the calculated age of this coral and assuming that it behaved as a closed geochemical system for ^{226}Ra-^{238}U series, the $^{226}Ra/^{230}Th$ activity ratio must have attained the transient equilibrium state, thus allowing a theoretical ^{226}Ra content to be calculated. This theoretical value ((^{226}Ra) = 1.284 dpm/g) is consistent with the nine measured values within their errors ((^{226}Ra) = 1.279±0.007 dpm/g). This is illustrated in Figure II.2. which shows the ($^{226}Ra_{mean}/^{238}U_{mean}$) activity ratio *vs* the age of the coral in comparison with the theoretical evolution curve of this ratio with time. The excellent agreement between the measured and modelled values provides an external and robust validation of the accuracy of our ^{226}Ra measurements.

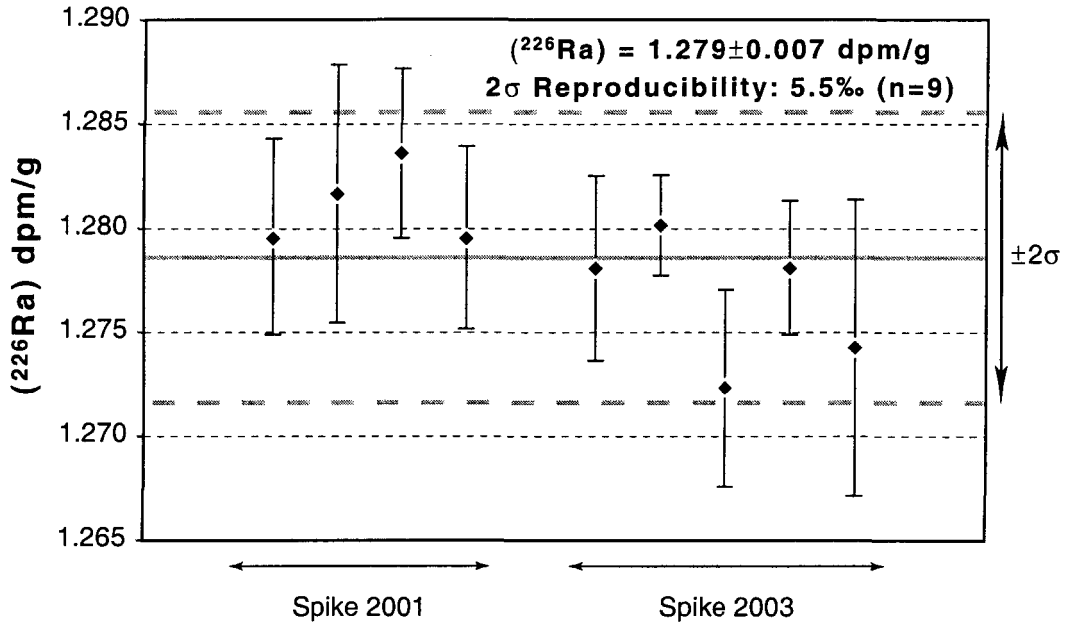

Figure II.1: Replicate analyses of ^{226}Ra in the GEOTOP in-house carbonate matrix standard (coral sample, Rendez-vous Hill, Barbados) by TIMS. Results (see Table 2) are expressed in activity (dpm/g) and are calculated using the ^{226}Ra half-life of 1602 y. Error bars indicate 2σ analytical precision. The total external reproducibility is ±5.5‰ (2σ, n = 9).

Furthermore, this result supports our hypotheses that both the secular equilibrium of the HU-1 solution for the ^{226}Ra-^{238}U series and the transient equilibrium of the coral standard for the ^{226}Ra-^{230}Th series are achieved. Therefore, it is very likely that the GEOTOP HU-1 standard is in a secular equilibrium state for the ^{226}Ra-^{238}U series within analytical errors (5.5‰, herein), despite this solution being out of equilibrium by ±3‰ with respect to the ^{230}Th-^{238}U series (see Cheng et al., 2000).

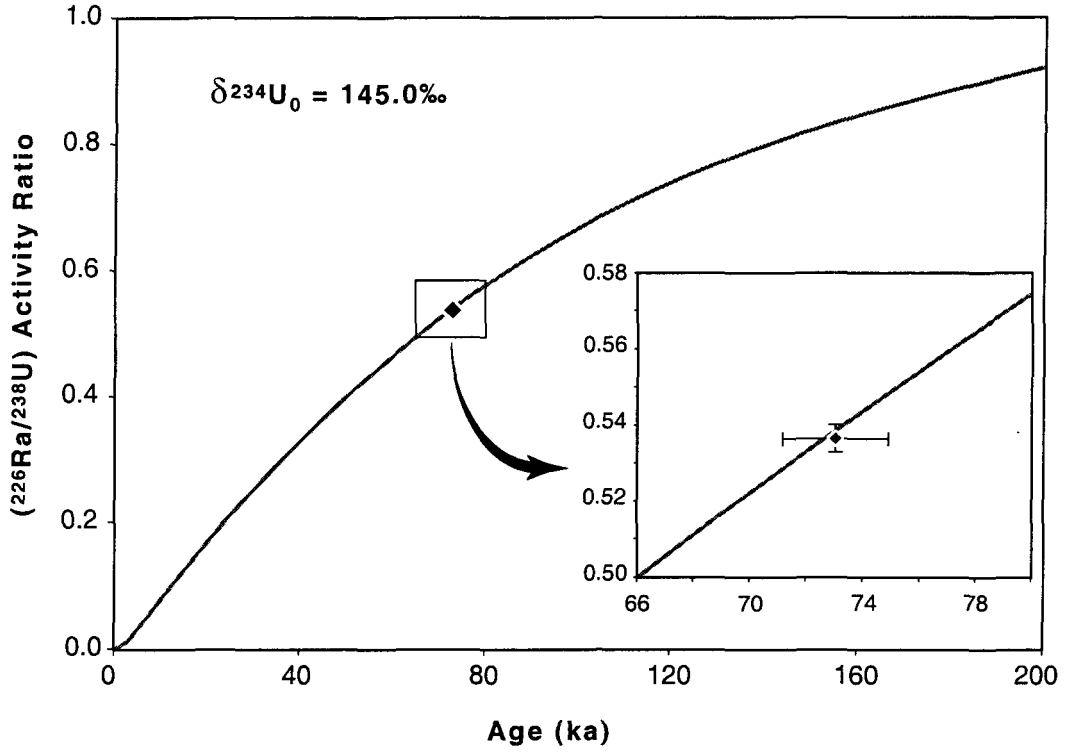

Figure II.2: ($^{226}Ra_{mean}/^{238}U_{mean}$) measured activity ratio of the GEOTOP in-house coral standard *vs* its age in comparison with the theoretical evolution curve of ($^{226}Ra/^{238}U$) activity ratio in a closed system. The theoretical curve has been determined from the measured the ($^{234}U/^{238}U$) activity ratio (1.1179±0.0014) and ^{230}Th age (73.0±1.9 ka) of the coral. The measured and modelled ($^{226}Ra/^{238}U$) values are highly consistent.

II.3.2. Seawater

Eight seawater samples collected in a near shore, along a 100m-depth profile at station BON-1 (48° 43.950 N, 52° 58.060 W) in the Labrador Sea, were analyzed following the procedure described above. Results are listed in Table 3. Five replicate measurements were made for sample #255968 (depth 94m) and 2 for sample # 255969 (depth 68m). The external reproducibility, as estimated by the 5 replicate measurements of the # 255969 sample, is ±2.3% (2σ) using 200ml of water (~ 10 fg of ^{226}Ra). In Figure II.3., ^{226}Ra concentrations (normalized to 35 salinity) are presented as a function of bathymetry. The reported error bars correspond to the external reproducibility quoted above (±2.3%, 2σ).

Table 3: ^{226}Ra concentration in seawater samples from the Labrador sea (station BON-1)

Sample	Depth (m)	Salinity (‰)	Temperature	Replicate	(^{226}Ra) (dpm/kg)	^{226}Ra (fg/kg)
# 255976	2	31.600	12°C		0.0756 ± 0.0005	34.49 ± 0.24
# 255974	7	32.562	9.654°C		0.0762 ± 0.0004	34.75 ± 0.21
# 255973	18	32.980	2.160°C		0.0888 ± 0.0004	40.50 ± 0.20
# 255972	29	32.517	-0.303°C		0.1132 ± 0.0004	51.64 ± 0.18
# 255971	39	32.216	-0.580°C		0.1190 ± 0.0003	54.28 ± 0.13
# 255970	49	32.685	-0.881°C		0.1237 ± 0.0004	56.44 ± 0.17
# 255969	68	32.743	-1.064°C	#1	0.1134 ± 0.0013	51.73 ± 0.59
				#2	0.1156 ± 0.0009	52.73 ± 0.40
				Mean	0.1145	
# 255968	94	32.816	-1.237°C	#1	0.1133 ± 0.0005	51.71 ± 0.23
				#2	0.1162 ± 0.0010	53.02 ± 0.47
				#3	0.1141 ± 0.0006	52.05 ± 0.27
				#4	0.1161 ± 0.0004	52.97 ± 0.18
				#5	0.1157 ± 0.0003	52.80 ± 0.13
			Mean (± 2σ)		0.1151 ± 0.0026	52.51 ± 1.19
				2σ (%)	**2.3%**	

All errors are given at the 95% confidence level (2σ).

Large variations in ^{226}Ra concentrations are observed along this profile. The ^{226}Ra concentrations increase with depth from 0.07 dpm/kg at the surface to a maximum of 0.12 dpm/g reached at 49m depth. Because the ^{226}Ra contents have been

normalized to a salinity of 35, dilution by fresh water inputs cannot explain the decrease of ^{226}Ra content in the upper part of the profile.

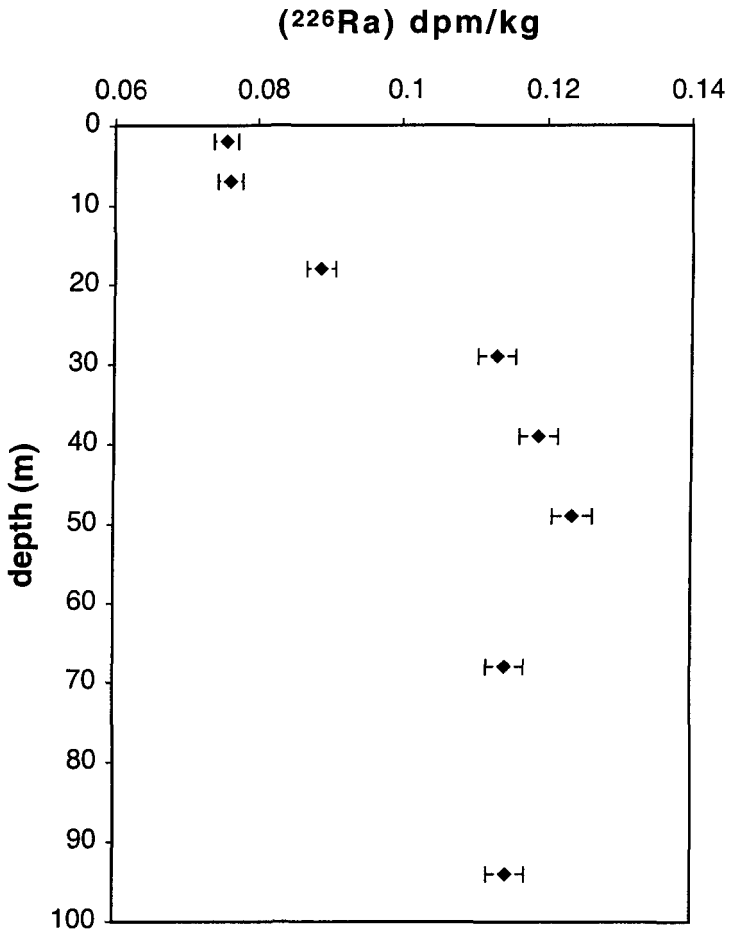

Figure II.3.: Depth profile of ^{226}Ra concentration in seawater from BON-1 near-shore Labrador Sea station. Analyses were performed by TIMS using 200 ml of seawater (~10 fg of ^{226}Ra). The reported errors correspond to 2σ reproducibility (±2.3%) obtained on 5 replicate measurements of the #255968 seawater sample (see Table 3).

This depth variation pattern can be explained by the fact that Ra is removed in the upper water column by biological cycling as proposed for Ba and Ra by Bacon and Edmond (1972 and references therein), Koide et al. (1976) and Falkner et al.

(1991). The exact nature of the mechanism responsible for the recycling of Ra (and Ba) in the water column (direct biological uptake, biological mediated barite precipitation...) is still subject to discussion (Dehairs et al., 1980; Bishop, 1988; Jeandel et al., 1996).

II.4. Conclusion

The present method for the measurement of ^{226}Ra in environmental samples, based on pre-concentration of Ra by MnO_2 precipitation, is particularly relevant for $CaCO_3$ matrix and water samples for which the usual chromatographic separation does not provide a sufficient chemical purification of Ra from Ca for precise TIMS determination. The high reproducibility and accuracy achieved for $CaCO_3$ matrix sample (5.5‰), open new prospects for the ^{226}Ra dating of Holocene marine and continental carbonates (Berkman and Ku, 1998; Pons-Branchu, 2001; Staubwasser et al., submitted).

This method can also be applied to seawater samples. It allowed here accurate measurements (±2.3%) of ^{226}Ra quantities as low as 10 fg (i.e. 200 ml of seawater). Compared with the large quantities (10-20 l) of seawater generally used by conventional counting methods, the small quantity required using TIMS represents a significant improvement for oceanographic studies.

This method could also be considered for the extraction of other trace or ultra-trace elements (such as Hf, Nd...) that are naturally concentrated in Mn-Fe nodules.

Acknowledgements

The authors wish to thank Pr. C. Hillaire-Marcel, Pr. C. Gariépy; Dr. H. Isnard, Dr. D. Sinclair and Dr. C. Claude for their constructive helps and comments. We are also very grateful to Pr. G. Henderson and L. Robinson for agreeing to perform an

external analysis of our in-house coral standard on the Oxford University NU™ MC-ICP-MS. B.G. thanks Allyn Clark (B.I.O., Dartmouth, Canada) for providing facilities for seawater sampling during the Hudson 2002032 cruise. Financial support from NSERC-Canada and FQRNT (Fonds Québécois de Recherche Nature et Technologie) is acknowledged (awards to Hillaire-Marcel et al., and Risk et al.). ANDRA provided financial support for P.D.'s Ph.D.

References

Bacon, M.P. and Edmond, J.M., 1972. Barium at Geosecs III in the southwest Pacific. Earth and Planetary Science Letters, 16(1): 66-74.

Berkman, P.A. and Ku, T.-L., 1998. ^{226}Ra/Ba ratios for dating Holocene biogenic carbonates in the Southern Ocean: preliminary evidence from Antarctic coastal mollusc shells. Chemical Geology, 144(3-4): 331-334.

Birck, J.-L., 1986. Precision K-Rb-Sr isotopic analysis; application to Rb-Sr chronology. Chemical Geology, 56(1-2): 73-83.

Bishop, J.K.B., 1988. The barite-opal-organic carbon association in oceanic particulate matter. Nature, 332(6162): 341-343.

Bourdon, B., Joron, J.-L., Claude-Ivanaj, C. and Allègre, C.J., 1998. U-Th-Pa-Ra systematics for the Grande Comore volcanics: melting processes in an upwelling plume. Earth and Planetary Science Letters, 164(1-2): 119-133.

Broecker, W.S., Goddard, J. and Sarmiento, J.L., 1976. The distribution of ^{226}Ra in the Atlantic Ocean. Earth and Planetary Science Letters, 32(2, GEOSECS collected papers; 1973-1976): 220-235.

Chabaux, F. and Allègre, C.J., 1994. ^{238}U-^{230}Th-^{226}Ra disequilibria in volcanics; a new insight into melting conditions. Earth and Planetary Science Letters, 126(1-3): 61-74.

Chabaux, F., Ben Othman, D. and Birck, J.L., 1994. A new Ra-Ba chromatographic separation and its application to Ra mass-spectrometric measurement in volcanic rocks. Chemical Geology, 114(3-4): 191-197.

Chen, J.H., Edwards, R.L. and Wasserburg, G.J., 1986. ^{238}U, ^{234}U and ^{232}Th in seawater. Earth and Planetary Science Letters, 80(3-4): 241-251.

Cheng, H., Edwards, R.L., Hoff, J., Gallup, C.D., Richards, D.A. and Asmerom, Y., 2000. The half-lives of Uranium-234 and Thorium-230. Chemical Geology, 169(1-2): 17-33.

Claude-Ivanaj, C., Bourdon, B. and Allègre, C., 1998. Ra-Th-Sr isotope systematics in Grande Comore Island: a case study of plume-lithosphere interaction. Earth and Planetary Science Letters, 164(1-2): 99-117.

Cohen, A.S. and O'Nions, K., 1991. Precise determination of femtogram quantities of radium by Thermal Ionization Mass Spectrometry. Analytical Chemistry, 63: 2705-2708.

Curie, M. and Debierne, A., 1910. Sur le radium métallique. Comptes Rendus de l'Académie des Sciences, 151: 523.

Dehairs, F., Chesselet, R. and Jedwab, J., 1980. Discrete suspended particles of barite and the barium cycle in the open ocean. Earth and Planetary Science Letters, 49(2): 528-550.

Delanghe, D., Bard, E. and Hamelin, B., 2002. New TIMS constraints on the uranium-238 and uranium-234 in seawaters from the main ocean basins and the Mediterranean Sea. Marine Chemistry, 80(1): 79-93.

Deschamps, P., Doucelance, R., Ghaleb, B. and Michelot, J.L., 2003. Further investigations on optimized tail correction and high-precision measurement of Uranium isotopic ratios using Multi-Collector ICP-MS. Chemical Geology, 201(1-2): 141-160.

Falkner, K.K., O'Neill, D.J., Todd, J.F., Moore, W.S. and Edmond, J.M., 1991. Depletion of barium and radium-226 in Black Sea surface waters over the past thirty years. Nature, 350(6318): 491-494.

Hamelin, B., Bard, E., Zindler, A. and Fairbanks, R.G., 1991. $^{234}U/^{234}U$ mass spectrometry of corals; how accurate is the U-Th age of the last interglacial period? Earth and Planetary Science Letters, 106(1-4): 169-180.

Henderson, G.M., Slowey, N.C. and Haddad, G.A., 1999. Fluid flow through carbonate platforms: constraints from $^{234}U/^{238}U$ and Cl^- in Bahamas pore-waters. Earth and Planetary Science Letters, 169(1-2): 99-111.

Jeandel, C., Dupré, B., Lebaron, G., Monnin, C. and Minster, J.F., 1996. Longitudinal distributions of dissolved barium, silica and alkalinity in the western and southern Indian Ocean. Deep-Sea Research. Part I: Oceanographic Research Papers, 43(1): 1-31.

Koide, M., Bruland, K.W. and Goldberg, E.D., 1976. ^{226}Ra chronology of a coastal marine sediment. Earth and Planetary Science Letters, 31(1): 31-36.

Liebetrau, V., Eisenhauer, A., Gussone, N., Worner, G., Hansen, B.T. and Leipe, T., 2002. $^{226}Ra_{excess}/Ba$ growth rates and U-Th-Ra-Ba systematic of Baltic Mn/Fe crusts. Geochimica et Cosmochimica Acta, 66(1): 73-83.

Ludwig, K.R., Simmons, K.R., Szabo, B.J., Winograd, I.J., Landwehr, J.M., Riggs, A.C. and Hoffman, R.J., 1992. Mass-spectrometric ^{230}Th-^{234}U-^{238}U dating of the Devils Hole calcite vein. Science, 258(5080): 284-287.

Pons-Branchu, E., 2001. Datation haute résolution de spéléothèmes ($^{230}Th/^{234}U$ et $^{226}Ra/^{238}U$). Application aux reconstitutions environmentales autour des sites du Gard et de Meuse / Haute-Marne. Ph-D Thesis, Université Aix-Marseille III.

Rihs, S., Condomines, M. and Fouillac, C., 1997. U- and Th-series radionuclides in CO_2- rich geothermal systems in the French massif central. Journal of Radioanalytical and nuclear Chemistry, 226(1-2): 149-157.

Rihs, S., Condomines, M. and Sigmarsson, O., 2000. U, Ra and Ba incorporation during precipitation of hydrothermal carbonates: implications for ^{226}Ra-Ba dating of impure travertines. Geochimica et Cosmochimica Acta, 64(4): 661-671.

Sigmarsson, O., 1996. Short magma chamber residence time at an Icelandic volcano inferred from U-series disequilibria. Nature, 382(6590): 440-442.

Sigmarsson, O., Chmeleff, J., Morris, J. and Lopez, E.L., 2002. Origin of ^{226}Ra-^{230}Th disequilibria in arc lavas from southern Chile and implications for magma transfer time. Earth and Planetary Science Letters, 196(3-4): 189-196.

Staubwasser, M., Henderson, G.M., Berkman, P. and Hall, B.L., Submitted. Ba, Ra, Th and U in marine mollusc shells and the potential of $^{226}Ra/Ba$ dating of

Holocene marine carbonate shells. submitted to Geochimica et Cosmochimica Acta.

Vigier, N., Bourdon, B., Turner, S. and Allègre, C.J., 2001. Erosion timescales derived from U-decay series measurements in rivers. Earth and Planetary Science Letters, 193(3-4): 549-563.

Volpe, A.M. and Goldstein, S.J., 1993. ^{226}Ra-^{230}Th disequilibrium in axial and off-axis mid-ocean ridge basalts. Geochimica et Cosmochimica Acta, 57(6): 1233-1241.

Volpe, A.M., Olivares, J.A. and Murrrell, M.T., 1991. Determination of radium isotpe ratios and abundances in geologic sample by Thermal Ionization Mass Spectrometry. Analytical Chemistry, 63: 913-916.

PARTIE B:

CARACTÉRISATION DE LA MIGRATION DES RADIONUCLÉIDES AU SEIN DES FORMATIONS SÉDIMENTAIRES DU SITE ANDRA DE L'EST

PARTIE B: CARACTÉRISATION DE LA MIGRATION DES RADIONUCLÉIDES AU SEIN DES FORMATIONS SÉDIMENTAIRES DU SITE ANDRA DE L'EST

Présentation

Politique de gestion de déchets nucléaires en France

En France, c'est par une loi, promulguée le 30 Décembre 1991, dite loi Bataille, que le parlement français a fixé les conditions de mise en œuvre d'une politique de gestion à long terme des déchets nucléaires. Cette loi définit trois volets complémentaires de recherche, conduits en parallèle:

- la réduction de la nocivité à long terme de ces déchets (séparation, transmutation);
- le conditionnement des déchets pour un entreposage de longue durée en surface;
- l'étude de formations géologiques profondes, notamment grâce à la réalisation de laboratoires souterrains en vue d'un éventuel stockage en profondeur.

L'évaluation finale de ces différentes voies de recherche était initialement prévue en 2006, date à laquelle le Parlement devra se prononcer sur un choix de mode de gestion à long terme des déchets à vie longue et/ou de haute radioactivité issus de la filière nucléaire.

La mise en œuvre de cette dernière voie a été confiée à l'ANDRA, Agence Nationale pour la Gestion des Déchets Radioactifs. La loi stipule que plusieurs laboratoires souterrains devront être installés, et ce, si possible, dans des contextes

géologiques différents ("argiles", "granite"). Après une période de concertation menée dans le cadre d'une mission de médiation confiée à C. Bataille, trois sites ont finalement été proposés: la Vienne, le Gard rhodanien et l'Est du bassin de Paris. A la suite d'un programme de reconnaissance géologique conduit par l'Agence afin de s'assurer du caractère favorable du système géologique, le 9 Décembre 1998, le gouvernement français décide de ne retenir dans un premier temps, qu'un seul site, celui situé dans l'Est du bassin parisien. Le décret du 3 août 1999 autorise la création d'un laboratoire souterrain sur la commune de Bure, située à la limite entre les départements de la Meuse et de la Haute-Marne.

Description du site expérimental ANDRA de Bure situé dans la partie Est du bassin de parisien

Le site expérimental de type "argile" de l'ANDRA, retenu pour l'implantation d'un laboratoire de recherche souterrain, est localisé sur la bordure orientale du bassin sédimentaire parisien, domaine tectoniquement peu actif et pratiquement asismique, à la limite des départements de la Meuse et de la Haute-Marne, au sein des terrains Jurassiques. Cette série sédimentaire (voir Figure B.1.), affleurante dans la zone d'étude, a une hauteur cumulée de 1300 mètres. Elle est composée d'une alternance de calcaires, marnes et argilites. Une description complète des caractéristiques géologiques, minéralogiques, hydrogéologiques et géochimiques du site pourra être trouvée dans le Référentiel Géologique publié par l'ANDRA (2001) ainsi que dans la synthèse des reconnaissances hydrogéochimiques du site (1998). En guise de synthèse, voici quelques éléments essentiels à la présente étude.

La formation cible du Callovo-Oxfordien est une argilite silteuse carbonatée, contenant 40 à 50 % de minéraux argileux (ces variations lithologiques sont mineures), datée de 150 à 156 Ma. Plongeant légèrement vers le Nord-Ouest, cette couche, sub-horizontale et continue sur une surface de plus de 10 km^2, a une

épaisseur totale de l'ordre de 130 mètres et se situe à une profondeur de 420 mètres au droit du sondage EST 103 où l'implantation du laboratoire est prévue. Elle est encadrée à ses épontes par deux unités carbonatées: à son mur, les faciès oolithiques à gravelo-bioclastiques du Bathonien-Callovien (Dogger); à son toit, la puissante unité des calcaires micritiques puis récifaux de l'Oxfordien moyen à supérieur.

Caractéristiques hydrogéologiques et propriétés des argilites du Callovo-Oxfordien

Le niveau d'argilite du Callovo-Oxfordien est très faiblement perméable sur toute sa hauteur. Cette formation est en charge vis-à-vis des encaissants carbonatés et aucune venue d'eau significative n'a été décelée lors des différents forages réalisés par l'ANDRA. Les eaux interstitielles obtenues par pressage et déshydratation sous vide des échantillons d'argilite ont un faciès chloruro-sulfaté sodique et ont une salinité comprise entre 2,7 et 7,4 $g.l^{-1}$.

Les premiers résultats soulignent les bonnes propriétés de confinement de cette formation. La faible porosité (10 à 15 %), la forte surface spécifique des argilites ainsi que la nature minéralogique des argiles (illites et plus particulièrement smectites) garantissent une forte capacité de rétention des radionucléides.

Contexte hydrogéologique et hydrogéochimique

Au droit du site du futur laboratoire, l'Oxfordien est isolé des formations carbonatées aquifères (Tithonien), le plus souvent karstiques, par une couche de marnes silteuses à niveaux de calcaires marneux de faible perméabilité de plus de 100 mètres d'épaisseur (Kimméridgien). Si ce n'est aux zones d'affleurements où cette formation est aquifère, l'Oxfordien calcaire est en profondeur une nappe captive de très faible perméabilité ($\sim 10^{-9}$ $m.s^{-1}$). Aucune trace de karstification n'a été repérée et les venues d'eaux sont rares et faibles, le plus souvent limitées à des bancs plus poreux d'échelle métrique. La composition chimique du fluide serait bicarbonatée sodique pour une salinité d'environ 1,5 $g.l^{-1}$ ce qui contraste avec la composition des eaux superficielles.

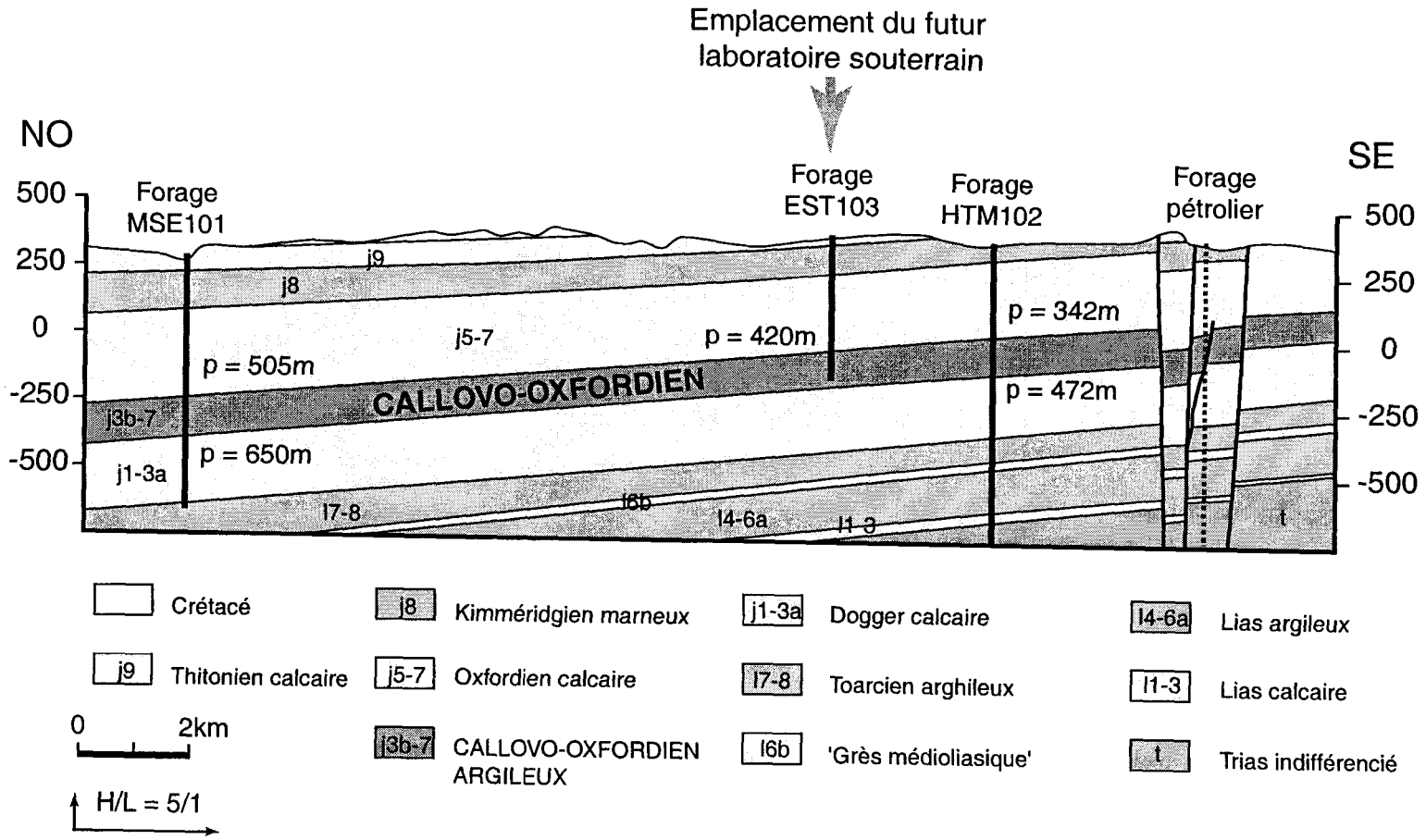

Figure B.1.: Coupe géologique Nord Ouest - Sud Est du site expérimental ANDRA de l'Est de la France
(extrait du rapport ANDRA, Recherches préliminaires à l'implantation des laboratoires de recherche souterrains, Bilan des travaux, 1996)

En profondeur, le Dogger présente une très faible perméabilité (~10^{-10} m.s^{-1}) augmentant parfois légèrement au voisinage de zones fissurées (~10^{-8} m.s^{-1}). Sur les deux forages réalisés par l'ANDRA traversant cette formation, seule une venue d'eau a été détectée dans le forage MSE 101. La composition chimique du fluide recueilli est de type chloruro-sulfatée sodique et possède une salinité de l'ordre de 4,3 g.l^{-1}.

Etant données les faibles perméabilités de ces deux formations en profondeur et les valeurs des gradients hydrauliques, les vitesses d'écoulement au droit du site du futur laboratoire sont faibles pour l'Oxfordien, voire quasiment nulles pour le Dogger.

Etude préalable

Les travaux menés durant cette thèse ont été initiés suite à une étude préliminaire réalisée par le BRGM (Casanova et Négrel, 1999). Cette étude avait pour objectif de retracer les éventuelles circulations souterraines ayant affecté la formation hôte du site de l'Est. L'approche méthodologique proposée s'appuyait sur l'utilisation conjuguée de différents traceurs isotopiques naturels (^{18}O, ^{13}C, ^{234}U, ^{238}U, ^{230}Th, ^{232}Th, ^{86}Sr, ^{87}Sr, Rb/Sr). Aucun indice prouvant une ouverture du système n'a pu être décelé au sein des argilites du Callovo-Oxfordien.

Ces travaux ont cependant mis en évidence des déséquilibres significatifs entre l'uranium-234 et son descendant le thorium-230 (($^{230}Th/^{234}U$)>1) sur des échantillons de roches carbonatées (analyses effectuées sur roche totale) situés au niveau des zones de transition entre la couche cible et ses épontes (voir Figure B.2.). En supposant que le processus responsable de ce flux négatif d'uranium soit dû à un événement sporadique et quasi actuel, les déséquilibres radioactifs ($^{230}Th/^{234}U$) de l'ordre de 1,4 et 1,6 observés sur les échantillons HTM 80638 (prof. 472.89) et MSE 01626 (prof. 650.79 m) correspondent à un départ minimum d'uranium respectivement de 29% et 37% par rapport au ^{230}Th, le thorium étant supposé

immobile. Ces estimations de flux sont de plus réalisées dans le cas le plus favorable au sens où les hypothèses émises minimisent la proportion d'uranium remobilisé.

Les deux articles présentés dans cette partie confirment ces résultats dans le sens où les formations carbonatées aux épontes de la formations argileuse cible ne sauraient être considérées comme totalement closes d'un point de vue chimique. La stratégie d'échantillonnage ainsi que la technique analytique choisie (MC-ICP-MS *vs* comptage α) qui améliore de deux ordres de grandeurs la précision analytique ont toutefois permis d'aller plus avant quant aux significations et conséquences des déséquilibres radioactifs observés dans ce système géologique.

Le premier article de cette partie (Chapitre III) a été soumis à la revue *Hydrology and Earth System Sciences*, sous le titre "*$^{234}U/^{238}U$ Disequilibrium along stylolitic discontinuities in deep Mesozoic limestone formations of the Eastern Paris basin: evidence for discrete uranium mobility over the last 1-2 million years*" et présente une partie des résultats ($^{234}U/^{238}U$) obtenus sur les échantillons provenant des formations carbonatées. Il aborde plus spécifiquement les déséquilibres ($^{234}U/^{238}U$) observés au niveau des zones caractérisées par des surfaces de pression-dissolution et mis en évidence par un sous-échantillonage du matériel stylolitique et de la matrice carbonatée associée.

Le dernier article (Chapitre IV) présente l'ensemble des résultats obtenus sur les échantillons du site de l'Est, tant au niveau de la formation argileuse cible que des formations carbonatées encaissantes (Bathonien et Oxfordien). Il aborde plus particulièrement les implications chronologiques qui découlent des déséquilibres radioactifs observés, ainsi que les processus responsables de la remobilisation de l'uranium dans le système. Ce manuscrit est encore en préparation et devrait faire l'objet à terme d'une soumission à la revue *Earth and Planetary Science Letters*.

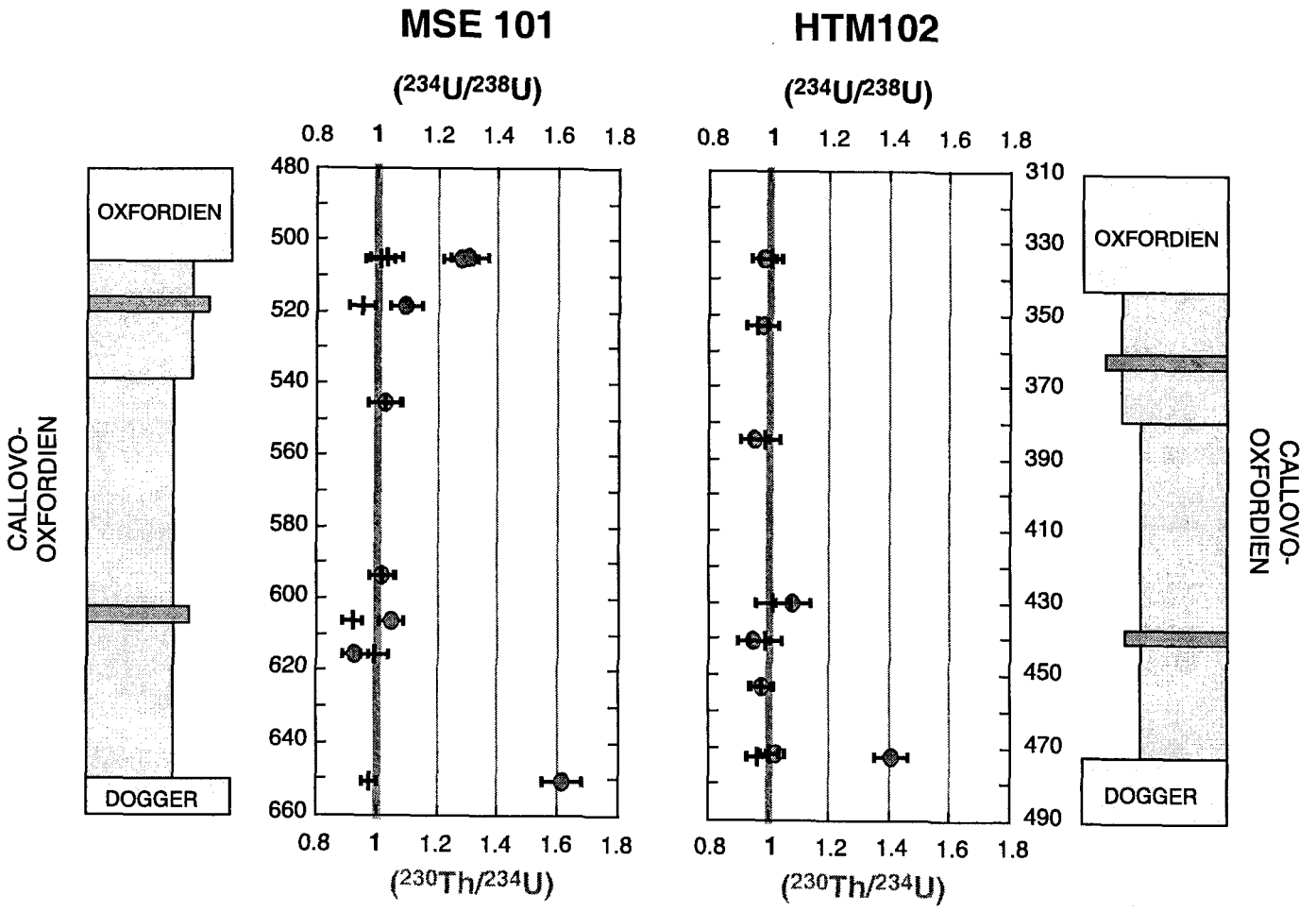

Figure B.2.: Variations des rapports ($^{234}U/^{238}U$) et ($^{230}Th/^{234}U$) dans des échantillons de roche totale des sondages MSE 101 et HTM 102 en fonction de la profondeur
(données BRGM, Casanova et Négrel, 1999)

Références

ANDRA, 1998. Site de l'Est- Synthèse des reconnaissances hydrogéochimiques. D RP 0ANT 97-069.

ANDRA, 2001. Référentiel Géologique du Site Meuse-Haute Marne. A RP ADS 99-005/B.

Casanova, J. et Négrel, P., 1999. Site de l'Est- Etude du système uranium-thorium dans la couche des argilites du Callovo-Oxfordien et ses épontes- Etude des forages MSE101 et HTM102. D RP 0ANT 98-026/A.

Chapitre III

$^{234}U/^{238}U$ Disequilibrium along stylolitic discontinuities in deep Mesozoic limestone formations of the Eastern Paris basin: evidence for discrete uranium mobility over the last 1-2 million years

Pierre Deschamps, Claude Hillaire-Marcel, Jean-Luc Michelot
Régis Doucelance, Bassam Ghaleb and Stéphane Buschaert

Submitted to Hydrology and Earth System Sciences

Abstract

The ($^{234}U/^{238}U$) equilibrium state of borehole core samples from the deep, low-permeability limestone formations surrounding the target argilite layer of the Meuse/Haute-Marne experimental site of the French agency for nuclear waste management -ANDRA- (Agence nationale pour la gestion des déchets radioactifs) was examined in order to improve our understanding of naturally occurring radionuclide behaviour in such geological settings. Highly precise, accurate MC-ICP-MS measurements of the ($^{234}U/^{238}U$) activity ratio show that limestone samples characterized by pressure dissolution structures (stylolites or dissolution seams) display systematic ($^{234}U/^{238}U$) disequilibria, while the pristine carbonate samples remain in the secular equilibrium state. The systematic feature is observed throughout the zones marked by pressure dissolution structures: i) the material within the seams shows a deficit of ^{234}U over ^{238}U (($^{234}U/^{238}U$) down to 0.80) and ii) the surrounding carbonate matrix is characterized by an activity ratio greater than unity (up to 1.05).

These results highlight a centimetric-scale uranium remobilization in the limestone formations along these sub-horizontal seams. Although their nature and modalities are not fully understood, the driving processes responsible for these disequilibria were active during the last 1-2 Ma.

Keywords: Uranium isotopes; Multiple-Collector ICP-MS; waste management; remobilization; migration.

III.1. Introduction

This study is part of geological investigations conducted by ANDRA since 1994 (Agence nationale pour la gestion des déchets radioactifs —the French agency for nuclear waste management) around the Underground Research Laboratory of Bure, excavated in a clay layer of the Eastern part of the sedimentary Paris Basin, France. ANDRA was given the responsibility of assessing the safety of High-Level-Radioactive Waste (HLRW) repositories in deep geological environment. The safety of such nuclear waste disposal generally relies on a multi-barrier approach. Engineered and natural barriers are combined to prevent, or at least retard, radionuclide migration from the disposal site to the biosphere. These barriers must isolate wastes for periods sufficiently long to allow radioactivity to decay at acceptable levels. Although artificial barriers play an important role in long-term waste containment, the natural barrier (the host rock and the geological environment in which the repository is constructed, termed the "far field"), plays a major role in the overall safety of the storage. In this framework, hydrological and geochemical behaviours of the potential host geological system must be taken into account to estimate its long-term confining capacities.

In this context, the systematics of naturally occurring uranium-decay series is a relevant tool providing site-specific, natural chemical analogue information for the assessment of *in situ*, short-to-long-term migration of radionuclides in the far field of the repository (see review in Ivanovich, 1991; Ivanovich et al., 1992). One of the various applications of U-series systematics relevant to the study of radioactive waste disposal is the assessment of the chemical stability of potential host formations with respect to transporting chemical species by determination of radioactive equilibrium state in the rock body (Schwarcz et al., 1982).

In this study, we examine the present state of equilibrium between uranium-238 and one of its daughters, uranium-234, in sedimentary rocks at the ANDRA experimental site located in the eastern part of the Paris basin. We report isotopic uranium analyses of whole-rock samples from the deep, low-permeability limestone formations surrounding the target clayey layer. The highly precise and accurate MC-ICP-MS measurements of the ($^{234}U/^{238}U$) activity ratio highlight disequilibrium in the vicinity of pressure dissolution structures. This enables us (i) to document the *in situ* mobility of uranium within this sedimentary environment; and (ii) to deduce temporal indications on U-remobilization in the system on a time scale of up to 1-2 Ma.

III.2. Principle of U-Th decay series study to radionuclide migration in rock matrix

Uranium and thorium are ubiquitous radioactive elements that occur naturally at trace levels in all Earth materials (Gascoyne, 1992). Their daughter nuclides are present in rocks in abundance, depending on: i) their initial concentrations at the time of the system closure; ii) the concentrations of their parents; and iii) the time span elapsed since the last closure of the system. In a geological system that has remained closed to radionuclide migration for at least 1-2 Ma (i.e. a few half-lives of the longest-lived daughter of the U-Th series: uranium-234, $T_{1/2}$ = 245,250 a), the activities (defined as disintegrations per minute per gram, or dpm/g) of the intermediate nuclides are equal to the activities of their parents. This state is known as secular equilibrium. Thus, for a host rock older than 2 Ma, the attainment of secular equilibrium in the U and Th series becomes a strong indicator of a closed-system behaviour, although it is possible, but highly unlikely, that inward or outward fluxes of all radionuclides occur at an equal rate in an open system.

Conversely, when a departure from the state of equilibrium between a parent and its daughter is observed, i.e. a daughter-parent activity ratio distinct from unity, the system has been disturbed by a process fractionationing the two nuclides from each other. This disruption from the secular equilibrium state originates from processes capable of fractionating nuclides from one another as a result of either their specific chemical properties or of a phenomenon directly related to the radioactive decay itself, known as the recoil effect.

In low-temperature environments on the Earth's surface, discriminating chemical processes essentially occur at the water-rock interface and proceed from distinct properties of the radionuclides during water-rock interactions such as solubility, adsorption, complexation or redox-sensitive behaviour. The recoil effect is a general term referring to the different physical mechanisms related to radioactive decay and inducing disequilibrium among radionuclides[1]. After the radioactive decay of a α-emitter parent, the resulting daughter is emitted with a finite kinetic energy. The crystalline lattice where the parent was located is damaged and the recoil atom is displaced from this initial position. Two main mechanisms are usually evoked to account for subsequent fractionation. When the α-emitter parent is located close to the edge of the grain, the recoil atom can be directly ejected from the grain into an adjacent phase, in most cases, the interstitial liquid phase (Kigoshi, 1971). Alternatively, after the parent disintegration, the daughter is located in a radiation-damaged site within the mineral grain, where it is more prone to subsequent removal or chemical remobilization by fluids, e.g. by oxidation (Fleischer and Raabe, 1978; Fleischer, 1980). These two phenomena account for the universal ($^{234}U/^{238}U$) radioactive disequilibria observed in the hydrosphere (Osmond and Cowart, 1976; Osmond and Cowart, 1992; Osmond and Ivanovich, 1992).

[1] For a more precise and exhaustive description of the recoil effect, refer to Gascoyne (1992), Ivanovich (1994) or Bourdon et al. (2003).

Regardless of the fractionating processes involved, the time scale in which this phenomenon occurs can be directly inferred from the half-lives of the radionuclides concerned. In the general case where the half-life of the daughter is shorter than that of its parent, as with the ^{234}U-^{238}U or ^{230}Th-^{234}U pairs, the time span required to return to equilibrium state is determined by the half-life of the daughter. Although ultimately dependent on analytical precision, it is generally stated that the return to equilibrium occurs after 4-6 half-lives of the daughter (Condomines et al., 1988; Gascoyne et al., 2002; Bourdon et al., 2003). Therefore, U-Th-series disequilibria are a sensitive tool to trace phenomena that have disturbed a given system and to constrain chronologically them by providing a wide range of time scales corresponding to the half-lives encountered in the ^{238}U, ^{235}U and ^{232}Th series.

The significance of these isotopic clocks to study radionuclide migration in deep geological formation was first addressed by Schwarcz et al. (1982). These authors discussed the chronological implications of radioactive disequilibrium observed on rock matrices. They focussed mainly on the ^{226}Ra, ^{230}Th, and ^{234}U nuclides since their half-lives (1,599 a, 75,690 a and 245,250 a, respectively) are most appropriate to the time scale in which the migration of radionuclides in the far field must be assessed. This approach was then applied with success to deep experimental sites relevant to storage of radioactive waste, located in granitoid bedrock (e.g. Smellie and Stuckless, 1985; Gascoyne and Schwarcz, 1986; Smellie et al., 1986; Gascoyne and Cramer, 1987; Griffault et al., 1993) or in volcanic tuff (Gascoyne et al., 2002). In these studies, the primary focus was the altered and/or fractured zones of the rock matrix where water/rock interaction may have preferentially taken place. This approach permits investigation of the time scales of such interactions and, consequently, to constrain in time groundwater circulation events, since it is often understood that the two phenomena are related.

III.3. Geological setting and sampling

The French government authorized ANDRA the construction of a scientific Underground Research Laboratory (URL) at a depth of 500 m in a 150-million-year-old clay formation in an area straddling the Meuse and Haute-Marne departments (Eastern France).

The target formation belongs to Mesozoic sedimentary rocks in the eastern Paris Basin and is a thick (130 m), Callovo-Oxfordian argilite unit that is 420-550 m deep at the URL site (Figure III.1.). This detrital clay-rich rock is composed of illite, ordered mixed-layered illite-smectite minerals dominated by illite, kaolinite, minor amounts of chlorite, and cemented by 25-30 wt % of micrite (ANDRA, 2001).

This formation is overlain and underlain by Oxfordian to Kimmeridgian and Bajocian/Bathonian (Dogger) limestones, respectively (Figure III.1.). These carbonate units display very low porosity (2-5%) and permeability, although some more porous (10-20%), metric scale levels located in the Oxfordian limestones are water productive. Sub-horizontal pressure dissolution structures are distributed throughout within these limestone formations (see Figures III.2. and III.3.). For the sake of simplicity, we will henceforth refer to such structures as "stylolites" or "stylolitized zones", although, they can actually be categorized either as "stylolites", in the strict sense, or "dissolution seams" according to the standard terminology proposed by Buxton and Sibley (1981) and Bathurst (1987).

At the regional scale, these stylolitic seams have been documented in all the Mesozoic limestone formations (Coulon, 1992). According to this author, they could have a tectonic origin and be related to the Oligocene extension in the western part of the Eurasian plate. However, some of them were probably formed earlier by overburden during sedimentary loading of the series (ANDRA, 2001).

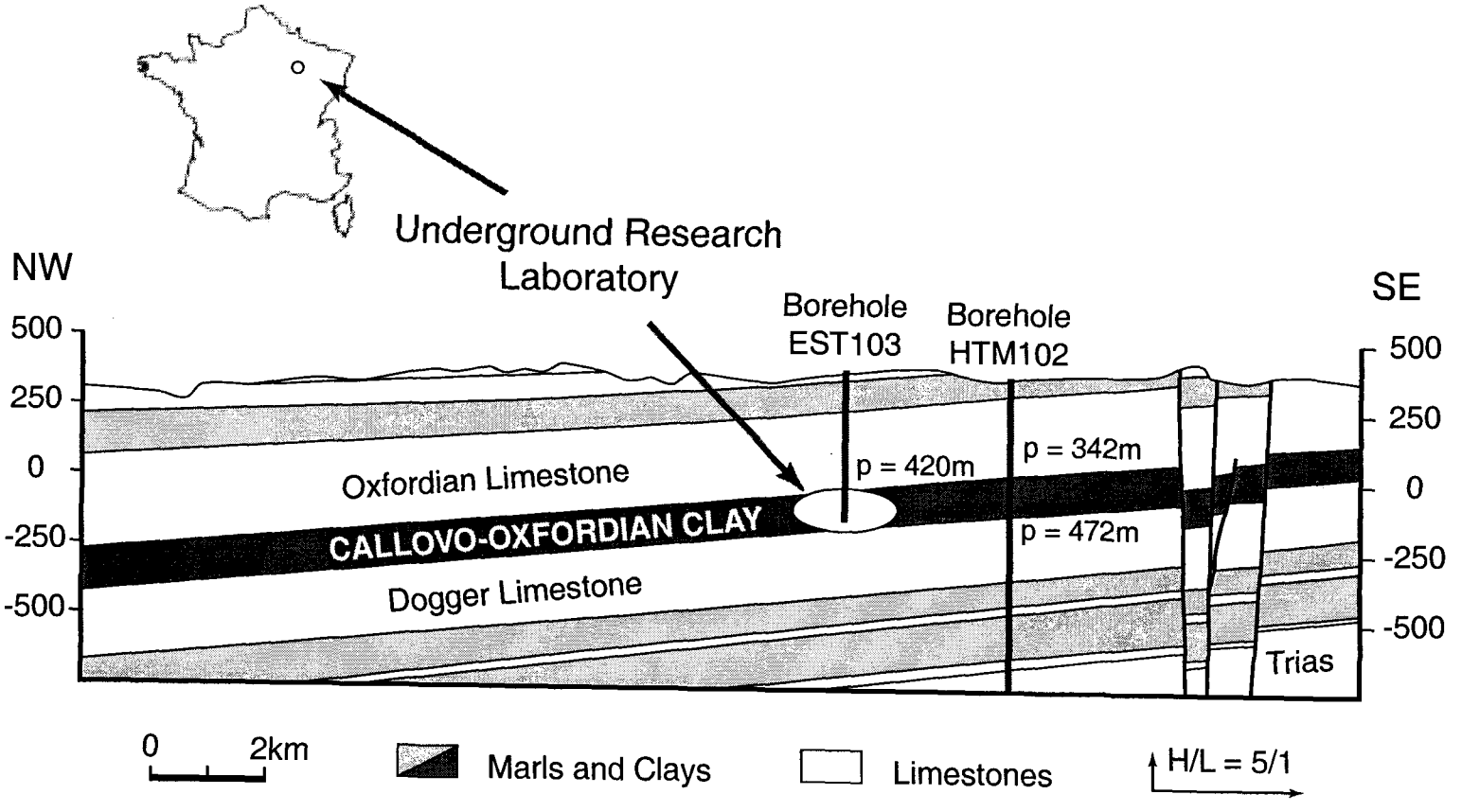

Figure III.1.: Location of the ANDRA Underground Research Laboratory (URL) in the eastern part of the Paris basin and Northwest/Southeast geological cross-section throughout the sedimentary target layers.

The core samples analyzed were obtained from the HTM 102 ANDRA prospecting borehole located near the site where the URL is being built. This 1,100 m deep borehole was drilled throughout the whole sedimentary series from the Kimmeridgian to the Bathonian unit. It cross-cuts the target Callovo-Oxfordian argilite unit found between 342.70 m and 472.16 m below core top.

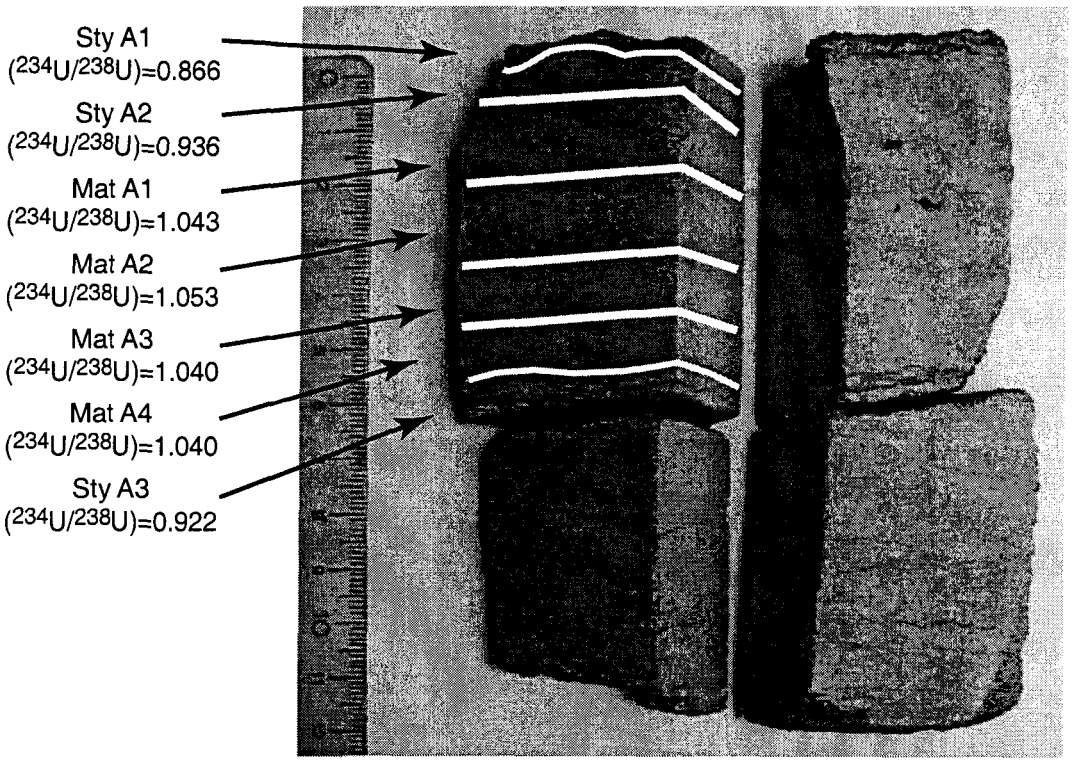

Figure III.2.: Subsampling of the HTM 02928 sample located in the Bathonian limestone formation (478 m depth). This sample is characterized by two major pressure dissolution structures (swarms of dissolution seams) that were sampled (Sty A1, Sty A2 and Sty A3 subsamples). The carbonate matrix located between these two stylolites was also sampled (Mat A1 to Mat A4 subsamples). The measured ($^{234}U/^{238}U$) activity ratio are reported.

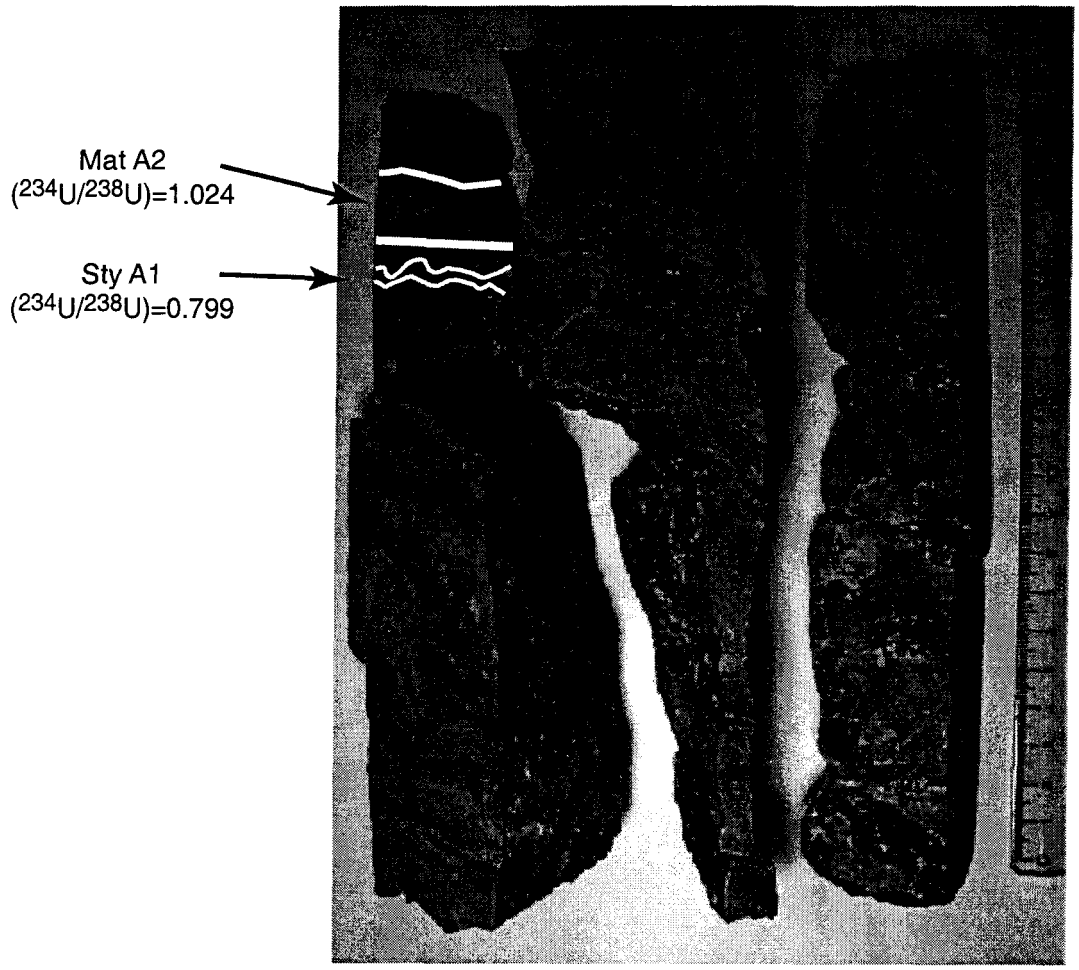

Figure III.3.: Subsampling of the HTM 80824 sample located in the Oxfordian limestone formation (306 m depth). This sample is characterized by several sub-millimetric stylolitic seams. One of these seams (Sty A1 subsample), together with the embedding carbonate matrix within close proximity (Mat A1 subsample) were sampled. The measured ($^{234}U/^{238}U$) activity ratio are reported.

Ten samples from the Bathonian and Oxfordian formations and two samples from the upper part of the Callovo-Oxfordian formation were examined. In the two limestones formations, sampling was mainly focused on zones displaying pressure dissolution structures. Seven of the ten limestone samples selected are characterized by sub-horizontal, millimetric to centimetric-scale seams. In these samples, the

material inside the joints as well as parts of the surrounding carbonate matrix were subsampled (see Figures III.2. and III.3.). For the sampling of the material within stylolitic seams, care was taken to exclude as much of the surrounding matrix rock as possible.

Finally, five samples that are not characterized by pressure dissolution structures (and which will be referred to as "pristine" samples hereafter) and twenty-five "stylolitic" subsamples were crushed, finely powdered and analyzed for their uranium content and $^{234}U/^{238}U$ isotopic composition.

III.4. Experimental techniques

III.4.1. Chemical procedure

Because of the large amount of clay and organic impurities in the carbonate matrix, the chemical procedure for uranium separation and purification developed for these samples was modified from the usual chemical procedures used for pure carbonate matrices (Edwards et al., 1987; Labonne and Hillaire-Marcel, 2000). More particularly, the digestion step needs to be adapted to ensure that the sample is totally dissolved.

Sample aliquots of 0.1 to 1 g were firstly weighed and burnt in a furnace at 650°C for 6 hours in order to oxidize the organic matter. Secondly, aliquots were digested by sequential treatment with concentrated nitric acid and aqua regia in PFA Teflon Savillex™ previously spiked with a ^{236}U-^{233}U mixed solution (Deschamps et al., 2003). The residues of insoluble material were centrifuged in nitric media, separated from the supernate liquid phase and further digested with concentrated nitric and hydrofluoric acids. At this step, the residues were totally dissolved. These solutions were dried before being dissolved in the previous supernate nitric solution. Uranium and thorium were then co-precipitated with Fe by the addition of ammonium hydroxide to pHs above 6 to 7 in order to optimize uranyl adsorption onto

amorphous $Fe(OH)_3$ (Hsi and Langmuir, 1985; Waite et al., 1994). Because of the large amount of clay in some samples, aluminum oxyhydroxides also co-precipitated with amorphous $Fe(OH)_3$. The mixture was centrifuged, the supernatant discarded, and the precipitate was rinsed twice with Milli-Q water. The residue was then dissolved in 7N HNO_3, loaded onto a 2 ml column of anionic exchange resin (AG 1X8) and rinsed with 2 ml 7N HNO_3. Uranium and thorium fractions were then eluted together with MQ water and 6N HCl. This pre-purification step allows most of the major elements, especially Al, to be discarded. The fraction containing U and Th was dried down before being re-dissolved in 6N HCl. Uranium and Thorium fractions were separated on a second 2ml column of anionic exchange resin (AG 1X8). The Th fraction was eluted with 6N HCl, then dried before being purified on a 0.5 ml column of anionic exchange resin (AG 1X8) in 7N HNO_3. This Th fraction was stored for later analysis. The U fraction was eluted with MQ water, dried and purified on a 0.2 ml column of extraction chromatographic resin (U/Teva Elchrom™) in 2N HNO_3. The chemical yield for uranium achieved using this protocol was always greater than 90%.

III.4.2. MC-ICP-MS analyses

The uranium analyses were performed on a Micromass IsoProbe™ MC-ICP-MS at the GEOTOP Research Center. In contrast to the methods usually carried out by other MC-ICP-MS users for uranium analyses (e.g. Luo et al., 1997), we used Faraday detectors in static mode only. This approach avoids the problems of inter-calibration of the Daly and Faraday detector gains. However, since we do not use a Daly detector and its associated energy filter, the high abundance sensitivity of our instrument (up to 28 ppm) raises another major difficulty: that of precise estimation of tailing effects. We therefore developed a method for tail correction, quite similar to the one proposed by Thirlwall (2001), based on the effective and precise quantification of tail

contribution underneath each peak due to adjacent ion beams, as independently determined by measurements of mono-isotopic ion beams.

For uranium analyses, mass discrimination bias is corrected for by the use of a ^{236}U-^{233}U double spike. Using an Aridus desolvating microconcentric nebulizer system, the amount of U consumed per $^{234}U/^{238}U$ analysis is about 200 ng, which is sufficient for obtaining a ^{234}U signal of 4 mV for 50 cycles of 5 seconds. The entire procedure is described in detail in Deschamps et al. (2003).

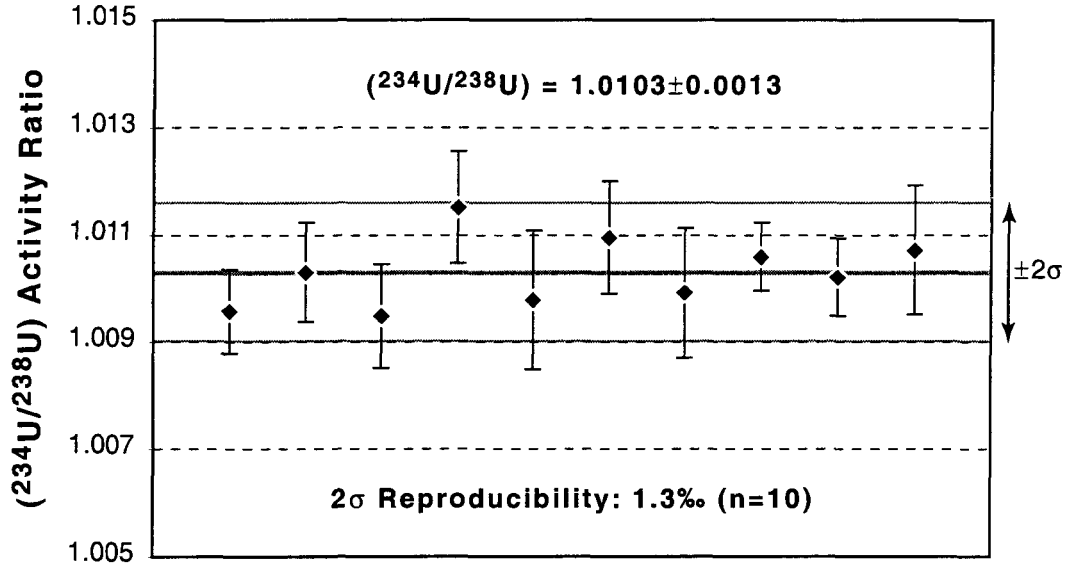

Figure III.4.: Replicate analyses of the ($^{234}U/^{238}U$) activity ratio of the HTM 02924 A #1 carbonate rock sample. The total external reproducibility is ±1.3‰ (2σ, n=10). Analyses were performed on a Micromass IsoProbe™ MC-ICP-MS at the GEOTOP Research Center using the method described in Deschamps et al. (2003). ($^{234}U/^{238}U$) activity ratios are calculated using the half-life values determined by Cheng et al. (2000). Error bars indicate 2σ internal precision.

The accuracy and precision of the analytical protocol was assessed by measurements of a reference material (the NBL-112a standard, also called CRM-145, or formerly, NBS SRM-960). Nineteen replicate analyses of this standard yielded a

mean $\delta^{234}U$ value of -36.42±0.80‰ (2σ) that is in excellent agreement with previously published values (see review in Deschamps et al., 2003). For this specific study, the actual reproducibility on natural samples was determined by replicate measurements of an in-house carbonate standard, a powdered Bathonian limestone sample (HTM 02924 Mat #1) from the ANDRA HTM 102 borehole. The results, reported in Table 1 and Figure III.4., yielded a mean ($^{234}U/^{238}U$) activity ratio of 1.103±0.0013 (2σ, n= 10), which yields a total reproducibility (analytical plus chemical) of ~1.3‰, at the 95% confidence level. For the uranium concentration, a total reproducibility of 5‰ was obtained ([^{238}U] = 526.8±2.9 ppb, 2σ, n= 10).

Table 1 : Replicate measurements of the ($^{234}U/^{238}U$) activity ratio and uranium content of an in-house limestone rock standard (HTM 02924 A #1 sample) with the GEOTOP MicroMass IsoProbe™ MC-ICP-MS.

Sub-Sample	^{238}U (ppb)	($^{234}U/^{238}U$) AR*
#1	526.736 ± 0.4	1.0096 ± 0.0008
#2	523.986 ± 0.5	1.0103 ± 0.0009
#3	527.906 ± 0.4	1.0095 ± 0.0010
#4	526.395 ± 0.4	1.0115 ± 0.0010
#5	528.397 ± 0.5	1.0098 ± 0.0013
#6	528.422 ± 0.5	1.0110 ± 0.0011
#7	528.023 ± 0.5	1.0099 ± 0.0012
#8	525.280 ± 0.5	1.0106 ± 0.0006
#9	526.605 ± 0.5	1.0102 ± 0.0007
#10	526.294 ± 0.5	1.0107 ± 0.0012
Mean (± 2σ, n = 10)	**526.8** ± 2.9	**1.0103** ± 0.0013
2σ (%)	**0.55%**	**0.13%**

* ($^{234}U/^{238}U$) activity ratios (AR) are calculated using the half-life values given by Cheng et al. (2000).
All errors are given at the 95% confidence level (2σ).

III.5. Results

Uranium concentrations and ($^{234}U/^{238}U$) activity ratios (AR) results of thirty samples, together with a brief description (host formation, depth, length and sample type –matrix vs. seams) are listed in Table 2. The errors listed in Table 2 and reported in Figures III.5. and III.6. are given at the 95% confidence level and represent the internal error of each analysis.

In the Oxfordian limestone formation, the uranium concentrations of the carbonate matrix samples vary from 1.2 to 1.9 ppm. For stylolite samples, the U concentrations increase to 3.7-4.3 ppm. The same pattern is observed in the Bathonian formation: the carbonate matrix samples display between 0.2 and 0.6 ppm of U, whereas the stylolite samples show U-contents as high as 4 ppm. These data are within the range of uranium abundance typically encountered in such sedimentary rocks (Gascoyne, 1992).

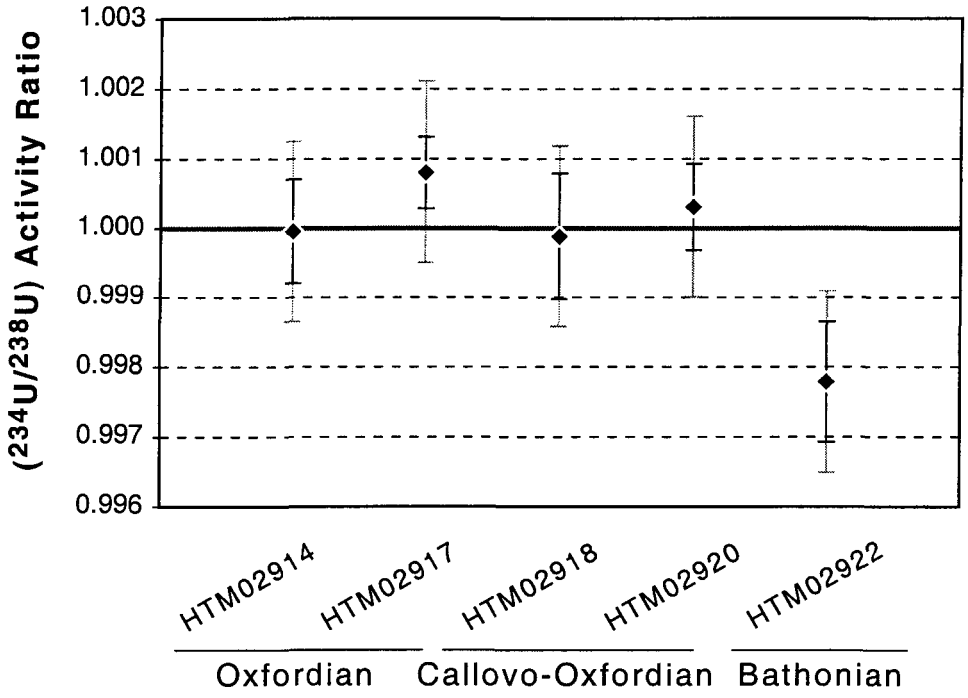

Figure III.5.: ($^{234}U/^{238}U$) activity ratio measurements of pristine samples from the ANDRA HTM 102 borehole core. ($^{234}U/^{238}U$) activity ratios are calculated using the half-life values determined by Cheng et al. (2000). Error bars indicate either 2σ internal precision (black) or 2σ external precision (grey).

Table 2 : Analyses of the ($^{234}U/^{238}U$) activity ratio and uranium content in samples from the ANDRA HTM 102 borehole with a MicroMass IsoProbe™ MC-ICP-MS at the GEOTOP research Center.

Sample	Unit	Top	Bottom	Sub-Sample	Type#	^{238}U (ppb)	($^{234}U/^{238}U$) AR*
Pristine Samples							
HTM 02914	Oxfordian	337.69	337.71			1638.7 ± 0.2	1.0000 ± 0.0008
HTM 02917	Oxfordian	340.30	340.66			1194.6 ± 1.0	1.0008 ± 0.0005
HTM 02918	Callovo-Oxfordian	345.72	346.03			657.8 ± 0.6	0.9999 ± 0.0009
HTM 02920	Callovo-Oxfordian	349.94	349.96			1407.4 ± 1.2	1.0003 ± 0.0006
HTM 02922	Bathonian	472.00	472.10			1876.2 ± 1.5	0.9978 ± 0.0009
Stylolitized Samples							
HTM 80824	Oxfordian	306.00	306.22	Mat A2	carbonate matrix	1503.6 ± 1.5	1.0244 ± 0.0003
				Sty A1	stylolitic material	3880.3 ± 5.8	0.7991 ± 0.0005
HTM 07325	Oxfordian	322.30	322.64	Mat A4	carbonate matrix	1881.5 ± 1.8	1.0023 ± 0.0003
				Sty A1	stylolitic material	4354.7 ± 4.2	0.9932 ± 0.0003
HTM 02601	Oxfordian	323.50	323.76	Mat A2	carbonate matrix	1439.0 ± 1.4	1.0028 ± 0.0004
				Sty A2	stylolitic material	3740.6 ± 3.5	0.9989 ± 0.0002
HTM 02924	Bathonian	472.81	472.96	A #1	carbonate matrix	526.9 ± 2.9	1.0106 ± 0.0013
				A #9	carbonate matrix	654.4 ± 0.6	1.0441 ± 0.0007
				A #10	carbonate matrix	557.3 ± 0.5	1.0344 ± 0.0009
				A #6a	stylolitic material	4082.4 ± 4.2	0.9628 ± 0.0005
				A #6b	stylolitic material	2196.4 ± 2.2	0.9799 ± 0.0005
HTM 02926	Bathonian	472.96	473.17	A #3	carbonate matrix	463.0 ± 0.4	1.0198 ± 0.0006
				A #23	carbonate matrix	388.5 ± 0.4	1.0203 ± 0.0010
				A #12	stylolitic material	618.2 ± 0.9	0.9361 ± 0.0021
				A #26	stylolitic material	559.0 ± 0.5	0.9154 ± 0.0008
HTM 07322	Bathonian	476.48	476.87	Mat A	carbonate matrix	774.9 ± 0.7	1.0303 ± 0.0005
				Sty A1	stylolitic material	1149.5 ± 1.1	1.0106 ± 0.0005
				Sty B2	stylolitic material	834.4 ± 0.8	0.9532 ± 0.0006
HTM 02928	Bathonian	477.66	477.77	Mat A1	carbonate matrix	260.7 ± 0.2	1.0427 ± 0.0010
				Mat A2	carbonate matrix	252.5 ± 0.2	1.0532 ± 0.0012
				Mat A3	carbonate matrix	262.1 ± 0.2	1.0399 ± 0.0011
				Mat A4	carbonate matrix	279.8 ± 0.3	1.0402 ± 0.0013
				Sty A1	stylolitic material	970.3 ± 0.9	0.8665 ± 0.0010
				Sty A2	stylolitic material	487.8 ± 0.5	0.9364 ± 0.0009
				Sty A3	stylolitic material	479.2 ± 0.4	0.9224 ± 0.0010

Carbonate matrix material refers to the embedding matrix sample in the vicinity of the stylolitic seams.

* ($^{234}U/^{238}U$) activity ratios (AR) are calculated using the half-life values given by Cheng et al. (2000). All errors are given at the 95% confidence level (2σ).

($^{234}U/^{238}U$) results of the pristine samples, illustrated in Figure III.5., show near secular equilibrium values. In this figure, we also report for each data the total analytical reproducibility achieved in the course of this study (1.3‰, 2σ). Figure III.6. presents the ($^{234}U/^{238}U$) AR of the stylolitized samples (surrounding carbonate matrix *vs* stylolite subsamples). Materials within the stylolitic joints are characterized by ($^{234}U/^{238}U$) AR from 0.999 to 0.799, while the surrounding carbonate matrix samples exhibit activity ratios between 1.002 and 1.053.

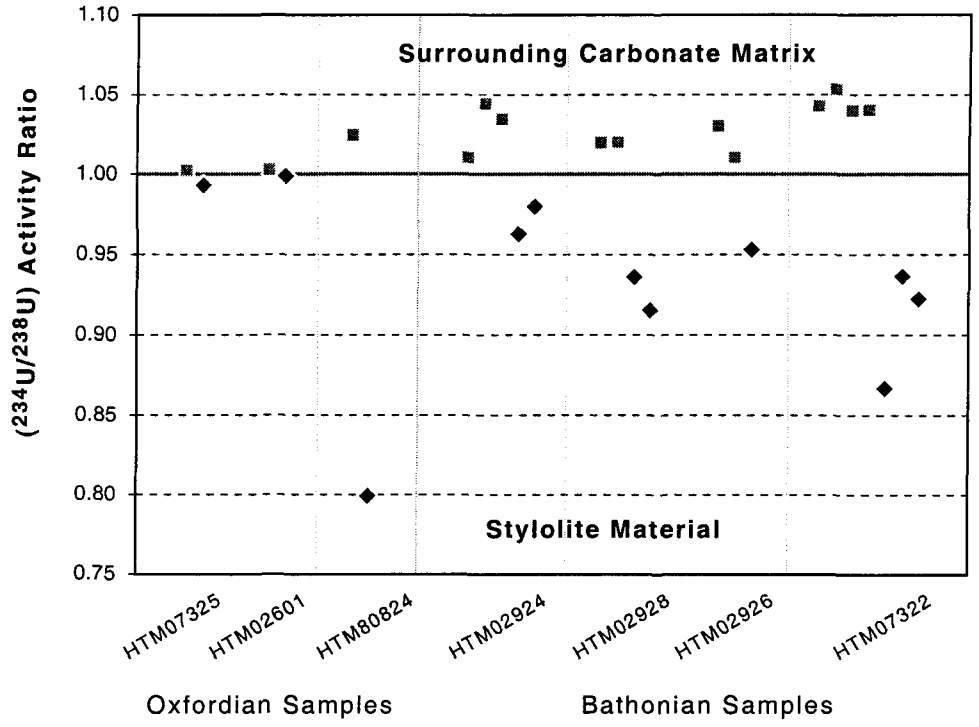

Figure III.6.: ($^{234}U/^{238}U$) activity ratio measurements on stylolitic material (black diamonds) and embedding carbonate matrix (grey squares) samples from the ANDRA HTM 102 borehole core. ($^{234}U/^{238}U$) activity ratios are calculated using the half-life values determined by Cheng et al. (2000). Error bars are in the points.

III.6. Discussion

The pristine limestone samples display secular equilibrium between ^{234}U and ^{238}U (Figure III.5.) indicating that there has been no differential migration of ^{234}U relative to ^{238}U in these samples in recent time and, likely, no U mobility at all. Indeed, it would be very unlikely that an opening in the chemical system could occur without any detectable fractionation between ^{234}U and ^{238}U, since such a phenomenon necessarily involves water/rock interactions and migration via interstitial fluids. ($^{234}U/^{238}U$) disequilibria, resulting from water/rock interaction and recoil effects at the water/rock interface, display generally highly significant departure from unity in fluid phases and, to a lesser extend, in solid matrix (Osmond and Cowart, 1992; Osmond and Ivanovich, 1992). Consequently, and although it depends ultimately on the water/rock ratio, one can expect that the disequilibria inherited by the matrix rock from such a phenomenon should be detectable by means of the high analytical precision achieved with the MC-ICP-MS technique (~1‰).

Concerning the HTM 02922 Bathonian sample, the disequilibrium observed (($^{234}U/^{238}U$) = 0.9978±0.0013) is significant at the 2σ level, whereas this is not the case at the 3σ level. If this disequilibrium is confirmed, it could be directly attributed to the presence in its vicinity of a stylolitized zone (sample HTM 02924), located 80 cm down, that shows significant disequilibrium (see below). Moreover, this sample was considered pristine at the macroscopic scale only. It is therefore possible that, in fact, barely visible sub-millimetric stylolitic joints could have been present.

All the stylolites and associated carbonate matrix subsamples display significant ($^{234}U/^{238}U$) disequilibria (see Figure III.6.). The following features are systematically observed throughout this type of samples. The material within the seams shows: i) a higher abundance of uranium than in the embedding carbonate matrix; and ii) a significant deficit of ^{234}U over ^{238}U (($^{234}U/^{238}U$) down to 0.80). In contrast, the surrounding matrix is systematically characterized by ($^{234}U/^{238}U$) activity

ratios greater than unity, up to 1.05 (see Figures III.2, III.3. and III.6.). The higher U-content in stylolitic material than in the embedding matrix can be explained by the presence of U-rich, insoluble residue, which consists mainly of clay minerals, organic matter and detrital accessory minerals. In this discontinuity, the accumulation of non-carbonate minerals arises from the pressure dissolution of host carbonate rocks along the stylolite interface as a response to overburden or tectonic stress (Wanless, 1979; Tucker, 1990).

This phenomenon is observed in both the Bathonian and Oxfordian samples. However, the intensity of these disequilibria is less pronounced in the Oxfordian samples than in the Bathonian samples. For instance, the HTM 07325 and HTM 02601 samples from the Oxfordian limestone exhibit only slightly significant disequilibria either in the stylolite ($(^{234}U/^{238}U)$ = 0.9932 and 0.9989, respectively) or in the surrounding carbonate matrix ($(^{234}U/^{238}U)$ = 1.0022 and 1.0028, respectively).

Two conclusions can be drawn from these results at this stage.

Firstly, although it is currently impossible to specify whether the system has been subject to a continuous process or whether it has been disturbed by a short and sudden event (see the distinction in Scott et al., 1992), a phenomenon of uranium migration has occurred within the last 1-2 Ma. Secondly, this uranium remobilization is directly associated with the presence of the pressure dissolution structure since the disequilibria observed are encountered only in samples within and within close proximity of such discontinuities.

Furthermore, the distribution of the uranium isotopes throughout the stylolitized zones suggests a relocation of uranium from the U-rich material within the seams into the surrounding U-low carbonate matrix. In this case, such a uranium transfer would be accompanied by an isotopic fractionation, the uranium remobilized from the stylolitic joint being characterized by a $(^{234}U/^{238}U)$ AR greater than unity.

The nature and the modality of the driving process(es) responsible for the remobilization and fractionation of uranium are not understood and cannot be inferred solely from the ($^{234}U/^{238}U$) data presented here. However, two mechanisms can be evoked to explain U-remobilization: 1) late epidiagenetic processes related to the pressure dissolution phenomenon, or 2) preferential fluid circulation along the stylolite pathway.

III.7. Conclusion

Although these results should be viewed as preliminary to a more exhaustive investigation of U-Series disequilibrium in the sedimentary formations of the ANDRA site, some conclusions can already be drawn.

The ($^{234}U/^{238}U$) disequilibria measured in this study highlight a discrete, recent uranium migration in the limestone formations that underlie and overlie the clay target formation of the French Meuse/Haute Marne Underground Research Laboratory. This is a major, surprising result since it is generally supposed that low-permeability limestone formations, such as those of the Meuse/Haute-Marne experimental site, behave as a chemically stable system after early diagenesis-related processes. Pressure dissolution structures play a major role in this remobilization, but the nature and the modality of the processes responsible for these disequilibria are not well understood. However, regardless of the processes involved, they have been active during at least the last 1-2 Ma. These last results are a significant contribution to our understanding of the dynamic behaviour of natural radionuclides in these Mesozoic series that can be considered as an analogue to the far field of potential disposals in clay layer.

Furthermore, methodological conclusions can be drawn from this study. Our results highlight the importance of using highly precise and accurate techniques, such as MC-ICP-MS or TIMS. In fact, until now, most of the published data in this field were obtained by α-spectrometry. Their quoted analytical errors are commonly no better than 5% at the 95% level confidence for the ($^{234}U/^{238}U$) activity ratio (e.g. Schwarcz et al., 1982; Smellie and Rosholt, 1984; Smellie and Stuckless, 1985; Gascoyne and Schwarcz, 1986; Smellie et al., 1986; Gascoyne and Cramer, 1987; Latham and Schwarcz, 1987; Griffault et al., 1993; Gascoyne et al., 2002). Since in most samples from this study the observed excess or deficit in ^{234}U *vs* ^{238}U does not exceed 5%, such disequilibria could not be highlighted by the current α-counting technique. Although, at this time, the MC-ICP-MS or TIMS techniques have not been fully exploited in this field, there is no doubt that they will open up new prospects.

Acknowledgements

The authors thank Dr. E. Pons-Branchu for her constructive help and comments on the manuscript. PD is grateful to ANDRA for providing drill-core samples and Ph.D. financial support.

References

ANDRA, 2001. Référentiel Géologique du Site Meuse-Haute Marne. A RP ADS 99-005/B.

Bathurst, R.G.C., 1987. Diagenetically enhanced bedding in argillaceous platform limestones; stratified cementation and selective compaction. Sedimentology, 34(5): 749-778.

Bourdon, B., Turner, S.P., Henderson, G.M. and Lundstrom, C.C., 2003. Introduction to U-series geochemistry. In: B. Bourdon, G.M. Henderson, C.C. Lundstrom and S.P. Turner (Editors), Uranium-Series Geochemistry. Reviews in Mineralogy and Geochemistry, pp. 1-21.

Buxton, T.M. and Sibley, D.F., 1981. Pressure solution features in a shallow buried limestone. Journal of Sedimentary Petrology, 51(1): 19-26.

Cheng, H., Edwards, R.L., Hoff, J., Gallup, C.D., Richards, D.A. and Asmerom, Y., 2000. The half-lives of Uranium-234 and Thorium-230. Chemical Geology, 169(1-2): 17-33.

Condomines, M., Hemond, C. and Allègre, C.J., 1988. U-Th-Ra radioactive disequilibria and magmatic processes. Earth and Planetary Science Letters, 90(3): 243-262.

Coulon, M., 1992. La Distension Oligocène dans le nord-est du bassin de Paris (perturbation des directions d'extension et distribution des stylolites). Bulletin de la Société Géologique de France, 163(5): 531-540.

Deschamps, P., Doucelance, R., Ghaleb, B. and Michelot, J.L., 2003. Further investigations on optimized tail correction and high-precision measurement of Uranium isotopic ratios using Multi-Collector ICP-MS. Chemical Geology (in press).

Edwards, R.L., Chen, J.H. and Wasserburg, G.J., 1987. ^{238}U-^{234}U-^{230}Th-^{232}Th systematics and the precise measurement of time over the past 500,000 years. Earth and Planetary Science Letters, 81(2-3): 175-192.

Fleischer, R.L., 1980. Isotopic disequilibrium of uranium; alpha-recoil damage and preferential solution effects. Science, 207(4434): 979-981.

Fleischer, R.L. and Raabe, O.G., 1978. Recoiling alpha-emitting nuclei; mechanisms for uranium-series disequilibrium. Geochimica et Cosmochimica Acta, 42(7): 973-978.

Gascoyne, M., 1992. Geochemistry of the actinides and their daughters. In: M. Ivanovich and R.S. Harmon (Editors), Uranium-series disequilibrium; applications to earth, marine, and environmental sciences. Clarendon Press, Oxford, United Kingdom, pp. 34-61.

Gascoyne, M. and Cramer, J.J., 1987. History of actinide and minor element mobility in an Archean granitic batholith in Manitoba, Canada. Applied Geochemistry, 2(1): 37-53.

Gascoyne, M., Miller, N.H. and Neymark, L.A., 2002. Uranium-series disequilibrium in tuffs from Yucca Mountain, Nevada, as evidence of pore-fluid flow over the last million years. Applied Geochemistry, 17(6): 781-792.

Gascoyne, M. and Schwarcz, H.P., 1986. Radionuclide migration over recent geologic time in a granitic pluton. Chemical Geology; Isotope Geoscience Section, 59(1): 75-85.

Griffault, L.Y., Gascoyne, M., Kamineni, C., Kerrich, R. and Vandergraaf, T.T., 1993. Actinide and Rare Earth Element characteristics of deep fracture zones in the Lac du Bonnet granitic batholith, Manitoba, Canada. Geochimica et Cosmochimica Acta, 57(6): 1181-1202.

Hsi, C.K.D. and Langmuir, D., 1985. Adsorption of uranyl onto ferric oxyhydroxides; application of the surface complexation site-binding model. Geochimica et Cosmochimica Acta, 49(9): 1931-1941.

Ivanovich, M., 1991. Aspects of uranium/thorium series disequilibrium applications to radionuclide migration studies. Radiochimica Acta, 52/53: 257-268.

Ivanovich, M., 1994. Uranium series disequilibrium: concepts and applications. Radiochimica Acta, 64: 81-94.

Ivanovich, M., Latham, A.G., Longworth, G. and Gascoyne, M., 1992. Applications to radioactive waste disposal studies. In: M. Ivanovich and R.S. Harmon (Editors), Uranium-series disequilibrium; applications to earth, marine, and environmental sciences. Clarendon Press, Oxford, United Kingdom, pp. 583-630.

Kigoshi, K., 1971. Alpha-recoil thorium-234; dissolution into water and the uranium-234/uranium-238 disequilibrium in nature. Science, 173: 47-48.

Labonne, M. and Hillaire-Marcel, C., 2000. Geochemical gradients within modern and fossil shells of Concholepas concholepas from Northern Chile: An insight into U-Th systematics and diagenetic/authigenic isotopic imprints in mollusk shells. Geochimica et Cosmochimica Acta, 64(9): 1523-1534.

Latham, A.G. and Schwarcz, H.P., 1987. The relative mobility of U, Th and Ra isotopes in the weathered zones of the Eye-Dashwa Lakes granite pluton, northwestern Ontario, Canada. Geochimica et Cosmochimica Acta, 51(10): 2787-2793.

Luo, X., Rehkämper, M., Lee, D.C. and Halliday, A.N., 1997. High precision $^{230}Th/^{232}Th$ and $^{234}U/^{238}U$ measurements using energy-filtered ICP Magnetic Sector Multi-Collector mass spectrometry. International Journal of Mass Spectrometry and Ion Processes, 171: 105-117.

Osmond, J.K. and Cowart, J.B., 1976. The theory and uses of natural uranium isotopic variations in hydrology, Atomic Energy Review, pp. 621-679.

Osmond, J.K. and Cowart, J.B., 1992. Ground water. In: M. Ivanovich and R.S. Harmon (Editors), Uranium-series disequilibrium; applications to earth, marine, and environmental sciences. Clarendon Press, Oxford, United Kingdom, pp. 290-333.

Osmond, J.K. and Ivanovich, M., 1992. Uranium-series mobilization and surface hydrology. In: M. Ivanovich and R.S. Harmon (Editors), Uranium-series disequilibrium; applications to earth, marine, and environmental sciences. Clarendon Press, Oxford, United Kingdom, pp. 259-289.

Schwarcz, H.P., Gascoyne, M. and Ford, D.C., 1982. Uranium-series disequilibrium studies of granitic rocks. Chemical geology, 36(1-2): 87-102.

Scott, R.D., MacKenzie, A.B. and Alexander, W.R., 1992. The interpretation of ^{238}U-^{234}U- ^{230}Th- ^{226}Ra disequilibria produced by rock-water interactions. In: N.A. Chapman, I.G. McKinley, M.E. Shea and J.A.T. Smellie (Editors), The Pocos de Caldas Project; natural analogues of processes in a radioactive waste repository, Part I. Journal of Geochemical Exploration. Elsevier, Amsterdam-New York, International, pp. 345-363.

Smellie, J.A.T., Mackenzie, A.B. and Scott, R.D., 1986. An analogue validation study of natural radionuclide migration in crystalline rocks using uranium-series disequilibrium studies. Chemical Geology, 55(4): 233-254.

Smellie, J.A.T. and Rosholt, J.N., 1984. Radioactive disequilibria in mineralised fracture samples from two uranium occurrences in northern Sweden. Lithos, 17(3): 215-225.

Smellie, J.A.T. and Stuckless, J.S., 1985. Element mobility studies of two drill-cores from the Goetemar Granite (Kraakemaala test site), Southeast Sweden. Chemical Geology, 51(1-2): 55-78.

Thirlwall, 2001. Inapropriate tail corrections can cause large inaccuracy in isotope ratio determination by MC-ICP-MS. Journal of Analytical Atomic Spectrometry, 16: 1121-1125.

Tucker, M., 1990. Diagenetic processes, products and environments. In: M.E. Tucker and V.P. Wright (Editors), Carbonate sedimentology. Blackwell Sci. Publ., Oxford, United Kingdom, pp. 314-364.

Waite, T.D., Davis, J.A., Payne, T.E., Waychunas, G.A. and Xu, N., 1994. Uranium(VI) adsorption to ferrihydrite; application of a surface complexation model. Geochimica et Cosmochimica Acta, 58(24): 5465-5478.

Wanless, H.R., 1979. Limestone response to stress; pressure solution and dolomitization. Journal of Sedimentary Petrology, 49(2): 437-462.

Chapitre IV

Active uranium relocation process in the last 2 Ma along pressure dissolution surfaces, in deep Mesozoic limestone formations, as inferred by $^{234}U/^{238}U$ disequilibria

Pierre Deschamps, Claude Hillaire-Marcel, Jean-Luc Michelot
Régis Doucelance, Bassam Ghaleb and Stéphane Buschaert

To be submitted to Earth and Planetary Science Letters

Abstract

Borehole core samples from the deep, low-permeability Mesozoic formations surrounding the target argilite layer of the Meuse/Haute-Marne experimental site of the French agency for nuclear waste management -ANDRA- (Agence nationale pour la gestion des déchets radioactifs) were analysed for their uranium isotopic abundance. This study attempts to decipher the history and the processes governing the mobility of uranium in such geological settings by means of precise measurements of the ($^{234}U/^{238}U$) activity ratio. The high analytical precision and accuracy achieved by MC-ICP-MS compel us to re-examine radioactive equilibrium/disequilibrium concepts and their geochemical implications.

Within Oxfordian and Bathonian limestone formations, zones characterized by pressure dissolution surfaces (stylolites or dissolution seams) display systematic ($^{234}U/^{238}U$) disequilibria, whereas pristine samples remain in secular equilibrium state. The systematic feature is observed throughout these zones: i) the material within the seams shows a deficit of ^{234}U over ^{238}U (($^{234}U/^{238}U$) down to 0.80) and ii) the

surrounding carbonate matrix is characterized by an activity ratio greater than unity (up to 1.05). Seriate measurements along a transect realized perpendicularly to a major stylolitic discontinuity permit us to depict the modality of the uranium remobilization. These results highlight a centimetric-scale relocation of uranium from the U-rich stylolitic material toward the U-poor surrounding matrix. Two potential driving processes responsible for the uranium relocation (fluid circulations vs late epidiagenetic phenomenon) are proposed and discussed. Although this debate is still open, it is highly likely that, whatever driving process is involved in this U relocation, it is also responsible for the U remobilization observed within all the stylolitized zones examined. Our results would therefore highlight a general and active relocation of uranium during the last 2 Ma in stylolitized zones of the limestone formations.

Conversely, samples from the target Callovo-Oxfordian argilites display ($^{234}U/^{238}U$) radioactive equilibrium. This is a fundamental result concerning the storage capacities of high level radioactive wastes in such argillaceous environments since it provides strong evidence for current chemical closure of the system with respect to uranium and, therefore, most probably to the other U-series radionuclides.

Keywords: Uranium isotopes; Multiple-Collector ICP-MS; waste management; remobilization; diagenesis; migration.

IV.1. Introduction

The safety of nuclear waste disposal in deep geological formation depends on the concept of multiple barriers that prevent or at least retard radionuclide migration from the storage site to the biosphere. Engineered and natural barriers are combined to isolate the High-Level-Radioactive Waste (HLRW) for time sufficiently long to allow the radioactivity to decay to acceptable levels for future societies.

Fluid circulations constitute a critical parameter for the confining capacities of the system, since they are the most effective and fastest mechanism by which radionuclides can reach the biosphere [1]. Consequently, knowledge of the past and present hydrological and geochemical regime within the geological system is fundamental to making predictions of the behaviour of radionuclides when they are released from the "near field," i.e. the engineered barriers and the immediately surrounding rock. Once in the "far field," the released radionuclides are considered diluted and therefore as minor components of a largely unperturbed natural medium, so that the natural hydrochemical and geochemical dynamics of the system control their behaviour.

From this viewpoint, the study of uranium and thorium-decay series naturally occurring in the far field provides in-situ, site-specific, natural analogue information for the assessment of short- to long-term migration of the radionuclides of a nuclear waste disposal site into the geological system. This interest relies on two main features of this geochemical system. Firstly, naturally occurring uranium, thorium or radium isotopes may be considered chemical analogues of the major and minor actinides (Np, Pu and of course U and Th) expected to be present in the radioactive waste inventory (see [2]). Secondly, the U-Th series provides a large panel of radioactive clocks, which corresponds to the range of half-lives encountered in the

three decay series over which physical and chemical processes that have disturbed the system and induced radioactive disequilibria may be characterized.

Various applications of the U-series systematics have been realized in the field of hydrological and geochemical characterization of geological systems of relevance to potential nuclear waste disposal (see review in [3]). These numerous studies deal notably with the characterization of (i) the fluid phase and groundwater dynamics (e.g. [4-6]), (ii) the dating of secondary minerals, such as fracture-infilling minerals (e.g. [7-9]) and finally, (iii) the state of radioactive equilibrium of the host rock.

In the latter case, the determination of the state of radioactive equilibrium -or disequilibrium- in the rock body makes it possible to assess the chemical stability of a potential host medium with respect to transport of chemical species by providing information on radionuclide migration on a time scale of up to 1-2 Ma. Indeed, any radioactive disequilibrium existing inside a radioactive chain implies that a chemical disturbance has affected the rock and fractionated its elements or isotopes. The time scale of such a disturbance can be directly inferred from the half-lives of the radionuclides and it is commonly stated that the fractionating phenomenon must have occurred within a period that does not exceed 4-6 times the half-life of the longest half-life of the daughter nuclide.

Basic theoretical considerations of this approach were outlined in detail by Schwarcz et al. [10]. Later applied studies concerned experimental sites essentially located in granitoid bedrocks [11-16] or, more recently, volcanic tuffs [17]. These studies focus on the ^{226}Ra-^{230}Th-^{234}U-^{238}U series, since the relatively long half-lives of these daughter radionuclides (1,599 a, 75,690 a and 245,250 a for ^{226}Ra, ^{230}Th and ^{234}U, respectively) provide the means to investigate the time scale at which the safety

of radioactive waste disposal needs to be addressed. They mainly investigate the altered and/or fractured zones of the rock matrix where extensive water/rock interactions may have preferentially taken place. In particular, this approach makes it possible to temporally constrain such interactions and consequently the groundwater circulation events, since it is often implicitly admitted that the two phenomena are related.

This study concerns sedimentary formations with low porosity and reduced hydraulic flows. It forms part of the geological investigations undertaken by the French agency for nuclear waste management, ANDRA (Agence nationale pour la gestion des déchets radioactifs) around the Underground Research Laboratory (URL) of Bure (Eastern part of the Paris Basin) in order to evaluate the feasibility of high-level radioactive waste repository in deep argilite formations. Among the different geological options that have been proposed as potential host formations for HLRW repository, argillaceous rocks and their surrounding sedimentary formations have not been nearly as thoroughly investigated with U-series systematic as fractured "granitic"-type sites. This is probably due to the widely accepted view that it is unlikely that such low-permeability sedimentary rocks could have been subjected to chemical instability at the time scale controlled by U series systematics (up to 1-2 Ma).

In an earlier phase of the present project, Deschamps et al. [18] demonstrated the systematic occurrence of ($^{234}U/^{238}U$) disequilibrium within and within close proximity of discontinuities resulting from pressure dissolution processes (stylolites) embedded in the deep, low permeability, low-porosity limestone formations surrounding the target clay layer of the Bure URL. Here, we present complementary isotopic analyses of uranium conducted along a transect through a pressure dissolution discontinuity in order to document the processes governing the mobility

of actinides in such an environment. We will show that, in the present case, radioactive disequilibria observed on the matrix rock definitely involve isotopic fractionation, short scale migration and relocation of uranium via the interstitial fluid phase along the pressure dissolution seams but not necessarily, as is often, andperhaps too readily assumed, groundwaters flowing through the system.

IV.2. Geological setting

The French government authorized ANDRA to excavate a scientific Underground Research Laboratory in an area straddling the Meuse and Haute-Marne regions in the Eastern part of the Paris Basin in France (Figure IV.1.). The target formation is part of the Mesozoic sedimentary rocks; it consists of a 130 m thick, Callovo-Oxfordian argilite found at 420-550 m below ground surface at the URL site. The target layer is a detrital clay-rich rock composed of illite, ordered mixed-layered illite-smectite minerals dominated by illite, kaolinite and minor amounts of chlorite, and is cemented by 25-30 wt % of micrite [19].

This formation is respectively overlain and underlain by Oxfordian/Kimmeridgian and Bajocian/Bathonian (Dogger) shelf limestones (see Figure IV.1.). They consist of oolitic to oncholoitic limestones and have very low porosity (2-5%) and permeability except for some more porous (10-20%), metric scale portions of the Oxfordian limestones that can sometimes be water productive [19].

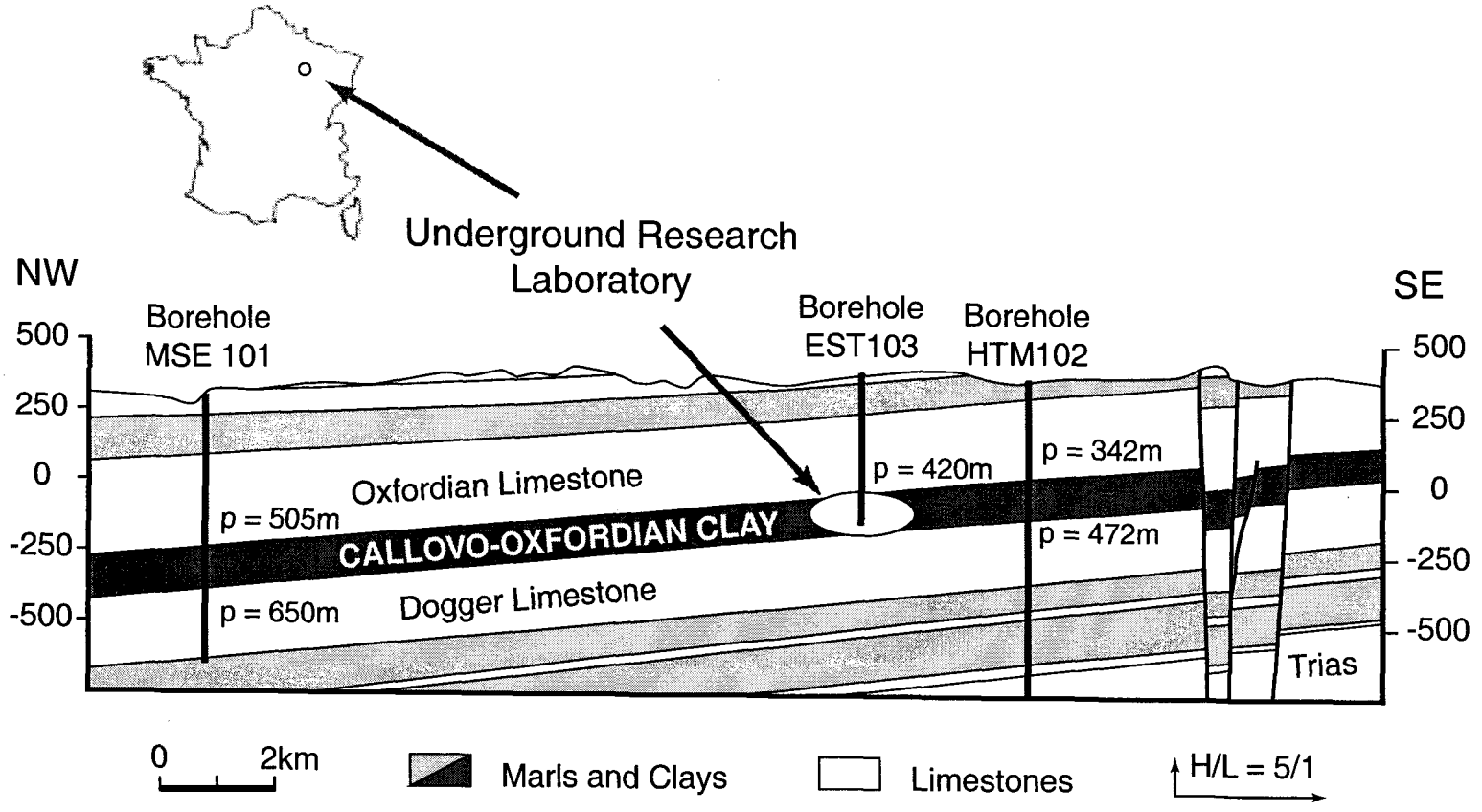

Figure IV.1.: Location of the ANDRA Underground Research Laboratory (URL) in the eastern part of the Paris basin and Northwest/Southeast geological cross-section throughout the sedimentary target layers.

Oxfordian and Bathonian formations are characterised by pressure dissolution surfaces [20-23] categorized either as "stylolites" *stricto sensu* or "dissolution seams" according to the terminology established by Buxton and Sibley [24] and Bathurst [25]. Henceforth, for simplification purposes, we will refer to such structures indistinctly as "stylolites" or "stylolitized zones" and to rock matrices that do not exhibit such discontinuities as "pristine" rock [18]. These sub-horizontal seams have been documented at the regional scale in all of the Mesozoic limestone formations [26]. Two generations have been distinguished [19]. The first generation was probably formed early by overburden during sedimentary loading of the series [19] while the second generation has a tectonic origin and is related to the Oligocene phase of extension in the Western part of the Eurasian plate [26]. It is important to note that such pressure dissolution structures are absent in Callovo-Oxfordian argilites.

IV.3. Samples and Experimental techniques

Core samples were obtained from three ANDRA prospecting boreholes located near the site where the Underground Research Laboratory is being constructed (Figure IV.1.). The HTM 102 and MSE 101 boreholes were drilled within the whole series from Kimmeridgian to Trias sediments (1,101 m depth) and from Kimmeridgian to Dogger sediments (950 m depth), respectively. They cross-cut the Callovo-Oxfordian argilite unit at depths of between 342 m and 472 m, and between 505 m and 650 m, respectively. The EST 103 borehole (526 m depth) reaches the Callovo-Oxfordian formation at 420 m depth.

Our sampling focused on the Callovo-Oxfordian formation and its bounding Bathonian and Oxfordian formations, more particularly on the two interfaces between argilite and limestone units and on stylolitized zones within limestones. Some results

from the HTM 102 borehole were already published in Deschamps et al. [18]. Four samples from the target Callovo-Oxfordian argilite in the EST 103 borehole and one sample from the Bathonian limestone in the MSE 101 borehole were also subsampled. For limestone samples characterized by pressure dissolution structures, we subsampled the material inside the seams as well as the surrounding carbonate matrix. From the series of samples used in our previous study, we selected the HTM 02924 sample that shows a sub-horizontal, centimetric-scale swarm of stylolitic seams in its middle. Thirteen subsamples were recovered along a perpendicular transect performed through this discontinuity (see Figure IV.4.).

Finally, nine pristine samples (6 Callovo-Oxfordian and 3 Bathonian or Oxfordian samples) and thirty-three subsamples associated with stylolitized zones were crushed, finely powdered and analyzed for their uranium content and $^{234}U/^{238}U$ isotopic composition.

The chemical procedure, and more particularly the digestion step, was slightly modified from the usual chemical procedures used for pure carbonate [18]. The uranium isotopic analyses were performed on a Micromass IsoProbe™ MC-ICP-MS instrument at the GEOTOP Research Centre. The analytical procedure we develop is described in details in Deschamps et al. [27]. Replicate analyses of the New Brunswick Laboratory Certified Reference Material 112a (NBL-112a standard, also called CRM-145 -formerly the NBS SRM-960) yielded a mean $\delta^{234}U$ value of -36.42±0.80‰ (2σ, n=19) that is in excellent agreement with previously published values [27]. For this study, the actual reproducibility on natural samples was determined by replicate measurements of a carbonate subsample from the HTM 02924 transect (HTM 02924 #1). The results yielded a mean ($^{234}U/^{238}U$) activity ratio of 1.0103±0.0013 (2σ, n = 10), which gives a total reproducibility (analytical plus

chemical) of ±1.3‰, at the 95% confidence level. For the uranium concentration, a total reproducibility of ±5‰ was obtained (526.8±2.9 ppb, 2σ, n = 10).

All subsamples from the HTM 02924 transect were also analyzed for major and trace elements. These analyses were performed at the CRPG Nancy by ICP-AES and ICP-MS, respectively.

IV.4. Results

Uranium concentrations and ($^{234}U/^{238}U$) activity ratios (AR), with relevant information about samples (host formation, depth, length and sample type) are listed in Table 1. ($^{234}U/^{238}U$) AR were calculated using the reference $^{234}U/^{238}U$ atomic ratio of $54{,}887.10^{-6}$ determined by Cheng et al. [28] by replicate analyses of materials at secular equilibrium. The errors listed in Table 1 and reported in figures are given at the 95% confidence level and represent the internal error of each analysis. Where replicate measurements were carried out, the weighted means and their associated errors are reported in the figures.

For comparison purposes, duplicate measurements of four samples were performed on a VG sector Thermal Ionization Mass Spectrometer equipped with a 10 cm electrostatic analyzer and a pulse-counting Daly detector. The TIMS analyses were carried out with a ^{236}U-^{233}U double spike different from the one that was used for MC-ICP-MS measurement. The TIMS results, also reported in Table 1, are in good agreement within error with the results obtained by MC-ICP-MS, thereby highlighting the robustness of the data set used here.

Table 1

Analyses of uranium contents and ($^{234}U/^{238}U$) activity ratios in samples from the ANDRA boreholes with a MicroMass IsoProbe™ MC-ICP-MS at the GEOTOP research Center.

Sample	Unit	Depth (m) Top	Depth (m) Bottom	Sub-Sample	Type[#]	^{238}U (ppb)	($^{234}U/^{238}U$) AR[*]
Pristine Samples							
EST 103 Borehole							
EST 03300	Callovo-Oxfordian	421.77	421.87			2318.7 ± 2.3	1.0018 ± 0.0004
EST 03302	Callovo-Oxfordian	422.6	422.63			1555.0 ± 1.5	1.0013 ± 0.0006
EST 03305	Callovo-Oxfordian	425.5	425.52			1024.5 ± 1.0	1.0020 ± 0.0015
EST 03306	Callovo-Oxfordian	427.32	427.35			1277.5 ± 1.3	1.0028 ± 0.0008
HTM 102 Borehole							
HTM 02914	Oxfordian	337.69	337.71			1638.7 ± 0.2	1.0000 ± 0.0008
						1639.2 ± 1.3	0.9994 ± 0.0008
						1641.7 ± 1.6	1.0005 ± 0.0005
HTM 02917	Oxfordian	340.30	340.66			1194.6 ± 1.0	1.0008 ± 0.0005
HTM 02918	Callovo-Oxfordian	345.72	346.03			657.8 ± 0.6	0.9999 ± 0.0009
						648.1 ± 0.6	0.9986 ± 0.0010
HTM 02920	Callovo-Oxfordian	349.94	349.96			1407.4 ± 1.2	1.0003 ± 0.0006
HTM 02922	Bathonian	472.00	472.10			1876.2 ± 1.5	0.9978 ± 0.0009
						1874.2 ± 1.8	0.9970 ± 0.0006
						1855.7 ± 1.9	0.9963 ± 0.0005
Stylolitized Samples							
MSE 101 Borehole							
MSE 01625	Bathonian	650.68	650.89	Mat #1	carbonate matrix	2431.1 ± 2.5	1.0046 ± 0.0003
				Mat #2	carbonate matrix	2630.9 ± 2.6	1.0078 ± 0.0003
				Mat #3	carbonate matrix	2246.3 ± 2.1	1.0043 ± 0.0004
				Sty #1	stylolitic material	1406.4 ± 1.5	0.9675 ± 0.0005
HTM 102 Borehole							
HTM 80824	Oxfordian	306.00	306.22	Mat A2	carbonate matrix	1503.6 ± 1.5	1.0244 ± 0.0003
				Sty A1	stylolitic material	3880.3 ± 5.8	0.7991 ± 0.0005
HTM 07325	Oxfordian	322.30	322.64	Mat A4	carbonate matrix	1881.5 ± 1.8	1.0023 ± 0.0003
						1879.6 ± 1.7	1.0021 ± 0.0002
				Sty A1	stylolitic material	4354.7 ± 4.2	0.9932 ± 0.0003
HTM 02601	Oxfordian	323.50	323.76	Mat A2	carbonate matrix	1439.0 ± 1.4	1.0028 ± 0.0004
				Sty A2	stylolitic material	3740.6 ± 3.5	0.9989 ± 0.0002
HTM 02926	Bathonian	472.96	473.17	A #3	carbonate matrix	463.0 ± 0.4	1.0198 ± 0.0006
				A #23	carbonate matrix	388.5 ± 0.4	1.0203 ± 0.0010
				A #12	stylolitic material	618.2 ± 0.9	0.9361 ± 0.0021
				A #26	stylolitic material	559.0 ± 0.5	0.9154 ± 0.0008
						552.0 ± 5.4	*0.9214 ± 0.0108*
HTM 07322	Bathonian	476.48	476.87	Mat A	carbonate matrix	774.9 ± 0.7	1.0303 ± 0.0005
				Sty A1	stylolitic material	1149.5 ± 1.1	1.0106 ± 0.0005
				Sty B2	stylolitic material	834.4 ± 0.8	0.9532 ± 0.0006
HTM 02928	Bathonian	477.66	477.77	Mat A1	carbonate matrix	260.7 ± 0.2	1.0427 ± 0.0010
				Mat A2	carbonate matrix	252.5 ± 0.2	1.0532 ± 0.0012
				Mat A3	carbonate matrix	262.1 ± 0.2	1.0399 ± 0.0011
						260.4 ± 2.3	*1.0382 ± 0.0071*
				Mat A4	carbonate matrix	279.8 ± 0.3	1.0402 ± 0.0013
				Sty A1	stylolitic material	970.3 ± 0.9	0.8665 ± 0.0010
				Sty A2	stylolitic material	487.8 ± 0.5	0.9364 ± 0.0009
						498.7 ± 4.3	*0.9332 ± 0.0085*
				Sty A3	stylolitic material	479.2 ± 0.4	0.9224 ± 0.0010
Transect							
HTM 02924	Bathonian	472.81	472.96	A #1	carbonate matrix	526.9 ± 2.9	1.0106 ± 0.0013
				A #2	carbonate matrix	589.2 ± 0.5	1.0158 ± 0.0008
				A #3	carbonate matrix	656.2 ± 0.6	1.0175 ± 0.0012
				A #4	carbonate matrix	768.6 ± 0.7	1.0385 ± 0.0007
					carbonate matrix	767.4 ± 0.8	1.0380 ± 0.0011
				A #5	carbonate matrix	1750.1 ± 1.8	0.9846 ± 0.0005
				A #6a	stylolitic material	4082.4 ± 4.2	0.9628 ± 0.0005
				A #6b	stylolitic material	2196.4 ± 2.2	0.9799 ± 0.0005
				A #7	carbonate matrix	1012.9 ± 1.0	1.0247 ± 0.0011
				A #8	carbonate matrix	680.4 ± 0.6	1.0468 ± 0.0007
					carbonate matrix	681.2 ± 0.6	1.0459 ± 0.0008
					carbonate matrix	678.2 ± 0.7	1.0452 ± 0.0013
				A #9	carbonate matrix	654.4 ± 0.6	1.0441 ± 0.0007
						656.4 ± 6.1	*1.0366 ± 0.0077*
				A #10	carbonate matrix	557.3 ± 0.5	1.0344 ± 0.0009
				A #11	carbonate matrix	524.5 ± 0.5	1.0276 ± 0.0007
				A #12	carbonate matrix	514.1 ± 0.5	1.0149 ± 0.0014
				A #13	stylolitic material	618.4 ± 0.6	0.9775 ± 0.0023

[#] Carbonate matrix material refers to the embedding matrix sample in the vicinity of the stylolitic seams.

[*] ($^{234}U/^{238}U$) activity ratios (AR) are calculated using the half-life values given by Cheng et al. (2000). All errors are given at the 95% confidence level (2σ).

Data in italic are duplicate measurements performed on a VG sector Thermo Ionization Mass Spectrometer.

In the Oxfordian limestone formations, the uranium concentrations in carbonate matrix samples varied from 1.2 to 1.9 ppm. In stylolite samples, the U concentrations increase to 3.7-4.3 ppm. A similar pattern is observed in the Bathonian formation: the carbonate matrix samples contains from 0.2 to 0.6 ppm of U and the stylolite samples up to 4 ppm. For the argilite Callovo-Oxfordian samples of the EST 103 borehole core, the U concentrations vary from 1 to 2.3 ppm. These data are consistent with the range of uranium abundance reported by Gascoyne [29] in such sedimentary rocks.

($^{234}U/^{238}U$) AR results of pristine samples are illustrated in Figure IV.2.. In this figure, the overall analytical reproducibility achieved in the course of this study (±1.3‰, 2σ) together with the internal error are reported for each point. All the pristine samples from Callovo-Oxfordian argilites and Oxfordian limestones fall within the zone of ^{234}U-^{238}U secular equilibrium as defined above. Only the pristine sample from the Bathonian formation (HTM 02922) that is located at the interface with the Callovo-Oxfordian unit shows a slight but undoubtedly significant ($^{234}U/^{238}U$) disequilibrium that was confirmed by three replicate measurements ($(^{234}U/^{238}U)_{\text{Weighted Mean}} = 0.9968\pm0.0013$; see Table 1). This appears to be related to the location of the sample within an area with abundant pressure dissolution seams (sample HTM 02924) that display significant disequilibrium (see below).

Figure IV.3. presents the ($^{234}U/^{238}U$) AR of the stylolite and associated carbonate matrix sub-samples, whereas Figure IV.4. illustrates the ($^{234}U/^{238}U$) AR and U-concentration, as well as major and trace element concentrations along the HTM 02924 transect. All samples characterized by the presence of stylolites display ($^{234}U/^{238}U$) disequilibria (see Figure IV.4.).

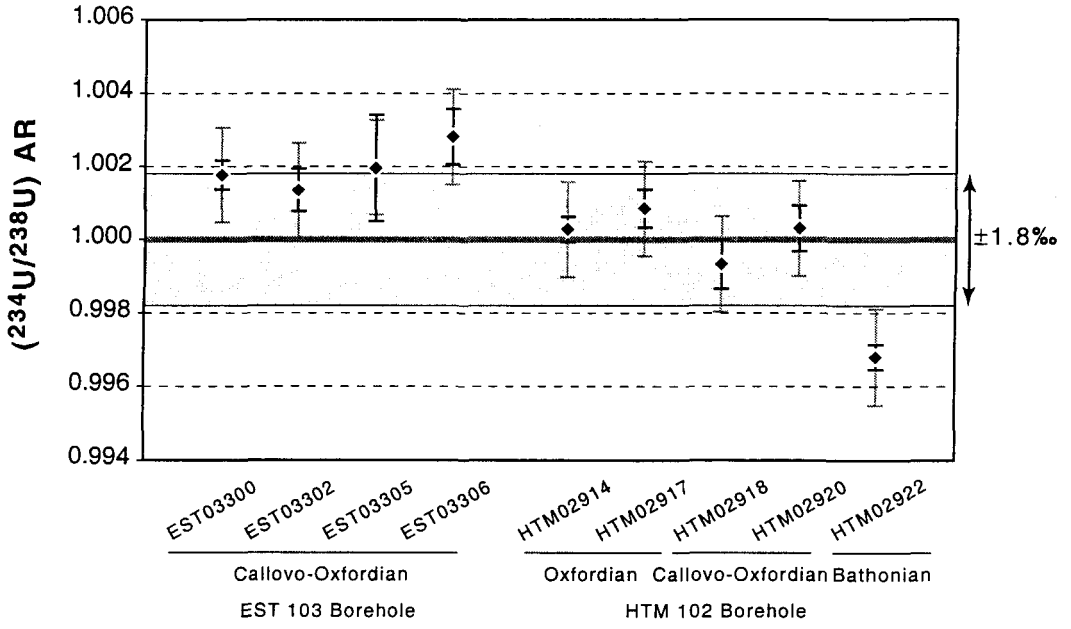

Figure IV. 2.: ($^{234}U/^{238}U$) activity ratio measurements on pristine samples from Bathonian and Oxfordian limestone and Calllovo-Oxfordian argilite formations. Core samples are from the ANDRA HTM 102 and EST 103 boreholes. ($^{234}U/^{238}U$) activity ratios are calculated using the $^{234}U/^{238}U$ atomic ratio determined by Cheng et al. [28] for secular equilibrium material ($^{234}U/^{238}U = 54{,}887.10^{-6}$). Reported error bars indicate either 2σ internal precision (black) or 2σ external reproducibility (grey).

The material inside the seams systematically shows a higher abundance of uranium than in the surrounding carbonate matrix and a significant deficit of ^{234}U *vs* ^{238}U, with ($^{234}U/^{238}U$) AR as low as 0.80. Conversely, the embedding matrix systematically shows a slight excess of ^{234}U *vs* ^{238}U, with ($^{234}U/^{238}U$) AR as high as 1.05 (see Figure IV.3.). The only exception was observed in sample MSE01626, where the stylolitic material is less enriched in uranium than the surrounding matrix. These disequilibria are observed in both the Bathonian and the Oxfordian samples, although they appear less pronounced in the latter.

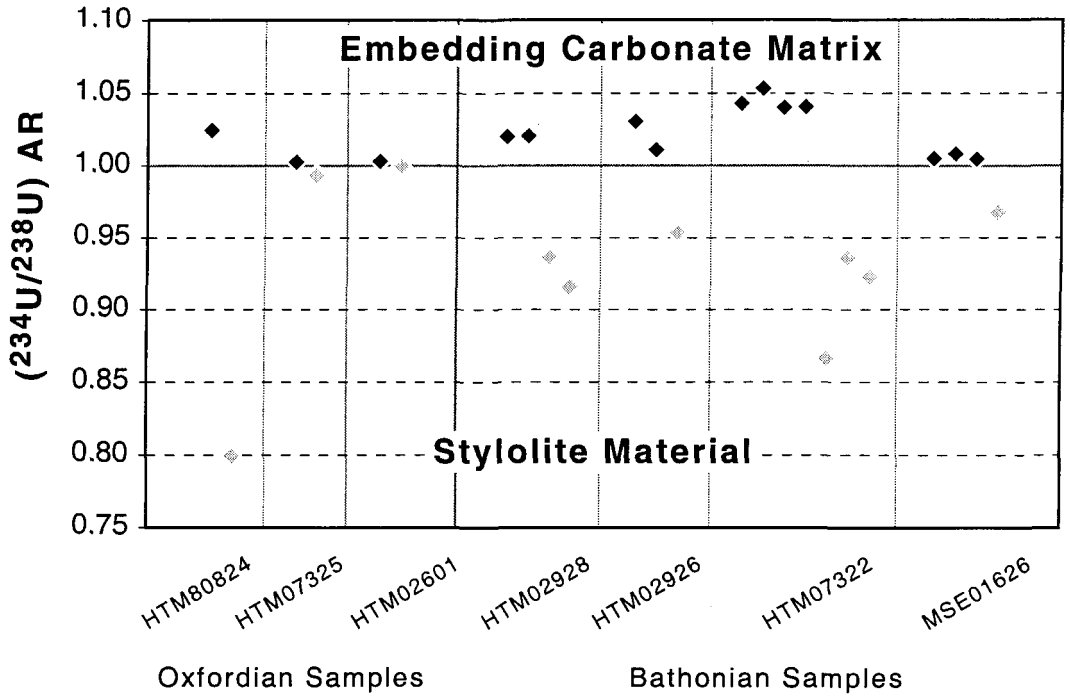

Figure IV.3.: ($^{234}U/^{238}U$) activity ratio measurements on stylolitic material (grey diamonds) and associated carbonate matrix (black diamonds) subsamples from Bathonian and Oxfordian limestone formations. Core samples are from the ANDRA HTM 102 and MSE 101 boreholes. ($^{234}U/^{238}U$) activity ratios are calculated using the $^{234}U/^{238}U$ atomic ratio determined by Cheng et al. [28] for secular equilibrium material ($^{234}U/^{238}U = 54{,}887.10^{-6}$). Error bars are smaller than symbol size.

In sample HTM 02924, similar features are also observed (Figure IV.4.). The transect exhibited a symmetric pattern in relation to the thick swarm of stylolitic seams (subsamples #6a and #6b) observed in the middle of the sample, with i) an increase of the U concentration towards the stylolitic seam and ii) a sharp transition between significant ($^{234}U/^{238}U$) < 1 disequilibria within the seam to an excess of ^{234}U (($^{234}U/^{238}U$) = 1.05) within close proximity of the seam, followed by a smooth decrease of the activity ratio away from the suture zone. Similar features are also depicted by the less thinner stylolitic joint located at the bottom of the sample (subsample #13).

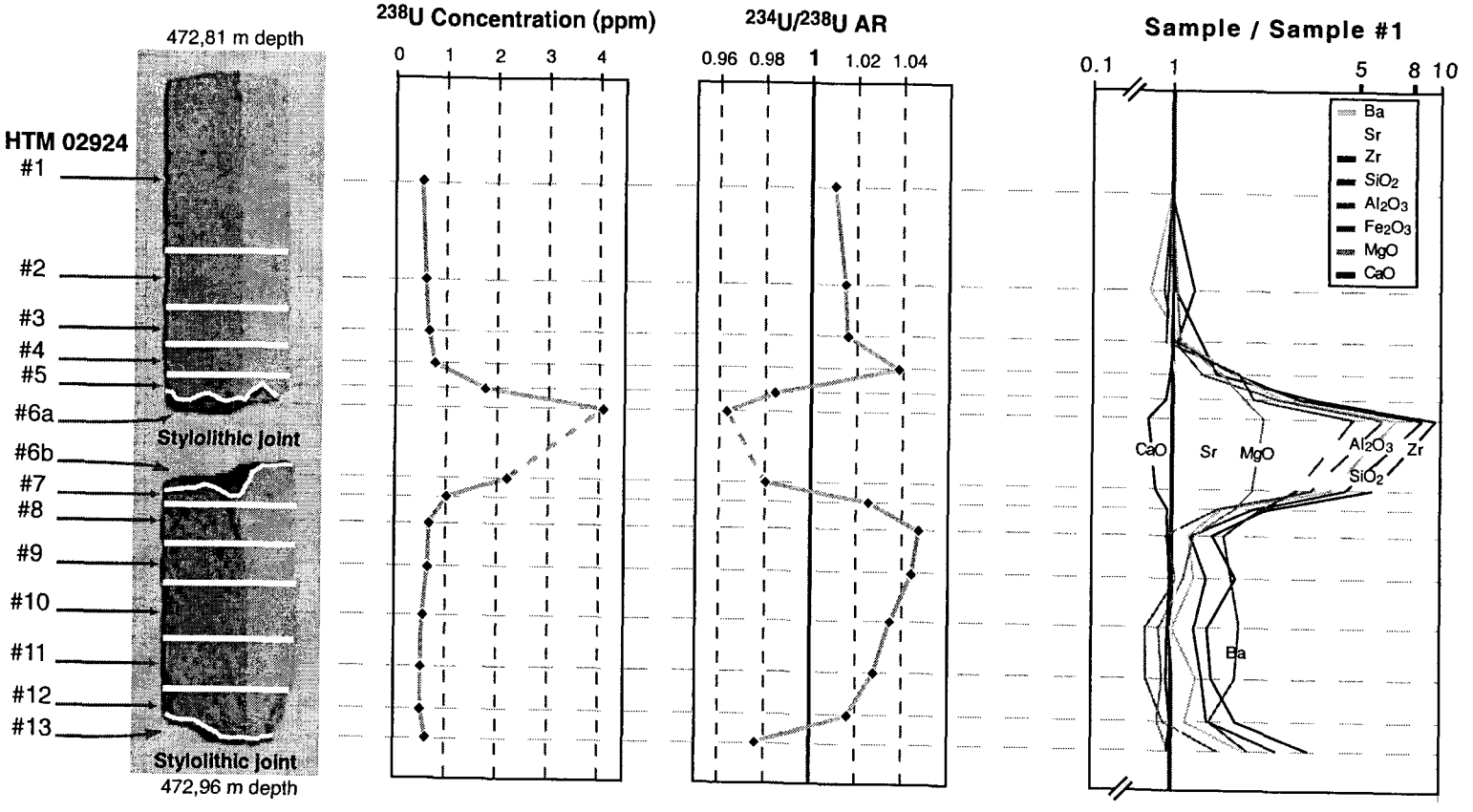

Figure IV.4.: Seriate measurement of uranium concentrations, $^{234}U/^{238}U$ activity ratios and major (Ca, Mg, Fe, Si, Al) and trace (Ba, Sr, Zr) elements along a transect realized within a stylolitized zone (sample HTM 02924) in the Bathonian limestones, collected 473 m downcore in HTM 102 borehole.

IV.5. Discussion

Before discussing the results, it is pertinent to examine in greater depth the concepts and significance of the radioactive equilibrium or disequilibrium, notably respect to the highly improved analytical precisions achieved by MC-ICP-MS or TIMS.

IV.5.1. Re-examination of the radioactive disequilibrium/equilibrium concepts and their geochemical implications

The main purpose of studies dealing with chemical stability of host rocks is to determine whether the rock matrix behaved as a closed system with respect to radionuclide migration, for a time span of the order of a few half-lives of uranium-234; in other words, whether the matrix remained at secular equilibrium or not. This purpose is thus intrinsically related to the definition of the secular equilibrium state and to the accuracy with which this equilibrium state can be determined.

With the recent improvements in mass spectrometry techniques, this question needs to be re-examined for studies dealing with the migration of key radionuclides of the U series (^{238}U-^{234}U-^{230}Th) in a rock matrix. Actually, until now, most of the published data on this topic were obtained by alpha spectrometry [10-17, 30, 31]. In these studies, the quoted analytical errors of the data were no better than ±5% at the 95% confidence level for the ($^{230}Th/^{234}U$) and ($^{234}U/^{238}U$) activity ratios of geological samples.

With recent developments in TIMS and MC-ICP-MS techniques, the analytical reproducibility has been improved, and is currently around ±1-2‰ (2σ) for the $^{234}U/^{238}U$ or the $^{230}Th/^{238}U$ atomic ratios (e.g. [27, 28, 32-38]). The most recent and accurate determination of the half-lives of uranium-234 and thorium-230 yields a precision (including systematic errors) of ±2‰ and ±3‰, respectively [28]. The quoted uncertainties of the half-lives are therefore of the same order as, or even

slightly higher than, the analytical reproducibility achieved by TIMS or MC-ICP-MS. Consequently, the question now arises as to how these uncertainties should be taken into account in the conversion of measured atomic ratios into activity ratios.

Two approaches can be envisaged to solve this question. The half-life uncertainties can be propagated into the activity ratios. This arbitrarily increases the total error beyond the actual reproducibility of the analytical data and, consequently, can make some results consistent within their calculated error, whereas in fact they are dissimilar. Therefore, this option results in a potential loss of information. For the purpose stated above, we used a second approach that defines the state of secular equilibrium with an uncertainty determined by propagating the error in the half-life values. In the case of the ($^{234}U/^{238}U$) AR, since the normalizing $^{234}U/^{238}U$ atomic ratio is known within a precision of ±1.8‰ [28], the state of secular equilibrium is not simply described by the unity, but by a range of activity ratios from 0.9982 to 1.0018. In practice, this may be illustrated, as in Figure IV.2., by a ±1.8‰ shaded zone around the best estimate of secular equilibrium. This approach permits a discussion of heterogeneities within a data set, even if all samples fall into the secular equilibrium zone.

A second purpose of this type of study is to infer chronological constraints on the chemical behaviour of the geological system from the observed radioactive disequilibrium or equilibrium state. In much the same way as above, the improved analytical accuracy and reproducibility make it also necessary to re-examine the question of the chronological implications of U series systematics. It is commonly stated that the return to a radioactive equilibrium state occurs within a time-span equal to 4-6 half-lives of the daughter radionuclide under consideration (e.g. [13, 17, 39, 40]). Conversely, if a disequilibrium is observed, one can assume that the system has been disturbed within a period spanning approximately 4-6 time the half-life of

the daughter up to the present. These assertions arise from the fact that, after a period of 4-5 half-lives, a radioactive excess or deficit has decreased to within ±5% of its initial value. For example, with the analytical error of 5% usually achieved by alpha spectrometry and assuming an initial activity ratio R_0 of 0 or 2, the residual activity ratio measured after 5 half-lives of the radionuclide (R = 0.97 or 1.03) is statistically indistinguishable from unity. Therefore, such assertions rely on the analytical precision of the data. This is illustrated in Figure IV.5., where the time-span of the return to equilibrium state is simulated for a daughter-parent pair for which the decay constant of the parent is much smaller in comparison with that of the daughter, as in the ^{238}U-^{234}U series. The evolution through time of a daughter/parent activity ratio, R, is modelled taking into account the analytical precision that can be achieved by alpha spectrometry (5%, 2σ) or by MC-ICP-MS or TIMS (1‰, 2σ), for varying values of the initial R_0 disequilibrium. The range of initial activity ratios (0 to 10) is representative of the range of disequilibria that are generally found in rocks of the upper crust for the key U-series radionuclides (^{234}U, ^{230}Th, ^{231}Pa).

As illustrated in Figure IV.5B, assuming an initial disequilibrium of 2 or 0, the time scale that can be controlled by a given radionuclide is indeed no better than five times its half-life for data with an analytical precision of ±5%. Using the same assumptions, but with an analytical precision improved to ±1‰, and taking into account the zone of secular equilibrium as defined above, one may conclude that the time scale controlled by a radionuclide increases to eight times its half-life or more (Figure IV.5C). With such precision, one can infer that a rock matrix sample, out of equilibrium for the ^{238}U-^{234}U series, has undergone a U remobilization event within a period of time equal to eight times the half-life of ^{234}U, i.e. during the last 2 Ma.

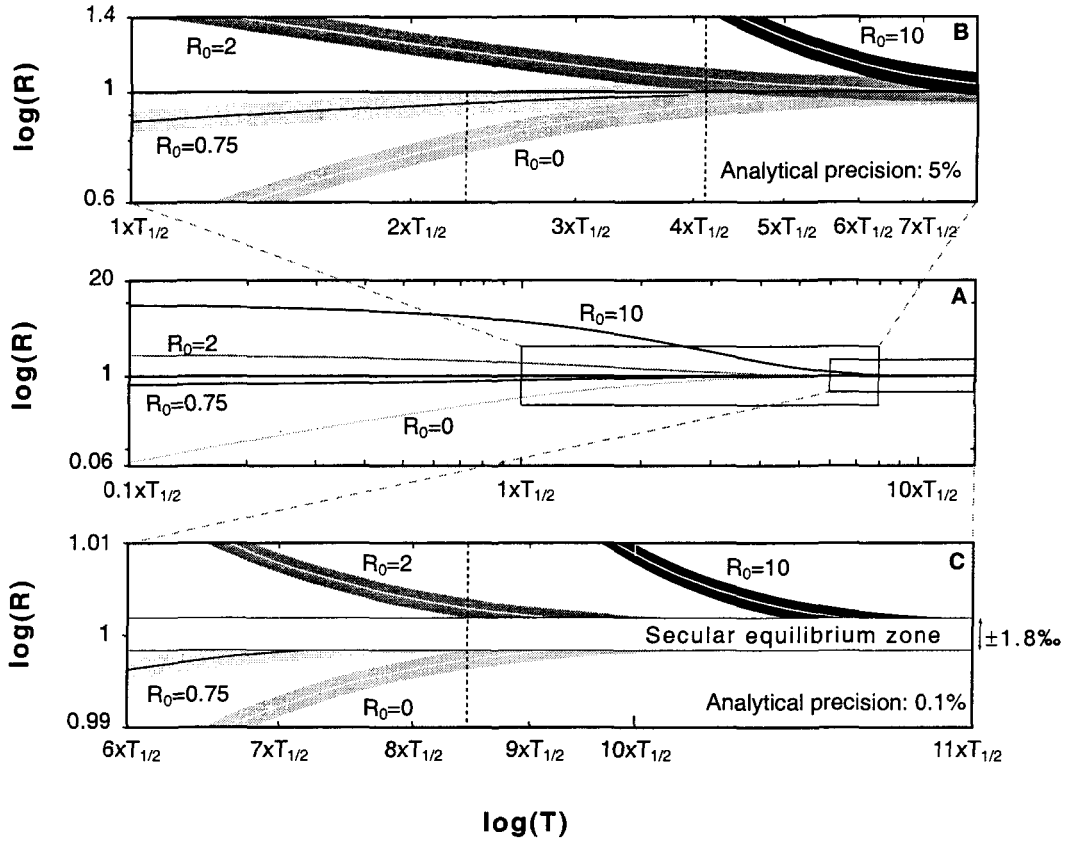

Figure IV.5.: Simulation of the return to equilibrium state for a parent-daughter pair for which the decay constant of the parent is negligible in comparison with the decay constant of the daughter, as for the ^{238}U-^{234}U series (Figure IV.5A). The evolution through time of a daughter/parent activity ratio, R, is modelled for varying values of the initial R_0 disequilibrium (0, 0.75, 2 and 10, respectively). The time scale "controlled" by the daughter nuclide depends on the analytical precision of the data. This is illustrated in Figures IV.5B and IV.5C where the evolution through time of the activity ratio R is modelled taking into account the analytical precision that can be achieved either by alpha spectrometry (5%, 2σ) or by MC-ICP-MS or TIMS (1‰, 2σ), respectively. With an initial deficit or excess arbitrarily fixed at 100% (R_0 = 0 or 2), the return to the equilibrium state occurs after a time span equal to either 4-5 times the half-life assuming an analytical precision of 5% or to 8-9 times the half-life assuming an analytical precision of 1‰. In the latter case, the uncertainty associated with the secular equilibrium (see full explanations in section 5.1.) is taken into

account by considering a shaded zone around the best estimate of secular equilibrium. This uncertainty is arbitrarily fixed at ±1.8‰, the uncertainty associated with the ^{234}U-^{238}U pair. For better visualisation, both axes (time expressed as half-life and R activity ratios) are expressed in log-scale.

Conversely, the question now arises: what chronological and chemical implications concerning the past can be inferred from sample assured to be in the secular equilibrium state? A secular equilibrium state implies that the chemical system does not experience any current relative migration of radionuclides and, consequently, that it certainly behaves as a closed system with respect to U series (see discussion in section 6.1.). In the "alpha counting" literature, it is often claimed that, in such cases of secular equilibrium states, the chemical systems have not experienced significant migration of radionuclides within the time interval equal to 4-5 times the half-life of ^{234}U, i.e. 1 Ma (e.g. [13, 16, 17]). Although one may question what is considered a "significant" migration, we think that such an assertion over-interprets the actual significance of the so-called secular equilibrium state. For example, if one assumes a uranium loss or gain of 25% relative to thorium (i.e. ($^{230}Th/^{238}U$) = 0.75 or 1.25) occurring 180 ka ago, the residual excess or deficit measured today is less than 5%. With analytical precision usually achieved by alpha spectrometry, such a remobilization event is indistinguishable from unity (Figure IV.5B).

For these reasons, it seems advisable to restrict the conclusions that can be drawn from the equilibrium state to the following one: the system is not being subjected to any radionuclide remobilization at present, nor in all likelihood has it been in very "recent" time.

IV.5.2. ($^{234}U/^{238}U$) equilibrium of the pristine samples

Although the pristine samples from the Callovo-Oxfordian and Oxfordian formations fall within their quoted errors in the zone of ^{234}U-^{238}U secular equilibrium, two clusters can be distinguished. The four samples from the HTM 102 borehole display ($^{234}U/^{238}U$) AR highly consistent with unity (($^{234}U/^{238}U)_{mean}$ = 1.0002±0.0010 at the 95% confidence level) whereas the four samples from the EST 103 borehole are in the upper fringe of the equilibrium zone (($^{234}U/^{238}U)_{mean}$ = 1.0020±0.0010 at the 95% confidence level). As discussed in section 5.1., this heterogeneity may highlight a slight radioactive disequilibrium state within the sample set examined.

These analyses were obtained with reference to a standard material, the Harwell Uraninite [27], which was certified to be at secular equilibrium for the ^{234}U-^{238}U series [28]. The four pristine samples from the HTM 102 borehole are highly consistent with this standard and, consequently, are certainly in radioactive equilibrium. Conversely, the EST 103 samples are statistically distinct from unity and therefore inconsistent with the HU-1 standard. It is therefore likely that these samples display a very slight disequilibrium. However, this disequilibrium most probably reflects an analytical artefact that is due to the petrologic characteristics of the corresponding samples, not to a geological phenomenon. The four EST 103 samples are from the target rich-clay layer of the Callovo-Oxfordian formation, whereas the pristine HTM 102 samples are subsampled either from the Oxfordian limestone or from the upper part of the Callovo-Oxfordian unit that is most carbonated. The chemical procedure was optimized on limestone samples and one cannot totally discard the possibility that some highly insoluble, detrital minerals in the argilites, such as refractory minerals, were not totally digested during the chemical dissolution step. The leaching of uranium associated with U-rich, non-soluble minerals may have resulted in the release of some fractionated uranium [41]. Complementary analyses will be carried out to confirm this hypothesis; whatever the results will be, it would

not be advisable to draw unequivocal conclusions concerning the geological nature of these slight disequilibria. In some sense, the very high precision achieved by the new analytical techniques raises new interpretative difficulties that were masked until now by poorer analytical uncertainties.

Therefore, the pristine rock samples (with the exception of the HTM 02922 Bathonian sample) will be considered to be at secular equilibrium state. This indicates that no preferential migration of either one of the two uranium isotopes should have occurred in current time within these samples. Given these results, the current occurrence of a migration of unfractionated uranium in the samples cannot be totally ruled out. However, it seems very unlikely that a U remobilization in the system could occur without any measurable, even small (i.e., at least of the order of a few 1‰) fractionation between ^{234}U and ^{238}U, since this phenomenon necessarily involves mass transfer by means of flowing fluids and, consequently exchanges at the rock/water interface. Due to recoil effects, isotopic fractionation of uranium is a widespread and prominent mechanism during rock/water interactions as proved by the universal occurrence of large ($^{234}U/^{238}U$) disequilibria observed in the hydrosphere [42-45]. The disequilibria observed along pressure dissolution seams (see below) provide a decisive argument for the sensitivity of this geochemical tool for tracing rock/water interaction processes and uranium remobilization in such a geological environment. Although they depend ultimately on water/rock ratios, the resulting disequilibria in the matrix rock should be disclosed by means of the high analytical precision achieved with the MC-ICP-MS technique (~1‰). For these reasons, we think that the ($^{234}U/^{238}U$) equilibrium state observed in most pristine samples provides strong evidence for a chemically closed system, currently, with respect to uranium. This conclusion should also hold for the other U-series radionuclides, since uranium is generally considered the most mobile element in the radioactive decay series.

IV.5.3. ($^{234}U/^{238}U$) disequilibria along stylolitic joints

The systematic ($^{234}U/^{238}U$) disequilibria encountered in zones characterized by pressure dissolution structures indicate that such zones have experienced some uranium fractionation and migration within the last 2 Ma. These structures must play a major role in uranium remobilization: radioactive disequilibria are observed only inside or within close proximity of the stylolitic seams, and the isotopic distribution of uranium systematically exhibit a symmetrical pattern in relation to these discontinuities. The seriate measurements performed perpendicularly to the centimetric-scale stylolitic swarm of HTM 02924 sample allow to document the geochemical processes involved.

Impact of stylolitization process on uranium concentration

The higher uranium content found in stylolitic material than in the host rock results from pressure dissolution processes. Dissolution of the carbonate matrix along stylolitic surfaces resulted in the accumulation of clay minerals, organic matter and detrital accessory minerals inside the seams [20, 21, 46, 47]. Consequently, the chemical elements present in non-soluble residues are concentrated in the seams. This is illustrated in Figure IV.4., which shows the relative enrichment of some major and trace elements through the major seam of sample HTM 02924 compared to its embedding rock matrix (assumed to be best represented by subsample HTM 02924 #1). Elements that are mainly associated with silicate or accessory minerals accumulated in this seam (Zr, Si, Al, Fe...) are enriched by a factor of up to 10, whereas elements that also co-precipitated with carbonates, such as alkaline earths (Mg^{2+}, Sr^{2+}, Ba^{2+}), display a lesser relative enrichment. The abundance of calcium (expressed as CaO) decreases from 53% in the carbonate matrix to 40% in the seam, thereby highlighting the pressure dissolution undergone by the calcium carbonate minerals. Since the distributions of U and Zr through the HTM 02924 transect are

similar (Figure IV.4.), the U distribution in the system is primarily controlled by the accumulation of U-rich detrital material in the seams.

Uranium relocation

This systematic deficit of ^{234}U in the stylolitic material concomitant with an excess of ^{234}U in the embedding matrix (see Figure IV.3.) strongly suggests a transfer of uranium from the U-rich stylolitic material to the surrounding U-poor carbonate matrix. This phenomenon is also clearly highlighted by the ^{234}U-^{238}U data obtained on the HTM 02924 transect when they are plotted in a standard ($^{234}U/^{238}U$) *vs* $1/^{238}U$ mixing diagram (Figure IV.6.). This diagram exhibits three trendlines that allow interpretation of these data in terms of mixing among four distinct end-members.

For clarification purposes, these end-members are defined *a priori* as follows:

M end-member: characterized by secular equilibrium state (($^{234}U/^{238}U$) = 1) and a low uranium concentration (~390 ppb). This end-member represents a pristine limestone matrix that would not have experienced any remobilization of uranium in the past.

AM1 and AM2 end-members: characterized by ($^{234}U/^{238}U$) activity ratios higher than unity (1.025 and 1.050, respectively) and uranium concentrations of 930 ppb and 715 ppb, respectively. These end-members represent the parts of the embedding matrix, on each side of the stylolitic swarm, that have undergone maximum secondary U fixation.

S end-member: characterized by a ($^{234}U/^{238}U$) activity ratio smaller than unity (0.963) and a high uranium concentration (4080 ppb). This end-member corresponds to the material within the stylolitic swarm and is composed of minerals that possess a lesser susceptibility to pressure dissolution: residual carbonates, non-soluble detrital minerals. It is also likely that secondary

authigenic minerals such as dolomite [47] are present. This end-member is represented by subsample #6a.

A trendline describes a mixture between, on the one hand, the S end-member and, on the other hand, the AM1 and AM2 end-members. The subsamples following this trend are located either inside the major stylolitic swarm or in very close proximity to it. This mixture of stylolitic material and altered carbonate matrix can be explained by the presence of a thin transition zone between the stylolitic material and the carbonate matrix. Some minor pressure dissolution structures may be located within this zone, thereby explaining the mixing trend observed. Sampling artefact could also account for this phenomenon although greatest care was taken to exclude as much of the embedding matrix as possible in sampling material inside the seam.

The other two trendlines show mixings between the M end-member and the AM1 and AM2 end-members, respectively (see Figure IV.6B). They correspond to subsamples located in the embedding carbonate matrix on each side of the major stylolitic discontinuity (subsample series #3 to #1 and #8 to #11, respectively). The decrease of the AR, together with a lower U content away from the seam, strongly suggests secondary deposition within the embedding matrix of uranium coming from the stylolitic discontinuity. Therefore, the AM1 and AM2 end-members are composed of the carbonate matrix component within which secondary fractionated uranium has been redeposited. The convergence of these two trend lines towards the single M end-member highlights the initial homogeneity of the carbonate rock matrix with respect to uranium at the scale of the transect. The amounts of secondary uranium fixed on each side of the stylolitic discontinuity are roughly equal since the U concentrations of the altered matrix are similar. These amounts can be estimated by looking at U contents in subsamples #1 to #4 and #7 to #11, and comparing them with the concentration of 390 ppb modelled for the pristine carbonate matrix M end-

member. The secondary uranium would represent from 26% to 49% of the total uranium found in these subsamples, 58% and 46% of the AM1 and AM2 end-members modelled, and finally 33% (19 μg of ^{238}U) of the total uranium of the embedding carbonate matrix.

The isotopic composition of the "secondary" uranium however differs on either sides of the pressure dissolution discontinuity. It is difficult to explain the existence of these two distinct isotopic signatures of the altered matrix end-members, AM1 and AM2. If the secondary uranium comes exclusively from the major pressure dissolution discontinuity observed in the middle of sample HTM 02924, there is no reason for the secondary uranium to leave distinct isotopic signatures on either sides of the discontinuity. Similarly, the intermediate position of subsample #4 between the AM1 and AM2 end-members in the diagram ($^{234}U/^{238}U$) *vs* $1/^{238}U$ (see Figure IV.6A), does not totally agree with the scenario of a single source of uranium in the system. For these reasons, we think that part of sample HTM 02924 located between the major stylolitic discontinuity (#6) and the small stylolitic joint (#13), as well as subsample #4, though with a lesser intensity, might have been influenced by the presence of other stylolitic seams in the near vicinity.

Although the process leading to the secondary fixation of uranium into the pristine carbonate rock is not fully understood, it is nevertheless very likely that secondary uranium comes from the stylolitic seams. This fact, together with the systematic deficit of ^{234}U inside the stylolitic material and the excess of ^{234}U in the embedding matrix, strongly suggests a relocation of uranium in the system.

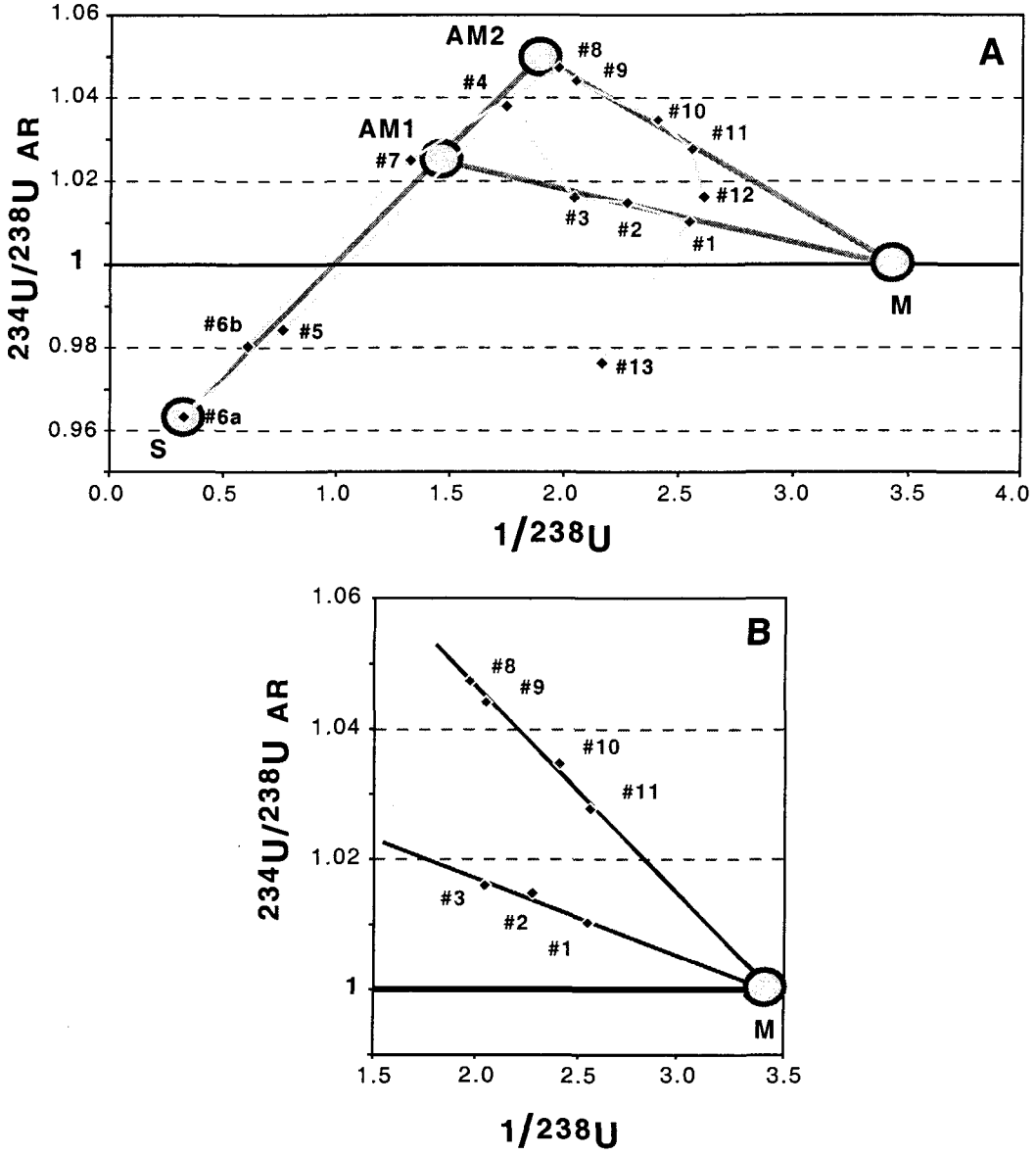

Figure IV.6.: A) $^{234}U/^{238}U$ AR vs. inverse of uranium activity (dpm/g) in subsamples of the HTM 02924 transect. Four end-members are identified. M: pristine matrix end-member; AM1 and AM2: altered matrix end-members; S: stylolitic material. The significance of the three mixing trendlines is explained in text.
B) Blow-up of right-hand portion of Fig. A.

The isotopic budget of uranium

According to the present scenario, the stylolitized zone should have behaved as a closed system. This assumption can be validated by estimating the isotopic budget of uranium. Since each subsample of the transect was weighed before being crushed, one can sum up the ^{234}U and ^{238}U activities of the whole HTM 02924 sample. This yields a ($^{234}U/^{238}U$) AR of 1.012±0.008 (2σ), i.e. a slight disequilibrium state at the 95% confidence level for the whole HTM 02924 sample. However, it is difficult to draw any unequivocal conclusion from this result concerning the chemical behaviour of the system (open vs closed). The small volume (the base of the subsampled core section does not exceed 4 cm^2 and the height of the sample is 15 cm) within which the uranium activities are integrated, is certainly not representative of the entire stylolitized zone column in the vicinity of sample HTM 02924. Moreover, the U-budget estimate does not include the stylolitic seams whose existence was previously suspected based on secondary uranium uptake in subsamples #8 to #11. Furthermore, subsampling artefact can account for the slight disequilibrium observed. The two parts on each side of the stylolitic discontinuity were found apart when received at the laboratory. It is therefore possible that some crumbly stylolitic material exhibiting a large ^{234}U deficit may have been lost. For these reasons, the isotopic budget that we calculated can only provide a rough indication about the chemical behaviour of the system that seems to tend to the radioactive equilibrium state for the ^{234}U-^{238}U series at the meso-scale of a stylolitized zone (i.e. a few cm to a few dm).

IV.5.4. Geological implications: fluid circulation or pressure dissolution-related phenomenon

The question arises now of the driving phenomena responsible for the "recent" (i.e. within the last 2 Ma) relocation of uranium within the stylolitized zones of the limestone formations. The processes involved require the presence of some interstitial

fluid since the fractionation of uranium entails exchanges at rock/water interfaces and mass transfer by means of a liquid phase.

Water/rock interactions induced by the physical and chemical perturbation associated with flowing fluids are often put forward to explain U-series disequilibria observed on rocks in the upper lithosphere. In the present case, this assumption cannot be totally ruled out. Pressure dissolution surfaces have been found to constitute fluid barriers for perpendicular fluid flow, but can act as preferential conduits for flowing fluids [48]. Fluids circulating through the stylolitic pathway could have remobilized fractionated uranium from the U-rich stylolitic material. Subsequently, these fluids could have infiltrated the surrounding matrix where some uranium had been redeposited. In this scenario, U relocation must have occurred after the stylolitization process itself. However, it is unlikely that this scenario can account for the practically balanced uranium budget found in the system. Considering the small volume of sample HTM 02924, the large amount of secondary uranium relocated in the surrounding carbonate matrix (19 μg of ^{238}U or 33% of the total uranium) can be considered proportionally very high. Since there are also some indications that the medium is characterized by reducing conditions (ubiquitous presence of pyrite rhombs in the carbonate matrix and high content of this mineral inside the stylolitic swarm), it seems highly unlikely that, under such redox conditions, fluids could be capable of remobilizing large quantities of uranium. Moreover, in this scenario, the geochemical processes involved in the deposition of the remobilized uranium in the embedding matrix are unclear.

Another plausible driving process may be invoked to explain radioactive disequilibria observed in stylolitized zones. Uranium fractionation and relocation can be directly related to the pressure dissolution process. During stylolitization, pressure dissolution that occurs in stressed domains of the rock leads to mass transfer through

an aqueous phase, either by diffusion or bulk flow [20]. The uranium associated with the carbonate material that was dissolved within stylolitic seams was redistributed in the surrounding carbonate matrix together with other dissolution products (major or trace elements). This may be done by precipitation of secondary carbonate cement within pore spaces of less stressed domain, thereby reducing the porosity and permeability of the host matrix [20, 21, 47, 48]. Such a phenomenon has been proposed to explain the low porosity of Dogger and Oxfordian limestones in the vicinity of the Bure site [19]. The high enrichment by a factor of up to 10 of elements that are mainly associated with detrital minerals (e.g. Zr) in stylolitic subsamples (#6a and #6b) indicates that a large quantity of the carbonate rock was dissolved inside the stylolitic swarm. The dissolved uranium that has been released into the matrix by the pressure dissolution process can represent the redeposited secondary uranium currently observed in the surrounding matrix (~33% of the total uranium of the carbonate matrix).

This scenario can account fully for the local uranium relocation and is consistent with the large transfer of uranium observed in the system. Unlike the fluid circulation scenario, this last model takes into account the products of the pressure dissolution phenomenon that were released into the embedding carbonate matrix. The isotopic fractionation of uranium arises from the preferential leaching of ^{234}U from the U-rich non-soluble minerals concomitant with the pressure dissolution of the carbonate within the seams. A similar mechanism was proposed by Bonotto and Andrews [49] in order to explain the enhancement of ($^{234}U/^{238}U$) AR in karstic limestone groundwater.

The formation of the stylolitic structures in the Mesozoic formations of the Bure site was initiated either during the burial of the sedimentary series [19] or during the tectonic Oligocene phase [26]. According to the second hypothesis, the data presented here would demonstrate that the pressure dissolution processes have been active until now or were at least reactivated in the last 2 Ma. The reasons for the

active stylolitization until recent time are not fully understood. Pressure dissolution usually results from gravitational loading by overburden or from tectonic forces, and occurs preferentially on surfaces statistically perpendicular to the maximum principal compressive normal stress [50]. Since the extensive Oligocene phase, the area is thought to have remained in compressive stress regime [19]. The active phenomenon currently observed could therefore not be attributed to tectonic forces. Stylolitization has been documented in limestone formations that experienced shallow burial from 1000m to 90m [21, 48, 51-53]. Since the maximum denudation of the upper part of the sedimentary series (Kimmeridgian, Tithonian and Cretaceous), as determined by fluid inclusion paleothermometry [19], does not exceed a few hundred meters (~200m), the burial depth of the Bathonian and Oxfordian limestone formation could not have varied significantly within time. Therefore, whatever the process that initiated the pressure dissolution (overburden or tectonic stress), it is possible that the current gravitational loading was responsible for the active phenomenon observed. In this case, the uranium relocation can be considered as an epidiagenetic phenomenon.

IV.6. Conclusion

As the ($^{234}U/^{238}U$) disequilibria observed in all the stylolitic zones analyzed systematically display features similar to those observed in sample HTM 02924, it is likely that these zones were subject to the same geochemical processes as those that control the isotopic distribution of uranium along this transect. Although one cannot rule out a small inward flux of uranium in the system, we rather believe that the ($^{234}U/^{238}U$) disequilibria observed indicate a discrete relocation of uranium from the U-rich material within the stylolitic seam toward the U-poor surrounding matrix. The system would behave as a balanced system with respect to uranium. Since this element is generally considered the most mobile element in the radioactive decay

series (with the exception of ^{222}Rn), this conclusion would also hold for other U-series radionuclides.

The driving processes responsible for the uranium relocation remain for the moment unclear. We have proposed and discussed two potential processes (fluid circulations vs late epidiagenetic phenomenon), but other phenomena could possibly be put forth. However, whatever the driving process involved, they have been active in the last 2 Ma and have affected all the stylolitized zones examined and, consequently, a large part of the Bathonian and Oxfordian limestone formations. This is a major and surprising result since the deep, low-permeability, compact limestone formations, such as those of the Bure experimental site, are generally supposed to behave as a chemically stable system after early to syn-compaction diagenesis.

Outside the stylolitized zones found in limestone formations, the pristine rock displays ($^{234}U/^{238}U$) radioactive equilibrium, providing robust evidence for a chemically closed system, during the present, with respect to uranium, thus to U-series radionuclides. The secular equilibrium state of the target Callovo-Oxfordian argilites is a fundamental result with regard to the storage of high level radioactive wastes since it gives a strong clue for the present day chemical stability of this deep argillaceous formation.

Acknowledgements

For constructive help and comments on the manuscript, the authors thank Dr. E. Pons-Branchu and Dr. C. Plain. PD is grateful to ANDRA (the French agency for nuclear waste management) for providing drill-core samples and financial support for his Ph.D..

References

[1] G. de Marsily, A. Barbreau, E. Ledoux and J. Margat, Nuclear waste disposal; can the geologist guarantee isolation?, Science 197(4303), 519-527, 1977.

[2] N.A. Chapman and J.A.T. Smellie, Natural analogues to the conditions around a final repository for high-level radioactive waste, Chemical Geology 55(4), 167-173, 1986.

[3] M. Ivanovich, A.G. Latham, G. Longworth and M. Gascoyne, Applications to radioactive waste disposal studies, in: Uranium-series disequilibrium; applications to earth, marine, and environmental sciences, M. Ivanovich and R.S. Harmon, eds., pp. 583-630, Clarendon Press, Oxford, United Kingdom, 1992.

[4] S. Krishnaswami, W.C. Graustein, K.K. Turekian and J.F. Dowd, Radium, thorium and radioactive lead isotopes in groundwaters; application to the in situ determination of adsorption-desorption rate constants and retardation factors, Water Resources Research 18(6), 1663-1675, 1982.

[5] M. Ivanovich, K. Froehlich and M.J. Hendry, Dating very old groundwater, Milk River Aquifer, Alberta, Canada, Applied Geochemistry 6; 4, 112, 1991.

[6] S. Luo, T.L. Ku, R. Roback, M. Murrell and T.L. McLing, In-situ radionuclide transport and preferential groundwater flows at INEEL (Idaho); decay-series disequilibrium studies, Geochimica et Cosmochimica Acta 64(5), 867-881, 2000.

[7] G.M. Milton and R.M. Brown, Uranium series dating of calcite coatings in groundwater flow systems of the Canadian Shield, Chemical Geology; Isotope Geoscience Section 65(1), 57-65, 1987.

[8] M. Ivanovich, A. Hernandez Benitez, A.V. Chambers and S.E. Hasler, Uranium series isotopic study of fracture infill materials from el Berrocal Site, Spain, Radiochimica Acta 66/67, 485-494, 1994.

[9] L.A. Neymark, Y.V. Amelin and J.B. Paces, ^{206}Pb-^{230}Th-^{234}U-^{238}U and ^{207}Pb-^{235}U geochronology of Quaternary opal, Yucca Mountain, Nevada, Geochimica et Cosmochimica Acta 64(17), 2913-2928, 2000.

[10] H.P. Schwarcz, M. Gascoyne and D.C. Ford, Uranium-series disequilibrium studies of granitic rocks, Chemical geology 36(1-2), 87-102, 1982.

[11] J.A.T. Smellie and J.S. Stuckless, Element mobility studies of two drill-cores from the Goetemar Granite (Kraakemaala test site), Southeast Sweden, Chemical Geology 51(1-2), 55-78, 1985.

[12] J.A.T. Smellie, A.B. Mackenzie and R.D. Scott, An analogue validation study of natural radionuclide migration in crystalline rocks using uranium-series disequilibrium studies, Chemical Geology 55(4), 233-254, 1986.

[13] M. Gascoyne and H.P. Schwarcz, Radionuclide migration over recent geologic time in a granitic pluton, Chemical Geology; Isotope Geoscience Section 59(1), 75-85, 1986.

[14] M. Gascoyne and J.J. Cramer, History of actinide and minor element mobility in an Archean granitic batholith in Manitoba, Canada, Applied Geochemistry 2(1), 37-53, 1987.

[15] L.Y. Griffault, M. Gascoyne, C. Kamineni, R. Kerrich and T.T. Vandergraaf, Actinide and Rare Earth Element characteristics of deep fracture zones in the Lac du Bonnet granitic batholith, Manitoba, Canada, Geochimica et Cosmochimica Acta 57(6), 1181-1202, 1993.

[16] M.Z. Min, J.P. Zhai and C.Q. Fang, Uranium-series radionuclide and element migration around the Sanerliu granite-hosted uranium deposit in southern China as a natural analogue for high-level radwaste repositories, Chemical Geology 144(3-4), 313-328, 1998.

[17] M. Gascoyne, N.H. Miller and L.A. Neymark, Uranium-series disequilibrium in tuffs from Yucca Mountain, Nevada, as evidence of pore-fluid flow over the last million years, Applied Geochemistry 17(6), 781-792, 2002.

[18] P. Deschamps, C. Hillaire-Marcel, J.L. Michelot, R. Doucelance, B. Ghaleb and S. Buschaert, $^{234}U/^{238}U$ Disequilibrium along stylolitic discontinuities in deep Mesozoic limestone formations of the Eastern Paris basin: evidence for discrete uranium mobility over the last 1-2 million years, Hydrology and Earth System Sciences, Submitted.

[19] ANDRA, Référentiel Géologique du Site Meuse-Haute Marne, in: ANDRA Report A RP ADS 99-005/B, pp. 5 Vol, 2001.

[20] R.G.C. Bathurst, Carbonate sediments and their diagenesis, 658 pp., Elsevier, 1975.

[21] R. Tada and R. Siever, Pressure solution during diagenesis, Annual Review of Earth and Planetary Sciences 17, 89-118, 1989.

[22] R.B. de Boer, On the thermodynamics of pressure solution; interaction between chemical and mechanical forces, Geochimica et Cosmochimica Acta 41(2), 249-256, 1977.

[23] R.B. de Boer, Pressure solution; theory and experiments, Tectonophysics 39(1-3), 287-301, 1977.

[24] T.M. Buxton and D.F. Sibley, Pressure solution features in a shallow buried limestone, Journal of Sedimentary Petrology 51(1), 19-26, 1981.

[25] R.G.C. Bathurst, Diagenetically enhanced bedding in argillaceous platform limestones; stratified cementation and selective compaction, Sedimentology 34(5), 749-778, 1987.

[26] M. Coulon, La Distension Oligocène dans le nord-est du bassin de Paris (perturbation des directions d'extension et distribution des stylolites), Bulletin de la Société Géologique de France 163(5), 531-540, 1992.

[27] P. Deschamps, R. Doucelance, B. Ghaleb and J.L. Michelot, Further investigations on optimized tail correction and high-precision measurement of Uranium isotopic ratios using Multi-Collector ICP-MS, Chemical Geology 201(1-2), 141-160, 2003.

[28] H. Cheng, R.L. Edwards, J. Hoff, C.D. Gallup, D.A. Richards and Y. Asmerom, The half-lives of Uranium-234 and Thorium-230, Chemical Geology 169(1-2), 17-33, 2000.

[29] M. Gascoyne, Geochemistry of the actinides and their daughters, in: Uranium-series disequilibrium; applications to earth, marine, and environmental sciences., M. Ivanovich and R.S. Harmon, eds., pp. 34-61, Clarendon Press, Oxford, United Kingdom, 1992.

[30] J.A.T. Smellie and J.N. Rosholt, Radioactive disequilibria in mineralised fracture samples from two uranium occurrences in northern Sweden, Lithos 17(3), 215-225, 1984.

[31] A.G. Latham and H.P. Schwarcz, The relative mobility of U, Th and Ra isotopes in the weathered zones of the Eye-Dashwa Lakes granite pluton, northwestern Ontario, Canada, Geochimica et Cosmochimica Acta 51(10), 2787-2793, 1987.

[32] X. Luo, M. Rehkämper, D.C. Lee and A.N. Halliday, High precision $^{230}Th/^{232}Th$ and $^{234}U/^{238}U$ measurements using energy-filtered ICP Magnetic Sector Multi-Collector mass spectrometry, International Journal of Mass Spectrometry and Ion Processes 171, 105-117, 1997.

[33] C.H. Stirling, T.M. Esat, K. Lambeck, M.T. McCulloch, S.G. Blake, D.C. Lee and A.N. Halliday, Orbital forcing of the marine isotope stage 9 interglacial, Science 291, 290-293, 2001.

[34] C.-C. Shen, L.R. Edwards, H. Cheng, J.A. Dorale, R.B. Thomas, M. Bradley, S., S.E. Weinstein and H.N. Edmonds, Uranium and thorium isotopic and concentration measurements by magnetic sector inductively coupled plasma mass spectrometry, Chemical Geology 185(3-4), 165-178, 2002.

[35] L.F. Robinson, G.M. Henderson and N.C. Slowey, U-Th dating of marine isotope stage 7 in Bahamas slope sediments, Earth and Planetary Science Letters 196(3-4), 175-187, 2002.

[36] G.M. Henderson, Seawater ($^{234}U/^{238}U$) during the last 800 thousand years, Earth and Planetary Science Letters 199(1-2), 97-110, 2002.

[37] D. Delanghe, E. Bard and B. Hamelin, New TIMS constraints on the uranium-238 and uranium-234 in seawaters from the main ocean basins and the Mediterranean Sea, Marine Chemistry 80(1), 79-93, 2002.

[38] A.J. Pietruszka, R.W. Carlson and E.H. Hauri, Precise and accurate measurement of ^{226}Ra-^{230}Th-^{234}U disequilibria in volcanic rocks using plasma ionization multicollector mass spectrometry, Chemical Geology 188(3-4), 171-191, 2002.

[39] M. Condomines, C. Hemond and C.J. Allègre, U-Th-Ra radioactive disequilibria and magmatic processes, Earth and Planetary Science Letters 90(3), 243-262, 1988.

[40] B. Bourdon, S.P. Turner, G.M. Henderson and C.C. Lundstrom, Introduction to U-series geochemistry, in: Uranium-Series Geochemistry, B. Bourdon, G.M. Henderson, C.C. Lundstrom and S.P. Turner, eds. 52, pp. 1-21, Reviews in Mineralogy and Geochemistry, 2003.

[41] Y. Eyal and R.L. Fleischer, Preferential leaching and the age of radiation damage from alpha decay in minerals, Geochimica et Cosmochimica Acta 49(5), 1155-1164, 1985.

[42] V.V. Cherdyntsev, Uranium-234, 234 pp., 1971.

[43] J.K. Osmond and J.B. Cowart, The theory and uses of natural uranium isotopic variations in hydrology, in: Atomic Energy Review 14, pp. 621-679, 1976.

[44] J.K. Osmond and J.B. Cowart, Ground water, in: Uranium-series disequilibrium; applications to earth, marine, and environmental sciences., M. Ivanovich and R.S. Harmon, eds., pp. 290-333, Clarendon Press, Oxford, United Kingdom, 1992.

[45] J.K. Osmond and M. Ivanovich, Uranium-series mobilization and surface hydrology, in: Uranium-series disequilibrium; applications to earth, marine, and environmental sciences., M. Ivanovich and R.S. Harmon, eds., pp. 259-289, Clarendon Press, Oxford, United Kingdom, 1992.

[46] M. Tucker, Diagenetic processes, products and environments, in: Carbonate sedimentology., M.E. Tucker and V.P. Wright, eds., pp. 314-364, Blackwell Sci. Publ., Oxford, United Kingdom, 1990.

[47] H.R. Wanless, Limestone response to stress; pressure solution and dolomitization, Journal of Sedimentary Petrology 49(2), 437-462, 1979.

[48] H.V. Dunnington, Aspects of diagenesis and shape change in stylolitic limestone reservoirs, Proceedings - World Petroleum Congress 2, 339-352, 1967.

[49] D.M. Bonotto and J.N. Andrews, The mechanism of $^{234}U/^{238}U$ activity ratio enhancement in karstic limestone groundwater, Chemical Geology 103(1-4), 193-206, 1993.

[50] D.W. Durney, Solution-transfer, an Important Geological Deformation Mechanism, Nature (London) 235(5337), 315-317, 1972.

[51] L.B. Railsback, Contrasting styles of chemical compaction in the Upper Pennsylvanian Dennis Limestone in the Midcontinent region, U.S.A, Journal of Sedimentary Petrology 63(1), 61-72, 1993.

[52] L.B. Railsback, Lithologic controls on morphology of pressure-dissolution surfaces (stylolites and dissolution seams) in Paleozoic carbonate rocks from the mideastern United States, Journal of Sedimentary Petrology 63(3), 513-522, 1993.

[53] W. Ricken, Diagenetic bedding, 210 pp., Springer-Verlag, Berlin, 1986.

Conclusions et Perspectives

Au terme de ce doctorat, il me semble qu'un certain nombre de conclusions peuvent être tirées, tant du point de vue de la méthodologie, que de l'intérêt de l'étude des déséquilibres radioactifs au sein des familles U-Th aux fins de caractérisation de la migration des radionucléides et de ses implications dans le contexte de la sûreté du stockage géologique des déchets nucléaires.

Apports méthodologiques

En premier lieu, un des enseignements majeurs qu'il faut déduire des résultats présentés ici est sans aucun doute d'ordre méthodologique. Parmi la quarantaine d'échantillons ou sous-échantillons analysés dans cette thèse montrant un déséquilibre ($^{234}U/^{238}U$) significatif, eu égard à la précision analytique (~1‰) obtenue grâce à l'utilisation de la spectrométrie de masse à source plasma, seuls six d'entre eux montrent un excès ou un défaut en ^{234}U supérieur à 5% (voir Chapitre III). En l'occurrence, il s'agit systématiquement de déficits en ^{234}U vis-à-vis de ^{238}U. Autrement dit, seuls ces six échantillons auraient pu indiquer une remobilisation de l'uranium si les analyses avaient été réalisées à l'aide de la technique analytique usuellement utilisée dans ce type d'étude, à savoir la spectrométrie alpha, pour laquelle la précision analytique ne dépasse que très rarement 5%. De plus, de telles analyses auraient certainement conduit à une interprétation erronée des résultats puisque les excès d'uranium-234 que nous avons observés dans la matrice carbonatée au voisinage des joints stylolitiques auraient été occultés par l'imprécision analytique. Une étude "alpha" aurait donc certainement conclu par: "un lessivage préférentiel de l'uranium-234 le long des joints stylolitiques". Il est, qui plus est, fort probable que la faible quantité de matériel recueilli pour les échantillons de type "stylolite" (parfois

100 mg, soit ~300 ng d'uranium) n'aurait pas permis, dans la pratique, de limiter l'erreur analytique à environ ±5% (2σ), mais plus probablement à ±10 %. La conclusion aurait alors été: "le milieu est clos".

A la défense de la spectrométrie d'émission α, on peut arguer avec raison que la sensibilité de la méthode des déséquilibres radioactifs appliquée au traçage des migrations de radionucléides repose usuellement sur le rapport $^{230}Th/^{234}U$. Ceci est certainement vrai lorsque l'on se limite aux phénomènes d'altération de surface où, dans des conditions oxydantes, l'oxydation de l'uranium sous sa forme (VI+) augmente significativement sa mobilité comparativement à celle du thorium. Toutefois, dans les milieux profonds qui nous préoccupent ici, les conditions physico-chimiques sont réductrices et seule la formation de complexes uranyles carbonatés (cf. Annexe B) peut expliquer une différence de mobilité significative (hors effet de recul) entre l'uranium et le thorium. Dans ces conditions, il est fort probable que l'intensité des déséquilibres radioactifs entre les deux couples ^{230}Th-^{234}U et ^{234}U-^{238}U soit du même ordre de grandeur. Ceci est en partie confirmé par les résultats obtenus par Gascoyne et al. (2002) dans les tuffs du site expérimental de Yucca Mountain, Nevada, où les déséquilibres $^{230}Th/^{234}U$ et $^{234}U/^{238}U$ observés au sein de la matrice sont du même ordre de grandeur et s'établissent entre 0,85 et 1,1 pour le rapport d'activité ($^{234}U/^{238}U$), et entre 0,9 et 1,4 pour le rapport ($^{230}Th/^{234}U$).

A priori, la détermination du rapport d'activité ($^{230}Th/^{234}U$) ne m'apparaît donc pas comme primordiale tant l'interprétation des rapports d'activité ($^{230}Th/^{234}U$) repose sur des postulats (uranium mobile *vs* thorium immobile) contestables dans les milieux étudiés ici. Les analyses isotopiques du thorium n'auraient donc probablement pas permis d'aller beaucoup plus loin dans le traçage et l'identification des phénomènes responsables de la remobilisation des radionucléides telle que mise en évidence à l'aide du rapport ($^{234}U/^{238}U$). Seules les indications chronologiques apportées par les analyses des rapports d'activité ($^{230}Th/^{234}U$) auraient sans aucun doute été précieuses.

A posteriori, les quelques analyses isotopiques du thorium que nous avons pu obtenir, le Dr. Régis Doucelance et moi-même, par spectrométrie de masse à ionisation thermique (TIMS VG-54™ équipé d'un WARP) au Laboratoire "Magmas et Volcans" de l'Université Blaise Pascal de Clermont-Ferrand, abondent dans ce sens. Les rapports ($^{230}Th/^{234}U$) obtenus sur la plupart des échantillons analysés (7 sur 8) semblent indiquer un équilibre radioactif au sein de la série ^{230}Th-^{234}U à la barre d'erreur de 1-2% (reporductibilité totale) que nous pouvons pour l'instant raisonnablement afficher pour ces mesures. Ces résultats ne peuvent toutefois être donnés qu'à titre indicatif, la mesure des rapports $^{232}Th/^{230}Th$ (ce rapport atomique pouvant atteindre 650000 pour certains échantillons) constituant un véritable défi technique, et devront être confirmés par des analyses et tests complémentaires.

L'utilisation des techniques actuellement les plus précises (TIMS ou MC-ICP-MS) s'impose, à mon sens, aujourd'hui dans le domaine dans lequel s'inscrit cette thèse. On peut d'ailleurs trouver surprenant que les études de ce type n'aient pas, à de rares exceptions près (e.g. Pomiès, 1999; Neymark et Paces, 2000; et dans une moindre mesure Gascoyne et al., 2002), encore mis à profit les nouvelles perspectives qu'offraient les récents développements analytiques. Cette recherche de précision et de justesse analytique a cependant un prix, tant en équipement, évidemment, qu'en temps nécessaire à la mise au point des techniques analytiques. La multiplication des précautions et des vérifications analytiques (préparation chimique: voir Chapitres II et III; instrumentation: voir Chapitre I) devient inévitable et requiert une compétence spécifique de la part de l'utilisateur. Bref, il n'y a plus d'analyse de routine -si jamais il en a existé- lorsqu'il s'agit d'afficher une reproductibilité de l'ordre du 1‰.

Caractérisation de la migration de l'uranium au sein des formations sédimentaires profondes

En ce qui a trait à la caractérisation de la migration de l'uranium au sein des séries Mésozoïques profondes situées dans l'environnement immédiat du futur laboratoire souterrain de l'ANDRA, deux conclusions majeures doivent être tirées des résultats obtenus.

Tout d'abord, l'état d'équilibre radioactif $^{234}U/^{238}U$ et certainement, par extension, l'état d'équilibre séculaire observé au sein des argilites Callovo-Oxfordiennes, démontrent une non-mobilité des radionucléides naturels dans la formation cible, et, par suite, attestent d'un milieu chimiquement inactif et clos au cours de la période actuelle, tout au moins pour les actinides naturels (voir Chapitre IV). Ce résultat est fondamental au regard de la problématique d'enfouissement des déchets radioactifs car il procure une confirmation *in situ* des capacités de confinement de la couche argileuse cible, dans les conditions physico-chimiques actuelles, vis-à-vis des actinides majeurs ou mineurs.

A contrario, les déséquilibres ($^{234}U/^{238}U$) systématiquement observés au niveau des zones stylolitisées dans les formations carbonatées de l'Oxfordien et du Bathonien témoignent d'une remobilisation de l'uranium au cours des derniers deux millions d'années, et donc, de processus actifs et de transport de matière au sein de ces matrices (Chapitre III). La répartition isotopique de l'uranium telle qu'elle a été révélée soit par un sous-échantillonnage systématique au niveau des surfaces de pression-dissolution, soit par la réalisation d'analyses sériées perpendiculairement à un joint stylolitique, suggère fortement un transfert de l'uranium depuis la surface stylolitique vers la matrice environnante. Bien que soumise à des transferts de matière, une zone stylolitisée fonctionnerait en toute vraisemblance en système fermé vis-à-vis de l'uranium.

Ces résultats sont surprenants au moins à deux titres.

Tout d'abord, par rapport à la connaissance que nous avions jusqu'à présent de la géologie de la séquence sédimentaire impliquée. Jusqu'aux récents travaux du Dr. Stéphane Buschaert (2001; 2003), sur lesquels je reviendrai par la suite, les principaux processus diagénétiques ayant affecté ces séries étaient associés à la mésogenèse (processus liés à leur enfouissement) et étaient considérés pour l'essentiel comme antérieurs au Crétacé supérieur (voir par exemple Vincent, 2001). Dans ces conditions, l'existence de déséquilibres radioactifs, dont la répartition est, bien que discrète, ubiquiste dans ces formations carbonatées, est pour le moins inattendue et atteste au contraire de transferts récents de matière dans le système.

D'autre part, ces résultats sont étonnants par rapport à notre connaissance du comportement des radionucléides naturels, des processus responsables de leur fractionnement et des interprétations que l'on en fait généralement. La mise en évidence d'un phénomène de relocalisation de l'uranium à l'échelle centimétrique est un fait nouveau. Les interprétations qu'il est fait des déséquilibres radioactifs observés sur une matrice solide se limitent très souvent, et certainement trop souvent, à une remobilisation des radionucléides sous l'effet de processus d'interaction eau-roche suite à des circulations de fluides et sont conclues invariablement par un comportement en système "ouvert" du milieu. La réalisation d'un sous-échantillonnage pertinent (e.g. coupe sériée) couplée à l'utilisation d'une technique analytique précise m'a permis de rediscuter la chaîne de causalité entre les déséquilibres observés et les processus qui en sont la cause et de sortir ainsi du schéma "déséquilibre = milieu ouvert" qui dépend finalement étroitement de l'échelle géologique à laquelle on se place. Dans le cas présent, les déséquilibres radioactifs témoignent évidemment de processus dynamiques et de transferts de matière, mais ne sauraient être interprétés comme la preuve d'un fonctionnement en système ouvert à grande échelle du milieu, vis-à-vis des radionucléides. Ceci me semble en accord avec ce que nous connaissons des caractéristiques hydrodynamiques du système

(ANDRA, 1998; ANDRA, 2001). Ces formations carbonatées étant compactes, faiblement perméables et soumises à de très faibles gradients hydrauliques, le transfert de fluide ne peut donc y être que très limité. Il est donc fort peu probable que des circulations de fluides soient la cause de flux entrants ou sortants significatifs d'actinides à grande échelle spatiale et dans la gamme de temps imposée par la systématique U-Th (2 Ma).

Si de telles circulations sont difficilement concevables, il semble évident que le transfert de matière au niveau d'une zone stylolitisée ne puisse se faire que par l'intermédiaire de la phase fluide interstitielle, soit par diffusion moléculaire, soit par advection. Le ou les processus moteurs restent à déterminer, mais il semble certain que les surfaces stylolitiques jouent un rôle prépondérant dans les mécanismes mis en jeu. Dans le chapitre IV, deux hypothèses ont été avancées. Selon un premier scénario, des fluides percolant au niveau de ces surfaces, ces dernières jouant ici le rôle d'axe préférentiel d'écoulement, lessiveraient l'uranium localisé à leur niveau et le redistribueraient dans la matrice carbonatée encadrant le joint. Selon la seconde hypothèse, le processus de stylolitisation serait encore actif ou aurait été réactivé récemment (au cours des 2 derniers millions d'années). Le transfert d'uranium tracé par les déséquilibres ($^{234}U/^{238}U$) correspondrait à la redistribution dans la matrice carbonatée de l'uranium associé à la fraction carbonatée dissoute lors des processus de pression dissolution. Le matériel carbonaté dissous au niveau d'une surface de pression dissolution est évacué dans la porosité adjacente, via la phase interstitielle, où il reprécipite à la faveur de la sursaturation du fluide vis-à-vis de la calcite. Les quantités importantes d'uranium secondaire réparties de part et d'autre du joint telles que j'ai pu les déterminer sur l'échantillon HTM 02924 représentent certainement l'uranium ayant co-précipité avec la calcite sparitique secondaire. Ce scénario présente l'avantage de rendre compte, d'une part du budget isotopique du système

(l'état d'équilibre sur l'ensemble d'une zone stylolitisée) et, d'autre part, du bilan de masse inhérent à la stylolitisation, elle-même.

Perspectives

Bien que l'on ne puisse, de façon univoque, conclure quant aux processus responsables de la relocalisation récente de l'uranium, le second scénario présenté a le mérite de proposer un modèle paléohydrologique général cohérent, en particulier, avec les résultats acquis par le Dr. S. Buschaert (2001; 2003) sur les phases carbonatées secondaires (géodes, fractures, fente de tension), ainsi que sur les ciments de type sparitique qui obturent la porosité des encaissants carbonatés. Les analyses $\delta^{18}O$ de ces phases minérales montrent que celles-ci sont certainement cogénétiques et associées à un épisode relativement tardif de percolation de fluides d'origine météorique et continentale (Buschaert, 2001). Cet évènement majeur de circulation de fluide serait lié à la formation des fossés distensifs régionaux (Gondrecourt, Neufchateau), situés à proximité du site et attribués à l'ouverture Oligocène du fossé Rhénan. A la faveur de ces accidents tectoniques, des fluides seraient remontés depuis les aquifères Triassiques et auraient pénétré les formations carbonatées du Dogger et de l'Oxfordien (Buschaert, 2001; Maes, 2002). Ces fluides seraient à l'origine de la cimentation / recristallisation intense de ces calcaires à porosité initiale importante (~25%) et donc responsables de leur colmatage, la perméabilité actuelle n'étant plus que de ~2-5%.

La composition isotopique du carbone de ces phases calcitiques secondaires indique quant à elle une origine locale pour cet élément (Buschaert, 2001). Il est donc aussi probable que le réservoir de calcium constitutif des carbonates secondaires tardifs soit lui aussi local. Selon toute vraisemblance, celui-ci a pour origine la stylolitisation, phénomène fréquemment invoqué pour expliquer la réduction de porosité observée dans les formations carbonatées (Bathurst, 1975; Wanless, 1979;

Tada et Siever, 1989). Selon Coulon (1992) ce processus aurait été initié à l'Oligocène, ou tout du moins en partie (ANDRA, 2001). Ainsi, se dégage un faisceau d'éléments cohérents tant d'un point de vue chronologique que du point de vue des bilans et transferts de masse dans le système. Les processus de pression dissolution et la compaction chimique résultante auraient donc joué un rôle essentiel sur l'évolution récente (0-30 Ma) des caractéristiques hydrodynamiques des formations carbonatées encadrant les argilites Callovo-Oxfordiennes. Les résultats présentés dans ce doctorat montreraient que ces processus sont encore actifs aujourd'hui ou, tout du moins, l'auraient été au cours des deux derniers millions d'années. Même s'il est probable que l'intensité de la stylolitisation ait été décroissante avec le temps (ne serait-ce que par l'impossibilité d'évacuer les produits de la pression dissolution, suite à la réduction de la porosité), ces éléments indiqueraient que le milieu serait en train de se colmater. Perfectionner

Tant du point de vue de la modalité et des relations existantes entre les différents phénomènes mis en jeu que de leur chronologie relative, des inconnues persistent. Dans ce contexte, l'apport d'informations chronologiques absolues sur la formation des phases carbonatées secondaires tardives (géodes, remplissages des fentes de tension et des failles) semble essentiel. Compte tenu des échelles de temps considérées (du Crétacé à aujourd'hui), les systèmes U-Th et U-Pb apparaissent être les chronomètres les plus pertinents à même d'apporter les contraintes temporelles recherchées. La "faisabilité" de la datation de ce type de matériel a déjà été établie tant par la méthode U-Th (voir par exemple: Milton, 1987; Milton et Brown, 1987; Winograd et al., 1988; Szabo et Kyser, 1990; Ludwig et al., 1992; Winograd et al., 1992; Ludwig et al., 1993; Pomiès, 1999), que par la méthode U-Pb (Richards et al., 1998; Grandia et al., 2000; Neymark et al., 2000; Getty et al., 2001; Neymark et al., 2002; Richards et Dorale, 2003).

Les quelques résultats ^{230}Th-^{234}U-^{238}U préliminaires que j'ai obtenus sur ce type d'échantillons (deux géodes du forage HTM 102 et trois remplissages de fractures associées au fossé de Gondrecourt), résultats par ailleurs confirmés par des analyses réalisées par le Dr. E. Pons-Branchu (com. pers.) indiquent que ces carbonates secondaires sont hors âge U-Th. Leur précipitation serait donc antérieure à 500 ka. Ceci constitue certes un renseignement important, mais insuffisant au regard des informations requises pour une meilleur compréhension de la paléohydrologie du système. La datation de ces phases minérales devra reposer donc sur le développement de la datation par la méthode U-Pb des minéraux carbonatés.

Références

ANDRA, 1998. Site de l'Est- Synthèse des reconnaissances hydrogéochimiques. D RP 0ANT 97-069.

ANDRA, 2001. Référentiel Géologique du Site Meuse-Haute Marne. A RP ADS 99-005/B.

Bathurst, R.G.C., 1975. Carbonate sediments and their diagenesis. Developments in sedimentology. Elsevier, 658 pp.

Buschaert, S., 2001. Origine, âge et processus physico-chimiques des circulations de fluides dans les fractures: Exemples de socle sous couverture (Vienne) et de formations riches en argiles (Gard, Est). Ph. D. Thesis, Université Henri Poincaré, Nancy-I, Nancy, 259 pp.

Buschaert, S., Foucade, S., Cathelineau, M., Deloule, E., Martineau, F., Ayt Ougougdal, M. et Trouiller, A., 2003. Widespreead cementation induced by inflow of continental water in the eastern part of the Paris Basin: O and C isotopic study of carbonate cements. Applied Geochemistry, Sous presse.

Coulon, M., 1992. La Distension Oligocène dans le nord-est du bassin de Paris (perturbation des directions d'extension et distribution des stylolites). Bulletin de la Société Géologique de France, 163(5): 531-540.

Gascoyne, M., Miller, N.H. et Neymark, L.A., 2002. Uranium-series disequilibrium in tuffs from Yucca Mountain, Nevada, as evidence of pore-fluid flow over the last million years. Applied Geochemistry, 17(6): 781-792.

Getty, S.R., Asmerom, Y. et Quinn, T.M., 2001. Accelerated Pleistocene coral extensions in the Caribbean basin from uranium-lead (U-Pb) dating. Geology, 29: 639-642.

Grandia, F., Asmerom, Y., Getty, S., Cardellach, E. et Canals, A., 2000. U-Pb dating of MVT ore-stage calcite: implications for fluid flow in a Mesozoic extensional basin from Iberian Peninsula. Journal of Geochemical Exploration, 69-70: 377-380.

Ludwig, K.R., Simmons, K.R., Szabo, B.J., Winograd, I.J., Landwehr, J.M., Riggs, A.C. et Hoffman, R.J., 1992. Mass-spectrometric ^{230}Th-^{234}U-^{238}U dating of the Devils Hole calcite vein. Science, 258(5080): 284-287.

Ludwig, K.R., Simmons, K.R., Szabo, B.J., Winograd, I.J. et Riggs, A.C., 1993. Dating of the Devils Hole calcite vein; reply. Science, 259: 1626-1627.

Maes, P., 2002. Circulations des fluides et interactions eau-roche passées et actuelles dans la pile sédimentaire du site Meuse / haute-Marne: Apport des isotopes du Sr et conséquences. Ph. D. Thesis, Université de Montpellier II.

Milton, G.M., 1987. Paleohydrological inferences from fracture calcite analyses; an example from the Stripa Project, Sweden. IApplied Geochemistry, 2; 1: 33-36.

Milton, G.M. et Brown, R.M., 1987. Uranium series dating of calcite coatings in groundwater flow systems of the Canadian Shield. Chemical Geology; Isotope Geoscience Section, 65(1): 57-65.

Neymark, L.A., Amelin, Y., Paces, J.B. et Peterman, Z.E., 2002. U-Pb ages of secondary silica at Yucca Mountain, Nevada: implications for the paleohydrology of the unsaturated zone. Applied Geochemistry, 17(6): 709-734.

Neymark, L.A., Amelin, Y.V. et Paces, J.B., 2000. ^{206}Pb-^{230}Th-^{234}U-^{238}U and ^{207}Pb-^{235}U geochronology of Quaternary opal, Yucca Mountain, Nevada. Geochimica et Cosmochimica Acta, 64(17): 2913-2928.

Neymark, L.A. et Paces, J.B., 2000. Consequences of slow growth for ^{230}Th/ U dating of Quaternary opals, Yucca Mountain, NV, USA. Chemical Geology, 164(1-2): 143-160.

Pomiès, C., 1999. Traçage isotopique des migrations d'uranium dans l'environnement granitique de la minéralisation uranifère de Palmottu (Sud-Ouest Finlande). Ph. D. Thesis, Université Montpellier 2.

Richards, D.A., Bottrell, S., Cliff, R.A., Stroehle, K. et Rowe, P.J., 1998. U-Pb dating of a speleothem of Quaternary age. Geochimica et Cosmochimica Acta, 62(23-24): 3683-3688.

Richards, D.A. et Dorale, J.A., 2003. U-series chronology and environmental applications of speleothems. In: B. Bourdon, G.M. Henderson, C.C. Lundstrom et S.P. Turner (Editors), Uranium-Series Geochemistry. Reviews in Mineralogy and Geochemistry, pp. 407-460.

Szabo, B.J. et Kyser, T.K., 1990. Ages and stable-isotope compositions of secondary calcite and opal in drill cores from Tertiary volcanic rocks of the Yucca Mountain area, Nevada. Geological Society of America Bulletin, 102(12): 1714-1719.

Tada, R. et Siever, R., 1989. Pressure solution during diagenesis. Annual Review of Earth and Planetary Sciences, 17: 89-118.

Vincent, B., 2001. Sédimentologie et Géochimie de la diagenèse des carbonates. Application au Malm de la Bordure Est du Bassin de Paris. Ph. D. Thesis, Université de Dijon.

Wanless, H.R., 1979. Limestone response to stress; pressure solution and dolomitization. Journal of Sedimentary Petrology, 49(2): 437-462.

Winograd, I.J., Coplen, T.B., Landwehr, J.M., Riggs, A.C., Ludwig, K.R., Szabo, B.J., Kolesar, P.T. et Revesz, K.M., 1992. Continuous 500,000-year climate record from vein calcite in Devils Hole, Nevada. Science, 258(5080): 255-260.

Winograd, I.J., Szabo, B.J., Coplen, T.B. et Riggs, A.C., 1988. A 250,000-year climatic record from Great Basin vein calcite; implications for Milankovitch theory. Science, 242(4883): 1275-1280.

Bibliographie générale

Alexandre, D., 1997. Conditionnement des déchéts nucléaires. In: R. Turlay (Editor), Les déchets nucléaires; un dossier scientifique. Les éditions de Physique, pp. 181-202.

Allègre, C.J. et Condomines, M., 1982. Basalt genesis and mantle structure studied through Th-isotopic geochemistry. Nature (London), 299(5878): 21-24.

ANDRA, 1998. Site de l'Est- Synthèse des reconnaissances hydrogéochimiques. D RP 0ANT 97-069.

ANDRA, 2001. Référentiel Géologique du Site Meuse-Haute Marne. A RP ADS 99-005/B.

Andrews, J.N., Ford, D.J., Hussain, N., Trivedi, D. et Youngman, M.J., 1989. Natural radioelement solution by circulating groundwaters in the Stripa Granite. Geochimica et Cosmochimica Acta, 53: 1791-1802.

Andrews, J.N., Giles, I.S., Kay, R.L.F., Lee, D.J., Osmond, J.K., Cowart, J.B., Fritz, P., Barker, J.F. et Gale, J., 1982. Radioelements, radiogenic helium and age relationships for groundwaters from the granites at Stripa, Sweden. Geochimica et Cosmochimica Acta, 46(9): 1533-1543.

Bacon, M.P. et Edmond, J.M., 1972. Barium at Geosecs III in the southwest Pacific. Earth and Planetary Science Letters, 16(1): 66-74.

Bard, E., Hamelin, B. et Fairbanks, R.G., 1990a. U-Th ages obtained by mass spectrometry in corals from Barbados; sea level during the past 130,000 years. Nature (London), 346(6283): 456-458.

Bard, E., Hamelin, B., Fairbanks, R.G. et Zindler, A., 1990b. Calibration of the ^{14}C timescale over the past 30,000 years using mass spectrometric U-Th ages from Barbados corals. Nature (London), 345(6274): 405-410.

Bard, E., Hamelin, B., Fairbanks, R.G., Zindler, A., Mathieu, G. et Arnold, M., 1990c. U/Th and ^{14}C ages of corals from Barbados and their use for calibrating the ^{14}C time scale beyond 9000 years BP. Nuclear Instrument and Methods in Physics Research, B-52: 461-468.

Barnes, J.W., Lang, E.J. et Potratz, H.A., 1956. Ratio of ionium to uranium in coral limestone. Science, 124(3213): 175-176.

Bathurst, R.G.C., 1975. Carbonate sediments and their diagenesis. Developments in sedimentology. Elsevier, 658 pp.

Bathurst, R.G.C., 1987. Diagenetically enhanced bedding in argillaceous platform limestones; stratified cementation and selective compaction. Sedimentology, 34(5): 749-778.

Berkman, P.A. et Ku, T.-L., 1998. $^{226}Ra/Ba$ ratios for dating Holocene biogenic carbonates in the Southern Ocean: preliminary evidence from Antarctic coastal mollusc shells. Chemical Geology, 144(3-4): 331-334.

Birck, J.-L., 1986. Precision K-Rb-Sr isotopic analysis; application to Rb-Sr chronology. Chemical Geology, 56(1-2): 73-83.

Bishop, J.K.B., 1988. The barite-opal-organic carbon association in oceanic particulate matter. Nature, 332(6162): 341-343.

Bonotto, D.M. et Andrews, J.N., 1993. The mechanism of $^{234}U/^{238}U$ activity ratio enhancement in karstic limestone groundwater. Chemical Geology, 103(1-4): 193-206.

Bourdon, B., Joron, J.-L., Claude-Ivanaj, C. et Allègre, C.J., 1998. U-Th-Pa-Ra systematics for the Grande Comore volcanics: melting processes in an upwelling plume. Earth and Planetary Science Letters, 164(1-2): 119-133.

Bourdon, B., Turner, S.P., Henderson, G.M. et Lundstrom, C.C., 2003. Introduction to U-series geochemistry. In: B. Bourdon, G.M. Henderson, C.C. Lundstrom et S.P. Turner (Editors), Uranium-Series Geochemistry. Reviews in Mineralogy and Geochemistry, pp. 1-21.

Broecker, W.S., Goddard, J. et Sarmiento, J.L., 1976. The distribution of ^{226}Ra in the Atlantic Ocean. Earth and Planetary Science Letters, 32(2, GEOSECS collected papers; 1973-1976): 220-235.

Buddemeier, R.W. et Hunt, J.R., 1988. Transport of colloidal contaminants in groundwater; radionuclide migration at the Nevada Test Site. Applied Geochemistry, 3(5): 535-548.

Buschaert, S., 2001. Origine, âge et processus physico-chimiques des circulations de fluides dans les fractures: Exemples de socle sous couverture (Vienne) et de formations riches en argiles (Gard, Est). Ph. D. Thesis, Université Henri Poincaré, Nancy-I, Nancy, 259 pp.

Buschaert, S., Foucade, S., Cathelineau, M., Deloule, E., Martineau, F., Ayt Ougougdal, M. et Trouiller, A., 2003. Widespreead cementation induced by inflow of continental water in the eastern part of the Paris Basin: O and C isotopic study of carbonate cements. Applied Geochemistry, Sous presse.

Buxton, T.M. et Sibley, D.F., 1981. Pressure solution features in a shallow buried limestone. Journal of Sedimentary Petrology, 51(1): 19-26.

Casanova, J. et Negrel, P., 1999. Site de l'Est- Etude du système uranium-thorium dans la couche des argilites du Callovo-Oxfordien et ses épontes- Etude des forages MSE101 et HTM102. D RP 0ANT 98-026/A.

Chabaux, F. et Allègre, C.J., 1994. ^{238}U-^{230}Th-^{226}Ra disequilibria in volcanics; a new insight into melting conditions. Earth and Planetary Science Letters, 126(1-3): 61-74.

Chabaux, F., Ben Othman, D. et Birck, J.L., 1994. A new Ra-Ba chromatographic separation and its application to Ra mass-spectrometric measurement in volcanic rocks. Chemical Geology, 114(3-4): 191-197.

Chapman, N.A. et McKinley, I.G., 1987. The geological disposal of nuclear waste. John Wiley & Sons, Chichester, United Kingdom, 280 pp.

Chapman, N.A. et Smellie, J.A.T., 1986. Natural analogues to the conditions around a final repository for high-level radioactive waste. Chemical Geology, 55(4): 167-173.

Chen, J.H., Edwards, R.L. et Wasserburg, G.J., 1986. ^{238}U, ^{234}U and ^{232}Th in seawater. Earth and Planetary Science Letters, 80(3-4): 241-251.

Chen, J.H., Edwards, R.L. et Wasserburg, G.J., 1992. Mass spectrometry and applications to uranium-series disequilibrium. In: M. Ivanovich et R.S. Harmon (Editors), Uranium-series disequilibrium; applications to earth, marine, and environmental sciences. Clarendon Press, Oxford, United Kingdom, pp. 174-206.

Chen, J.H. et Wasserburg, G.J., 1981a. The isotopic composition of uranium and lead in Allende inclusions and meteoritic phosphates. Earth and Planetary Science Letters, 52(1): 1-15.

Chen, J.H. et Wasserburg, G.J., 1981b. Isotopic determination of uranium in picomole and subpicomole quantities. Analytical Chemistry, 53: 2060-2067.

Cheng, H., Edwards, R.L., Hoff, J., Gallup, C.D., Richards, D.A. et Asmerom, Y., 2000. The half-lives of Uranium-234 and Thorium-230. Chemical Geology, 169(1-2): 17-33.

Cherdyntsev, V.V., 1971. Uranium-234, 234 pp.

Claude-Ivanaj, C., Bourdon, B. et Allègre, C., 1998. Ra-Th-Sr isotope systematics in Grande Comore Island: a case study of plume-lithosphere interaction. Earth and Planetary Science Letters, 164(1-2): 99-117.

Cohen, A.S. et O'Nions, K., 1991. Precise determination of femtogram quantities of radium by Thermal Ionization Mass Spectrometry. Analytical Chemistry, 63: 2705-2708.

Condomines, M. et Allègre, C.J., 1980. Age and magmatic evolution of Stromboli Volcano from (super 230) Th- (super 238) U disequilibrium data. Nature (London), 288(5789): 354-357.

Condomines, M., Hemond, C. et Allègre, C.J., 1988. U-Th-Ra radioactive disequilibria and magmatic processes. Earth and Planetary Science Letters, 90(3): 243-262.

Coulon, M., 1992. La Distension Oligocène dans le nord-est du bassin de Paris (perturbation des directions d'extension et distribution des stylolites). Bulletin de la Société Géologique de France, 163(5): 531-540.

Cowan, G.A. et Adler, H.H., 1976. The variability of the natural abundance of ^{235}U. Geochimica et Cosmochimica Acta, 40: 1487-1490.

Curie, M. et Debierne, A., 1910. Sur le radium métallique. Comptes Rendus de l'Académie des Sciences, 151: 523.

de Boer, R.B., 1977a. On the thermodynamics of pressure solution; interaction between chemical and mechanical forces. Geochimica et Cosmochimica Acta, 41(2): 249-256.

de Boer, R.B., 1977b. Pressure solution; theory and experiments. Tectonophysics, 39(1-3): 287-301.

de Marsily, G., 1997. Enfouissement des déchets nucléaires en formation géologique. In: R. Turlay (Editor), Les déchets nucléaires; un dossier scientifique. Les éditions de Physique, pp. 203-246.

de Marsily, G., Barbreau, A., Ledoux, E. et Margat, J., 1977. Nuclear waste disposal; can the geologist guarantee isolation? Science, 197(4303): 519-527.

Dehairs, F., Chesselet, R. et Jedwab, J., 1980. Discrete suspended particles of barite and the barium cycle in the open ocean. Earth and Planetary Science Letters, 49(2): 528-550.

Delanghe, D., Bard, E. et Hamelin, B., 2002. New TIMS constraints on the uranium-238 and uranium-234 in seawaters from the main ocean basins and the Mediterranean Sea. Marine Chemistry, 80(1): 79-93.

Deschamps, P., Doucelance, R., Ghaleb, B., Hillaire-Marcel, C. et Michelot, J.L., 2002. Evidence for micro-scale U-mobility along sedimentary discontinuities in a deep limestone formation as inferred by $^{234}U/^{238}U$ disequilibria. Abstracts of the 12th Annual V.M. Goldschmidt Conference, Geochimica et Cosmochimica Acta, Special Supplement, 66: 179.

Deschamps, P., Doucelance, R., Ghaleb, B. et Michelot, J.L., 2003a. Further investigations on optimized tail correction and high-precision measurement of Uranium isotopic ratios using Multi-Collector ICP-MS. Chemical Geology, 201(1-2): 141-160.

Deschamps, P. et Hillaire-Marcel, C., 1999. Bilan des connaissances sur le comportement des isotopes de l'uranium dissous en milieu réduit - Applications chronologiques. D RP 0 UNQ 99-001, ANDRA.

Deschamps, P., Hillaire-Marcel, C., Michelot, J.L., Doucelance, R. et Ghaleb, B., 2003b. $^{234}U/^{238}U$ Disequilibria along sedimentary discontinuities in a deep formation: late diagenetic U-relocation processes vs. large scale fluid circulation evidence?, EGU-AGU Joint Assembly. Geophysical Research Abstract, Nice, France.

Deschamps, P., Hillaire-Marcel, C., Michelot, J.L., Doucelance, R., Ghaleb, B. et Buschaert, S., Submitted. $^{234}U/^{238}U$ Disequilibrium along stylolitic discontinuities in deep Mesozoic limestone formations of the Eastern Paris basin: evidence for discrete uranium mobility over the last 1-2 million years. Hydrology and Earth System Sciences.

Dunnington, H.V., 1967. Aspects of diagenesis and shape change in stylolitic limestone reservoirs. Proceedings - World Petroleum Congress, 2: 339-352.

Durney, D.W., 1972. Solution-transfer, an Important Geological Deformation Mechanism. Nature, 235(5337): 315-317.

Edwards, R.L., 1988. High precision thorium-230 ages of corals and the timing of sea level fluctuations in the late Quaternary. Ph.D. Thesis, California Institute of Technology, Pasadena, United States.

Edwards, R.L., Chen, J.H., Ku, T.L. et Wasserburg, G.J., 1987a. Precise timing of the last interglacial period from mass spectrometric determination of thorium-230 in corals. Science, 236(4808): 1547-1553.

Edwards, R.L., Chen, J.H. et Wasserburg, G.J., 1987b. ^{238}U-^{234}U-^{230}Th-^{232}Th systematics and the precise measurement of time over the past 500,000 years. Earth and Planetary Science Letters, 81(2-3): 175-192.

Eyal, Y. et Fleischer, R.L., 1985. Preferential leaching and the age of radiation damage from alpha decay in minerals. Geochimica et Cosmochimica Acta, 49(5): 1155-1164.

Falkner, K.K., O'Neill, D.J., Todd, J.F., Moore, W.S. et Edmond, J.M., 1991. Depletion of barium and radium-226 in Black Sea surface waters over the past thirty years. Nature, 350(6318): 491-494.

Fleischer, R.L., 1980. Isotopic disequilibrium of uranium; alpha-recoil damage and preferential solution effects. Science, 207(4434): 979-981.

Fleischer, R.L. et Raabe, O.G., 1978. Recoiling alpha-emitting nuclei; mechanisms for uranium-series disequilibrium. Geochimica et Cosmochimica Acta, 42(7): 973-978.

Galer, S.J.G., 1999. Optimal double and triple spiking for high precision lead isotopic measurement. Chemical Geology, 157: 255-274.

Gallup, C.D., Cheng, H., Taylor, F.W. et Edwards, R.L., 2002. Direct determination of the timing of sea level change during termination II. Science, 295: 310-313.

Gascoyne, M., 1992. Geochemistry of the actinides and their daughters. In: M. Ivanovich et R.S. Harmon (Editors), Uranium-series disequilibrium; applications to earth, marine, and environmental sciences. Clarendon Press, Oxford, United Kingdom, pp. 34-61.

Gascoyne, M. et Cramer, J.J., 1987. History of actinide and minor element mobility in an Archean granitic batholith in Manitoba, Canada. Applied Geochemistry, 2(1): 37-53.

Gascoyne, M., Miller, N.H. et Neymark, L.A., 2002. Uranium-series disequilibrium in tuffs from Yucca Mountain, Nevada, as evidence of pore-fluid flow over the last million years. Applied Geochemistry, 17(6): 781-792.

Gascoyne, M. et Schwarcz, H.P., 1986. Radionuclide migration over recent geologic time in a granitic pluton. Chemical Geology; Isotope Geoscience Section, 59(1): 75-85.

Getty, S.R., Asmerom, Y. et Quinn, T.M., 2001. Accelerated Pleistocene coral extensions in the Caribbean basin from uranium-lead (U-Pb) dating. Geology, 29: 639-642.

Goldstein, S.J., Murrell, M.T. et Janecky, D.R., 1989. Th and U isotopic systematics of basalts from the Juan de Fuca and Gorda ridges by mass spectrometry. Earth and Planetary Science Letters, 96(1-2): 134-146.

Goldstein, S.J., Murrell, M.T., Janecky, D.R., Delaney, J.R. et Clague, D.A., 1991. Geochronology and petrogenesis of MORB from the Juan de Fuca and Gorda

ridges by ^{238}U-^{230}Th disequilibrium. Earth and Planetary Science Letters, 107(1): 25-41.

Grandia, F., Asmerom, Y., Getty, S., Cardellach, E. et Canals, A., 2000. U-Pb dating of MVT ore-stage calcite: implications for fluid flow in a Mesozoic extensional basin from Iberian Peninsula. Journal of Geochemical Exploration, 69-70: 377-380.

Griffault, L.Y., Gascoyne, M., Kamineni, C., Kerrich, R. et Vandergraaf, T.T., 1993. Actinide and Rare Earth Element characteristics of deep fracture zones in the Lac du Bonnet granitic batholith, Manitoba, Canada. Geochimica et Cosmochimica Acta, 57(6): 1181-1202.

Griffault, L.Y. et Shewchuk, T.A., 1994. Permeability effects on radionuclide migration in a highly fractured zone in the Lac du Bonnet batholith, Canada. Radiochimica Acta, 66/67: 495-503.

Halliday, A.N., Lee, D.C., Christensen, J.N., Rehkämper, M., Yi, W., Luo, X., Hall, C.M., Ballentine, C.J., Pettke, T. et Stirling, C., 1998. Applications of multiple collector-ICPMS to cosmochemistry, geochemistry and paleoceanography. Geochimica et Cosmochimica Acta, 62(6): 919-940.

Hamelin, B., Bard, E., Zindler, A. et Fairbanks, R.G., 1991. $^{234}U/^{234}U$ mass spectrometry of corals; how accurate is the U-Th age of the last interglacial period? Earth and Planetary Science Letters, 106(1-4): 169-180.

Hamelin, B., Manhès, G., Albarède, F. et Allègre, C.J., 1985. Precise lead isotope measurements by the double spike technique: a reconsideration. Geochimica et Cosmochimica Acta, 49: 173-182.

Henderson, G.M., 2002. Seawater ($^{234}U/^{238}U$) during the last 800 thousand years. Earth and Planetary Science Letters, 199(1-2): 97-110.

Henderson, G.M., Slowey, N.C. et Haddad, G.A., 1999. Fluid flow through carbonate platforms: constraints from $^{234}U/^{238}U$ and Cl^- in Bahamas pore-waters. Earth and Planetary Science Letters, 169(1-2): 99-111.

Hillaire-Marcel, C., Gariepy, C., Ghaleb, B., Goy, J.L., Zazo, C. et Barcelos, J.C., 1996. U-series measurements in Tyrrhenian deposits from Mallorca; further evidence for two last-interglacial high sea levels in the Balearic Islands. Quaternary Science Reviews, 15(1): 53-62.

Hofmann, A.W., 1971. Fractionation corrections for mixed-isotope spikes of Sr, K and Pb. Earth and Planetary Science Letter, 10: 397-402.

Hsi, C.K.D. et Langmuir, D., 1985. Adsorption of uranyl onto ferric oxyhydroxides; application of the surface complexation site-binding model. Geochimica et Cosmochimica Acta, 49(9): 1931-1941.

Ivanovich, M., 1991. Aspects of uranium/thorium series disequilibrium applications to radionuclide migration studies. Radiochimica Acta, 52/53: 257-268.

Ivanovich, M., 1994. Uranium series disequilibrium: concepts and applications. Radiochimica Acta, 64: 81-94.

Ivanovich, M., Froehlich, K. et Hendry, M.J., 1991. Dating very old groundwater, Milk River Aquifer, Alberta, Canada. Applied Geochemistry, 6; 4: 112.

Ivanovich, M., Hernandez Benitez, A., Chambers, A.V. et Hasler, S.E., 1994. Uranium series isotopic study of fracture infill materials from el Berrocal Site, Spain. Radiochimica Acta, 66/67: 485-494.

Ivanovich, M., Latham, A.G., Longworth, G. et Gascoyne, M., 1992. Applications to radioactive waste disposal studies. In: M. Ivanovich et R.S. Harmon (Editors), Uranium-series disequilibrium; applications to earth, marine, and environmental sciences. Clarendon Press, Oxford, United Kingdom, pp. 583-630.

Jarvis, K.E., Gray, A.L. et Houk, R.S., 1992. Handbook of Inductively Coupled Plasma Spectrometry. Blackie, Glasgow.

Jeandel, C., Dupré, B., Lebaron, G., Monnin, C. et Minster, J.F., 1996. Longitudinal distributions of dissolved barium, silica and alkalinity in the western and southern Indian Ocean. Deep-Sea Research. Part I: Oceanographic Research Papers, 43(1): 1-31.

Kersting, A.B., Efurd, D.W., Finnegan, D.L., Rokop, D.J., Smith, D.K. et Thompson, J.L., 1999. Migration of plutonium in ground water at the Nevada Test Site. Nature, 397: 56-59.

Kigoshi, K., 1971. Alpha-recoil thorium-234; dissolution into water and the uranium-234/uranium-238 disequilibrium in nature. Science, 173: 47-48.

Koide, M., Bruland, K.W. et Goldberg, E.D., 1976. ^{226}Ra chronology of a coastal marine sediment. Earth and Planetary Science Letters, 31(1): 31-36.

Krishnamoorthy, T.M., Nair, R.N. et Sarma, T.P., 1992. Migration of radionuclides from a granite repository. Water Resources Research, 28(7): 1927-1934.

Krishnaswami, S., Graustein, W.C., Turekian, K.K. et Dowd, J.F., 1982. Radium, thorium and radioactive lead isotopes in groundwaters; application to the in situ determination of adsorption-desorption rate constants and retardation factors. Water Resources Research, 18(6): 1663-1675.

Labonne, M. et Hillaire-Marcel, C., 2000. Geochemical gradients within modern and fossil shells of Concholepas concholepas from Northern Chile: An insight into U-Th systematics and diagenetic/authigenic isotopic imprints in mollusk shells. Geochimica et Cosmochimica Acta, 64(9): 1523-1534.

Lalou, C. et Brichet, E., 1980. Anomalously high uranium contents in the sediment under Galapagos hydrothermal mounds. Nature (London), 284(5753): 251-253.

Latham, A.G. et Schwarcz, H.P., 1987a. On the possibility of determining rates of removal of uranium from crystalline igneous rocks using U-series disequilibria; 1: a U-leach model, and its applicability to whole-rock data. Applied Geochemistry, 2(1): 67-71.

Latham, A.G. et Schwarcz, H.P., 1987b. On the possibility of determining rates of removal of uranium from crystalline igneous rocks using U-series disequilibria;

2: Applicability of a U-leach model to mineral separates. Applied Geochemistry, 2(1): 67-71.

Latham, A.G. et Schwarcz, H.P., 1987c. The relative mobility of U, Th and Ra isotopes in the weathered zones of the Eye-Dashwa Lakes granite pluton, Northwestern Ontario, Canada. Geochimica et Cosmochimica Acta, 51(10): 2787-2793.

Liebetrau, V., Eisenhauer, A., Gussone, N., Worner, G., Hansen, B.T. et Leipe, T., 2002. $^{226}Ra_{excess}$/Ba growth rates and U-Th-Ra-Ba systematic of Baltic Mn/Fe crusts. Geochimica et Cosmochimica Acta, 66(1): 73-83.

Ludwig, K.R., 1997. Optimization of multicollector isotope-ratio measurement of strontium and neodymium. Chemical Geology, 135(3-4): 325-334.

Ludwig, K.R., Simmons, K.R., Szabo, B.J., Winograd, I.J., Landwehr, J.M., Riggs, A.C. et Hoffman, R.J., 1992. Mass-spectrometric ^{230}Th-^{234}U-^{238}U dating of the Devils Hole calcite vein. Science, 258(5080): 284-287.

Ludwig, K.R., Simmons, K.R., Szabo, B.J., Winograd, I.J. et Riggs, A.C., 1993. Dating of the Devils Hole calcite vein; reply. Science, 259: 1626-1627.

Luo, S., Ku, T.L., Roback, R., Murrell, M. et McLing, T.L., 2000. In-situ radionuclide transport and preferential groundwater flows at INEEL (Idaho); decay-series disequilibrium studies. Geochimica et Cosmochimica Acta, 64(5): 867-881.

Luo, X., Rehkämper, M., Lee, D.C. et Halliday, A.N., 1997. High precision $^{230}Th/^{232}Th$ and $^{234}U/^{238}U$ measurements using energy-filtered ICP Magnetic Sector Multi-Collector mass spectrometry. International Journal of Mass Spectrometry and Ion Processes, 171: 105-117.

Maes, P., 2002. Circulations des fluides et interactions eau-roche passées et actuelles dans la pile sédimentaire du site Meuse / haute-Marne: Apport des isotopes du Sr et conséquences. Ph. D. Thesis, Université de Montpellier II.

Milton, G.M., 1987. Paleohydrological inferences from fracture calcite analyses; an example from the Stripa Project, Sweden. IApplied Geochemistry, 2; 1: 33-36.

Milton, G.M. et Brown, R.M., 1987a. Adsorption of uranium from groundwater by common fracture secondary minerals. Canadian Journal of Earth Sciences, 24(7): 1321-1328.

Milton, G.M. et Brown, R.M., 1987b. Uranium series dating of calcite coatings in groundwater flow systems of the Canadian Shield. Chemical Geology; Isotope Geoscience Section, 65(1): 57-65.

Min, M.Z., Zhai, J.P. et Fang, C.Q., 1998. Uranium-series radionuclide and element migration around the Sanerliu granite-hosted uranium deposit in southern China as a natural analogue for high-level radwaste repositories. Chemical Geology, 144(3-4): 313-328.

Neymark, L.A., Amelin, Y., Paces, J.B. et Peterman, Z.E., 2002. U-Pb ages of secondary silica at Yucca Mountain, Nevada: implications for the

paleohydrology of the unsaturated zone. Applied Geochemistry, 17(6): 709-734.

Neymark, L.A., Amelin, Y.V. et Paces, J.B., 2000. ^{206}Pb-^{230}Th-^{234}U-^{238}U and ^{207}Pb-^{235}U geochronology of Quaternary opal, Yucca Mountain, Nevada. Geochimica et Cosmochimica Acta, 64(17): 2913-2928.

Neymark, L.A. et Paces, J.B., 2000. Consequences of slow growth for ^{230}Th/ U dating of Quaternary opals, Yucca Mountain, NV, USA. Chemical Geology, 164(1-2): 143-160.

Osmond, J.K. et Cowart, J.B., 1976. The theory and uses of natural uranium isotopic variations in hydrology, Atomic Energy Review, pp. 621-679.

Osmond, J.K. et Cowart, J.B., 1992. Ground water. In: M. Ivanovich et R.S. Harmon (Editors), Uranium-series disequilibrium; applications to earth, marine, and environmental sciences. Clarendon Press, Oxford, United Kingdom, pp. 290-333.

Osmond, J.K. et Ivanovich, M., 1992. Uranium-series mobilization and surface hydrology. In: M. Ivanovich et R.S. Harmon (Editors), Uranium-series disequilibrium; applications to earth, marine, and environmental sciences. Clarendon Press, Oxford, United Kingdom, pp. 259-289.

Paces, J.B., Ludwig, K.R., Peterman, Z.E. et Neymark, L.A., 2002. 234U/238U evidence for local recharge and patterns of ground-water flow in the vicinity of Yucca Mountain, Nevada, USA. Applied Geochemistry, 17(6): 751-779.

Pietruszka, A.J., Carlson, R.W. et Hauri, E.H., 2002. Precise and accurate measurement of ^{226}Ra-^{230}Th-^{234}U disequilibria in volcanic rocks using plasma ionization multicollector mass spectrometry. Chemical Geology, 188(3-4): 171-191.

Pomiès, C., 1999. Traçage isotopique des migrations d'uranium dans l'environnement granitique de la minéralisation uranifère de Palmottu (Sud-Ouest Finlande). Ph. D. Thesis, Université Montpellier 2.

Pons-Branchu, E., 2001. Datation haute résolution de spéléothèmes ($^{230}Th/^{234}U$ et $^{226}Ra/^{238}U$). Application aux reconstitutions environnementales autour des sites du Gard et de Meuse / Haute-Marne. Ph-D Thesis, Université Aix-Marseille III.

Railsback, L.B., 1993a. Contrasting styles of chemical compaction in the Upper Pennsylvanian Dennis Limestone in the Midcontinent region, U.S.A. Journal of Sedimentary Petrology, 63(1): 61-72.

Railsback, L.B., 1993b. Lithologic controls on morphology of pressure-dissolution surfaces (stylolites and dissolution seams) in Paleozoic carbonate rocks from the mideastern United States. Journal of Sedimentary Petrology, 63(3): 513-522.

Rehkämper, M. et Mezger, K., 2000. Investigation of matrix effects for Pb isotope ratio measurements by multiple collector ICP-MS: verification and application of optimized analytical protocols. Journal of Analytical Atomic Spectrometry, 15: 1451-1460.

Richards, D.A., Bottrell, S., Cliff, R.A., Stroehle, K. et Rowe, P.J., 1998. U-Pb dating of a speleothem of Quaternary age. Geochimica et Cosmochimica Acta, 62(23-24): 3683-3688.

Richards, D.A. et Dorale, J.A., 2003. U-series chronology and environmental applications of speleothems. In: B. Bourdon, G.M. Henderson, C.C. Lundstrom et S.P. Turner (Editors), Uranium-Series Geochemistry. Reviews in Mineralogy and Geochemistry, pp. 407-460.

Ricken, W., 1986. Diagenetic bedding. Springer-Verlag, Berlin, 210 pp.

Rihs, S., Condomines, M. et Fouillac, C., 1997. U- and Th-series radionuclides in CO_2- rich geothermal systems in the French massif central. Journal of Radioanalytical and nuclear Chemistry, 226(1-2): 149-157.

Rihs, S., Condomines, M. et Sigmarsson, O., 2000. U, Ra and Ba incorporation during precipitation of hydrothermal carbonates: implications for ^{226}Ra-Ba dating of impure travertines. Geochimica et Cosmochimica Acta, 64(4): 661-671.

Robinson, L.F., Henderson, G.M. et Slowey, N.C., 2002. U-Th dating of marine isotope stage 7 in Bahamas slope sediments. Earth and Planetary Science Letters, 196(3-4): 175-187.

Rosholt, J.N., 1983. Isotopic composition of uranium and thorium in crystalline rocks. Journal of Geophysical Research. B, 88(9): 7315-7330.

Rosholt, J.N., Shields, W.R. et Garner, E.L., 1963. Isotopic fractionation of uranium in sandstone. Science, 139(3551): 224-226.

Rubin, K.H., 2001. Analysis of ^{232}Th/^{230}Th in volcanic rocks: a comparison of thermal ionization mass spectrometry and other methodologies. Chemical Geology, 175(3-4): 723-750.

Schwarcz, H.P., 1987. Uranium-series disequilibrium as a criterion for stability of radwaste sites. Isotope geochemistry of groundwater and fracture material in plutonic rock., 2(1): 136.

Schwarcz, H.P., Gascoyne, M. et Ford, D.C., 1982. Uranium-series disequilibrium studies of granitic rocks. Chemical geology, 36(1-2): 87-102.

Scott, R.D., MacKenzie, A.B. et Alexander, W.R., 1992. The interpretation of ^{238}U-^{234}U- ^{230}Th- ^{226}Ra disequilibria produced by rock-water interactions. Journal of Geochemical Exploration, 45(1-3): 345-363.

Shen, C.-C., Edwards, L.R., Cheng, H., Dorale, J.A., Thomas, R.B., Bradley, M., S., Weinstein, S.E. et Edmonds, H.N., 2002. Uranium and thorium isotopic and concentration measurements by magnetic sector inductively coupled plasma mass spectrometry. Chemical Geology, 185(3-4): 165-178.

Sigmarsson, O., 1996. Short magma chamber residence time at an Icelandic volcano inferred from U-series disequilibria. Nature, 382(6590): 440-442.

Sigmarsson, O., Chmeleff, J., Morris, J. et Lopez, E.L., 2002. Origin of ^{226}Ra-^{230}Th disequilibria in arc lavas from southern Chile and implications for magma transfer time. Earth and Planetary Science Letters, 196(3-4): 189-196.

Smellie, J.A.T., Mackenzie, A.B. et Scott, R.D., 1986. An analogue validation study of natural radionuclide migration in crystalline rocks using uranium-series disequilibrium studies. Chemical Geology, 55(4): 233-254.

Smellie, J.A.T. et Rosholt, J.N., 1984. Radioactive disequilibria in mineralised fracture samples from two uranium occurrences in northern Sweden. Lithos, 17(3): 215-225.

Smellie, J.A.T. et Stuckless, J.S., 1985. Element mobility studies of two drill-cores from the Goetemar Granite (Kraakemaala test site), Southeast Sweden. Chemical Geology, 51(1-2): 55-78.

Staubwasser, M., Henderson, G.M., Berkman, P. et Hall, B.L., Submitted. Ba, Ra, Th and U in marine mollusc shells and the potential of $^{226}Ra/Ba$ dating of Holocene marine carbonate shells. submitted to Geochimica et Cosmochimica Acta.

Stein, M., Wasserburg, G.J., Lajoie, K.R. et Chen, J.H., 1991. U-series ages of solitary corals from the California coast by mass spectrometry. Geochimica et Cosmochimica Acta, 55: 3709-3722.

Stirling, C.H., Esat, T.M., Lambeck, K., McCulloch, M.T., Blake, S.G., Lee, D.C. et Halliday, A.N., 2001. Orbital forcing of the marine isotope stage 9 interglacial. Science, 291: 290-293.

Stirling, C.H., Lee, D.C., Christensen, J.N. et Halliday, A.N., 2000. High-precision in situ ^{238}U-^{234}U-^{230}Th isotopic analysis using laser ablation multiple-collector ICP-MS. Geochimica et Cosmochimica Acta, 64(21): 3737-3750.

Szabo, B.J. et Kyser, T.K., 1990. Ages and stable-isotope compositions of secondary calcite and opal in drill cores from Tertiary volcanic rocks of the Yucca Mountain area, Nevada. Geological Society of America Bulletin, 102(12): 1714-1719.

Tada, R. et Siever, R., 1989. Pressure solution during diagenesis. Annual Review of Earth and Planetary Sciences, 17: 89-118.

Taylor, H.E., 2001. Inductively Coupled Plasma Mass Spectrometry. Practice and Techniques. Academic Press, San Diego, California, 294 pp.

Taylor, P., De Bievre, P., Walder, A. et Entwistle, A., 1995. Validation of the analytical linearity and mass discrimination correction model exhibited by a multiple collector inductively coupled plasma mass spectrometer by means of a set of synthetic uranium isotope mixtures. Journal of Analytical Atomic Spectrometry, 10: 395-398.

Thirlwall, 2001. Inapropriate tail corrections can cause large inaccuracy in isotope ratio determination by MC-ICP-MS. Journal of Analytical Atomic Spectrometry, 16: 1121-1125.

Thirlwall, M.F., 2002. Multicollector ICP-MS analysis of Pb isotopes using a ^{207}Pb-^{204}Pb double spike demonstrates up to 400 ppm/amu systematic errors in Tl-normalization. Chemical Geology, 184(3-4): 255-279.

Tucker, M., 1990. Diagenetic processes, products and environments. In: M.E. Tucker et V.P. Wright (Editors), Carbonate sedimentology. Blackwell Sci. Publ., Oxford, United Kingdom, pp. 314-364.

Vigier, N., Bourdon, B., Turner, S. et Allègre, C.J., 2001. Erosion timescales derived from U-decay series measurements in rivers. Earth and Planetary Science Letters, 193(3-4): 549-563.

Vilks, P., Caron, F. et Haas, M.K., 1998. Potential for the formation and migration of colloidal material from a near-surface waste disposal site. Applied Geochemistry, 13; 1: 31-42.

Vilks, P., Cramer, J.J., Bachinski, D.B., Doern, D.C. et Miller, H.G., 1993. Studies of colloids and suspended particles in the groundwaters of the Cigar Lake uranium deposit in Saskatchewan. In: J.F. McCarthy et F.J. Wobber (Editors), Manipulation of groundwater colloids for environmental restoration. Lewis Publishers, Boca Raton, FL, United States, pp. 331-334.

Vilks, P., Miller, H.G. et Doern, D.C., 1991. Natural colloids and suspended particles in the Whiteshell Research Area, Manitoba, Canada, and their potential effect on radiocolloid formation. Applied Geochemistry, 6(5): 565-574.

Vincent, B., 2001. Sédimentologie et Géochimie de la diagenèse des carbonates. Application au Malm de la Bordure Est du Bassin de Paris. Ph. D. Thesis, Université de Dijon.

Volpe, A.M. et Goldstein, S.J., 1993. ^{226}Ra-^{230}Th disequilibrium in axial and off-axis mid-ocean ridge basalts. Geochimica et Cosmochimica Acta, 57(6): 1233-1241.

Volpe, A.M., Olivares, J.A. et Murrrell, M.T., 1991. Determination of radium isotpe ratios and abundances in geologic sample by Thermal Ionization Mass Spectrometry. Analytical Chemistry, 63: 913-916.

Waite, T.D., Davis, J.A., Payne, T.E., Waychunas, G.A. et Xu, N., 1994. Uranium(VI) adsorption to ferrihydrite; application of a surface complexation model. Geochimica et Cosmochimica Acta, 58(24): 5465-5478.

Wanless, H.R., 1979. Limestone response to stress; pressure solution and dolomitization. Journal of Sedimentary Petrology, 49(2): 437-462.

Winograd, I.J., Coplen, T.B., Landwehr, J.M., Riggs, A.C., Ludwig, K.R., Szabo, B.J., Kolesar, P.T. et Revesz, K.M., 1992. Continuous 500,000-year climate record from vein calcite in Devils Hole, Nevada. Science, 258(5080): 255-260.

Winograd, I.J., Szabo, B.J., Coplen, T.B. et Riggs, A.C., 1988. A 250,000-year climatic record from Great Basin vein calcite; implications for Milankovitch theory. Science, 242(4883): 1275-1280.